Aalborg Universitet

AALBORG UNIVERSITY
DENMARK

Patient Radiation Dose from the EOS Low-Dose Scanner and other X-Ray Modalitites in Scoliosis Patients

an evaluation of organ dose and effective dose

Pedersen, Peter Heide

Publication date:
2019

Document Version
Publisher's PDF, also known as Version of record

Link to publication from Aalborg University

Citation for published version (APA):
Pedersen, P. H. (2019). *Patient Radiation Dose from the EOS Low-Dose Scanner and other X-Ray Modalitites in Scoliosis Patients: an evaluation of organ dose and effective dose*. Aalborg Universitetsforlag. Aalborg Universitet. Det Sundhedsvidenskabelige Fakultet. Ph.D.-Serien

General rights
Copyright and moral rights for the publications made accessible in the public portal are retained by the authors and/or other copyright owners and it is a condition of accessing publications that users recognise and abide by the legal requirements associated with these rights.

- Users may download and print one copy of any publication from the public portal for the purpose of private study or research.
- You may not further distribute the material or use it for any profit-making activity or commercial gain
- You may freely distribute the URL identifying the publication in the public portal -

Take down policy
If you believe that this document breaches copyright please contact us at vbn@aub.aau.dk providing details, and we will remove access to the work immediately and investigate your claim.

Downloaded from vbn.aau.dk on: May 04, 2023

PATIENT RADIATION DOSE FROM THE EOS LOW-DOSE SCANNER AND OTHER X-RAY MODALITIES IN SCOLIOSIS PATIENTS

AN EVALUATION OF ORGAN DOSE
AND EFFECTIVE DOSE

BY
PETER HEIDE PEDERSEN

DISSERTATION SUBMITTED 2019

AALBORG UNIVERSITY
DENMARK

PATIENT RADIATION DOSE FROM THE EOS LOW-DOSE SCANNER AND OTHER X-RAY MODALITIES IN SCOLIOSIS PATIENTS

AN EVALUATION OF ORGAN DOSE AND EFFECTIVE DOSE

PhD Dissertation by

Peter Heide Pedersen

Department of Clinical Medicine

AALBORG UNIVERSITY
DENMARK

Submitted November 2019

Dissertation submitted: November 27th, 2019

PhD supervisor: Associate Prof., MD, Søren Peter Eiskjær
Aalborg University Hospital, Denmark

Assistant PhD supervisorss: Associate Prof., MD, PhD, Svend Erik Østgaard
Aalborg University Hospital, Denmark

Medical Physicist, Asger Greval Petersen
Røntgenfysik, Region Nordjylland, Denmark

PhD committee: Thomas Jakobsen, Clinical Associate Professor, MD (chair)
Aalborg University

Peter Helmig, Professor, MD
Aarhus University Hospital

Benny Dahl, Professor, MD
Baylor College of Medicine/Texas Children's Hospital

PhD Series: Faculty of Medicine, Aalborg University

Department: Department of Clinical Medicine

ISSN (online): 2246-1302
ISBN (online): 978-87-7210-547-5

Published by:
Aalborg University Press
Langagervej 2
DK – 9220 Aalborg Ø
Phone: +45 99407140
aauf@forlag.aau.dk
forlag.aau.dk

© Copyright: Peter Heide Pedersen

Printed in Denmark by Rosendahls, 2020

“There are no secrets to success. It is the result of preparation, hard work, and learning from failure"

Colin Powell

Preface

The first brick for this PhD study was laid already the day that I was hired for my current position as an orthopedic staff-specialist. My future clinical chief, the future main supervisor of this PhD, asked me if I would be willing to do a "small project" once hired for my new position. What does one say when asked such a question at the job interview?

The journey of arriving at the point of submission of this PhD thesis has been a true adventure, one of dedication and challenges. Long dark hours in solitude at the X-ray lab and wandering the hallways of the surgical department at nighttime and on weekends in order to obtain radiographic exposures to my "family" of anthropomorphic phantoms. The fantastic experience of international collaboration in France. Learning by doing; project management, handling sophisticated x-ray equipment as well as keeping up with deadlines and performance goals.

In the course of this study, I have come to truly understand the importance of collaboration, both internal as well as external. The importance of the resulting domestic and international network is priceless. Science is the result of teamwork and the presented work could not have been effectuated had it not been for the collaboration of, and help from numerous people.

The work on which this PhD thesis is based was conducted over the years 2016-2019 while employed part-time as an orthopedic staff-specialist at the University Hospital of Aalborg, and enrolled part-time as a PhD student at the Department of Clinical Medicine, Aalborg University.

The experimental work was carried out at the following institutions: Department of Orthopedic Surgery, Aalborg University Hospital, Denmark. University College Nordjylland (Radiografskolen), Aalborg, Denmark. Institut de Biomécanique Humaine Georges Charpak, Paris, France. Department of Pediatric Orthopedics, and the Department of Radiology at Armand Trousseau Hospital, Sorbonne Université, APHP Paris, France.

The studies for this PhD are in continuation of the work initiated and conducted by Petersen and Eiskjær in 2012 on radiation dose optimization during assessment and treatment of spinal pathologies.

Acknowledgements

I would like to express my utmost and sincere gratitude to all the people and institutions involved one way or another in this project. This project could not have been accomplished if not for the combined effort from all of you.

Søren Eiskjær, my boss, my main supervisor, thank you for challenging me and continuously pushing my limits allowing me to reach higher goals than I anticipated possible. You let me manage this project, believed in me and got me back on track if needed. Had it not been for you, I would never have undertaken and succeeded with this project. Who, if not you, would have expected a one week crash course in French would allow me to actively include more than 40 French patients into this project. Thank you my dear colleagues at the Spine unit for carrying on while I was away for research, I owe you much gratitude. Many thanks also go to the Orthopedic Research Unit (OFE) at the department of Orthopedic Surgery at Aalborg University Hospital for financing my time off from clinical work. Thank you Asger Greval for being co-supervisor of this PhD as well as facilitating access through Røntgenfysik to the precious anthropomorphic phantoms used in this project. Thank you Torben Tvedebrink at the Institute for Mathematical Sciences, Aalborg University, for helping with statistics and thank you Svend Østgaard for critical revision and new ideas for my work. Thank you Michael and Christian at the UCN for providing lab facilities as well as technical support for my countless dose measurements. Thank you Elsebeth, for helping me conduct conventional x-ray images and for helping me with the EOS scanner. Raphaël Vialle, thank you for your invaluable help with facilitating my stay in France and providing a strong scientific team allowing me to successfully conduct two clinical studies. Thank you Claudio Vergari for being my main scientific sparring partner in France. Thank you Wafa Skalli for facilitating collaboration with your biomechanical institute and for inspiring me to conduct two scientific papers based on this collaboration. Thank you Fred Xavier, Alexia Tran and the rest of the team in Paris, as well as Prof. Ducout Le Pointe at the radiological department, at Armand Trousseau Hospital.

Much gratitude is also owed to private as well as public co-funders of this project, Among these: Region Nordjyllands forskningsfond, Aalborg University, the Danish State (Statens legatbolig, Paris), CC Klestrup og Hustrus mindelegat, Speciallæge Heinrich Kopps legat.

Finally, but not the least, I want to thank my loving family. My dear wife Priya, thank you for always being patient and supportive, and for believing in me. Without your support this PhD would never have been realized. Thank you my dear children, Meera, Vidya and Divyan, for bearing over with your busy father and for showing me your unconditional love.

List of Papers

This PhD thesis is based on the following papers:

I. EOS Micro-dose Protocol: First Full-spine Radiation Dose Measurements in Anthropomorphic Phantoms and Comparisons with EOS Standard-dose and Conventional Digital Radiology
Peter H. Pedersen, Asger G. Petersen, Svend E. Østgaard, Torben Tvedebrink and Søren P. Eiskjær.
(Published in Spine 2018)

II. A reduced micro-dose protocol for 3D reconstruction of the spine in children with scoliosis: results of a phantom based and clinically validated study using stereo-radiography
Peter H. Pedersen, Claudio Vergari, Abdulmajeed Alzakri, Raphaël Vialle and Wafa Skalli.
(Published in European Radiology 2019)

III. A Nano-Dose Protocol For Cobb Angle Assessment in Children With Scoliosis: Results of a Phantom-based and Clinically Validated Study
Peter H. Pedersen, Claudio Vergari, Raphaël Vialle et Al.
(Published in Clinical Spine Surgery 2019)

IV. EOS, O-arm, X-Ray; what is the cumulative radiation exposure during current scoliosis management?
Ari Demirel, Peter H. Pedersen and Søren P. Eiskjær.
(Submitted to: Danish Medical Journal)

V. How many dosemeters are needed for correct mean organ dose assessment when performing phantom dosimetry? A phantom study evaluating liver organ dose and investigating TLD numbers and ways of dosemeter placement.
Peter H. Pedersen, Asger G. Petersen, Svend E. Østgaard, Torben Tvedebrink and Søren P. Eiskjær.
(Submitted to: Radiation Protection Dosimetry)

The papers will be referenced in the text by their Roman numerals(I-V).

This thesis has been submitted in partial fulfillment of the PhD degree. The thesis is based on the scientific papers which are listed above. The thesis is not in its present form acceptable for open electronic publication but only in limited and closed circulation as copyrights for papers number II and III have not been ensured.

Table of Contents

Thesis at Glance

PAPER I

Aims: To report absorbed organ dose and effective dose using the new EOS imaging micro-dose scan protocol for full-spine imaging. Secondly, to compare these measurements to EOS standard-dose protocol and convention digital radiology (CR).
Design: A comparative study exploring radiation dose exposure measured in anthropomorphic dosimetry phantoms.
Primary outcome: A 5 to 17-fold reduction in radiation dose when using micro-dose protocol compared with standard-dose protocol and CR.
Conclusions: Full-spine imaging with EOS micro-dose protocol yields less radiation dose exposure than other currently available x-ray modalities. Measurements were reliable and comparable to literature.

PAPER II

Aim: To clinically validate a dose-optimized reduced micro-dose protocol for 3D reconstruction of the spine.
Design: A prospective study on clinical validation of a reduced micro-dose protocol for 3D reconstruction of the spine developed from semi-quantitative anthropomorphic phantom image analysis.
Primary Outcome: Clinical validation of the reduced micro-dose protocol for acceptable 3D reconstruction of the spine.
Conclusion: The reduced micro-dose protocol provided reproducible 3D reconstruction of the spine and allowed for screening and radiographic follow-up of pediatric patients with low to moderate degrees of scoliosis. The reduced micro-dose protocol could replace the micro-dose protocol in such patients. Standard-dose protocol remains superior to both reduced micro-dose protocol and regular micro-dose protocol.

PAPER III

Aim: To clinically validate a new ultra-low-dose protocol for reliable 2D Cobb angle measurements.
Design: A prospective clinical validation study.
Primary Outcome: An ultra-low-dose protocol (the “nano-dose” protocol) was established and subsequently clinically validated for reliable 2D Cobb angle measurements. Variability was <5° from the mean using 95% confidence intervals.

Conclusion: The proposal to use this clinically validated nano-dose protocol for routine radiographic follow-up of scoliotic pediatric patients, reducing radiation dose to a minimum while still obtaining reliable measurements of Cobb angles.

PAPER IV

Aim: To evaluate type and frequency of radiographic imaging and total cumulative radiation exposure to patients treated for scoliosis.
Design: A single center retrospective review study, and a survey study on trends of management and radiological follow-up algorithms for scoliotic patients between international spine centers.
Primary Outcomes: Surgically treated patients with scoliosis received a median dose of cumulative radiation dose 10-fold higher than conservatively treated patients. A substantial variability was found for radiographic follow-up protocols among eight international spine-centers.
Conclusion: The full-body absorbed radiation dose for surgically treated scoliotic patients varies greatly as a result of different radiographic follow-up protocols and the use of intraoperative CT based navigation. It is possible to keep dose rates low when applying new low-dose stereography and low-dose protocols for intraoperative navigation, and still provide state of the art treatment for scoliosis.

PAPER V

Aim: To evaluate different variables influencing measurements of radiation dose absorption in the liver and to evaluate the minimum of TLDs needed to accurately measure absorbed radiation dose to the liver.
Design: A methodological study evaluating the number of dosimeters and the location of these needed to ensure acceptable accuracy of organ dose measurements for the liver in the anthropomorphic ATOM phantom.
Primary outcome: Results using generalized linear mixed effects model analysis and subset analysis showed that TLD position, rotation of the phantom and the specific TLD tablet influenced radiation dose measurements. Four to six TLDs out of 28 could ensure an accurate measurement of absorbed liver dose.
Conclusion: It is possible to reduce the time spent on organ dosimetry by more than 75%, in the case of the liver, and still get valid mean organ dose results, lying within 95% CI of “true” mean organ dose values based on all 28 dosimeter locations.

Abbreviations

AIS	Adolescent Idiopathic Scoliosis
ALARA	As Low As Reasonable Achievable
AP	Anterior-Posterior
APL	Anterior-Posterior-Lateral
AVR	Apical Vertebra Rotation
BMI	Body Mass Index
CIRS	Computerized Imaging Reference System
CR	Conventional Digital Radiology
DAP	Dose Area Product
DRL	Diagnostic Reference Levels
IAEA	International Atomic Energy Agency
IAR	Intra-vertebral-Axial-Rotation
ICD	International Classification of Diseases
ICRP	International Commission on Radiological Protection
IS	Idiopathic Scoliosis
ISO	International Organization for Standardization
LAT	Lateral
LNT	Linear-Non-Threshold Model
PA	Posterior-Anterior
PACS	Picture Archiving and Communication System
PAL	Posterior-Anterior-Lateral
PT	Pelvic Tilt
TI	Torsional Index of the spine
TLD	Thermoluminescent Dosimeter
PCXMC	Monte Carlo dose-simulation program

English Summary

Radiographic imaging is the second most significant cause of ionizing radiation. The use of medically induced ionizing radiation, especially Computed Tomography (CT) has been on the rise for the past many decades. The Atom bomb survivor studies have shown that the risk of adverse health effects such as radiation induced cancer is proportional to the amount of radiation dose absorbed to the human body. Studies from historic cohorts of scoliosis patients undergoing repeat x-ray imaging show an increased risk of cancer compared to the background population. Especially breast cancer has been of concern. Children and young adults are believed to be more sensitive to the adverse effects of ionizing radiation.

When first diagnosed with scoliosis, patients are primarily children or young adults. Primary assessments of scoliosis, followed by monitoring of curve progression as well as intraoperative imaging result in repeated radiographic imaging. The consequence is potential high levels of cumulative dose absorption, and subsequent potential risk of increased adverse effects from ionizing radiation. To this day, there is no known lower dose limit to which amount of radiation that could potentially be harmful and lead to detrimental changes within the body and development of malignant disease. Thus, keeping radiation exposure to our patients as low as possible while still providing adequate imaging is of great importance.

Dose optimization is an issue of great concern and much effort has gone into revising dose-protocols, optimizing/modernizing x-ray equipment as well as developing new techniques. To address the issue of dose optimization, the low-dose EOS scanner was taken into use at our institution in the fall of 2014. This particular scanner has been shown to markedly reduce radiation dose compared with standard x-ray modalities, while at the same time providing images of high quality.

The aims of the studies in this PhD thesis was to investigate this new EOS scanner both with regard to radiation dose exposure and to investigate ways of optimizing low-dose protocols even further. Another aim was making an overall view of total dose accumulation in patients treated for idiopathic scoliosis at our institution including conventional x-rays, EOS scans, intraoperative imaging and ancillary CT scans and compare these findings with literature. Finally, to investigate and develop a method to reduce time spent on precise organ dosimetry with thermoluminescent dosimeters (TLDs).

Five studies were conducted, three of these published in international peer reviewed journals. Study I was the first study to report and publish results on organ doses and effective dose for the new EOS micro-dose protocol. Claims by manufacturer of level of dose exposure was confirmed. Findings on regular standard-dose were comparable to previous reports.

Studies II and III investigated, and found a way of establishing new reduced dose full-spine protocols. This was achieved by semi-quantitative phantom image analysis, resulting in two clinically validated reduced dose protocols; in study II a protocol for 3D reconstruction of the spine, and in study III a protocol allowing repeatable 2D Cobb angle measurements.

In study IV a first report was made on total radiation dose from CR, EOS, O-arm and ancillary CT during the course of current scoliosis treatment at our institution. A survey forwarded to nine international spine centers asking for information on current routines regarding scoliosis treatment and radiographic follow-up was used for comparison with own institution. The survey showed varying degrees of inter center agreement and no strict adherence to current consensus guidelines.

Study V investigated a way of possibly determining a reduced number of dosimeters to be used for organ dosimetry without compromising validity of results. The study was based on phantom liver organ dosimetry after exposure in the EOS. By statistical and practical analysis, it was found that reliable mean organ dose measurements could be performed using less than 25% of available dosimeter allocations.

The aims of the studies were met. Reliability of measurements were confirmed within studies and when compared with literature. Two new dose-optimized reduced-dose protocols are ready for clinical application. By evaluating the total amount of accumulated radiation dose during treatment of scoliosis a measure to evaluate potential risk of radiation induced cancer is at hand. A tool was presented proposing a way of reducing time spent on organ dosimetry without compromising certainty of dose measurements. Currently a strategy of how to implement one or both reduced-dose protocols is being worked out at our institution. The tools and methods presented in the thesis and those published in international journals are at hand for other institutions and for future research.

Dansk Resume

Medicinsk røntgenstråling er den næststørste årsag til at den menneskelige organisme udsættes for ioniserende bestråling. Gennem de seneste årtier har brugen af medicinske røntgenstråler med deraf følgende ioniserende stråling, specielt fra CT skanninger, været stigende. Studier af de som overlevede de amerikanske atombombesprængninger i henholdsvis Nagasaki og Hiroshima, har vist at der er en direkte årsagssammenhæng mellem den mængde af radioaktiv stråling som den menneskelige organisme udsættes for og den deraf følgende risiko for skadelige virkninger, som f.eks. stråleinduceret cancer. Flere historiske kohorte studier har indikeret at der er en øget forekomst af cancer blandt skoliosepatienter end i baggrundsbefolkningen. Dette begrundet i gentagne røntgenundersøgelser af skoliosepatienterne. Især den øgede forekomst af mamma cancer hos disse patienter har vakt bekymring. Børn og unge mennesker menes at være særligt modtagelige over for de skadelige virkninger af ioniserende stråler.

Diagnosen skoliose bliver oftest stillet i barndommen eller i den tidlige ungdom. Forundersøgelser, efterfølgende kontroller af mulig kurve progression, så vel som eventuel intraoperativ gennemlysning resulterer i, at denne patientgruppe skal igennem gentagne røntgenundersøgelser. Konsekvensen af dette er en potentielt høj akkumuleret dosis af ioniserende røntgenstråling, og en deraf øget risiko for skadevirkninger. Indtil videre er der ikke nogen kendt nedre grænse for hvilken mængde af røntgenstråling der kan lede til skadevirkninger og stråleinduceret cancer. Så længe dette er tilfældet er det yderst vigtigt at den mængde stråler som vores patienter udsættes for holdes på det lavest mulige niveau, samtidig med at vi sikrer os korrekt diagnosticering og behandling.

Dosisoptimering er et vigtigt fokusområde og mange ressourcer er blevet, og bliver fortsat, brugt på at revidere dosis protokoller, modernisere røntgenudstyr og på at udvikle nye teknikker.

For at imødekomme dette behov, tog vi i efteråret 2014 en ny EOS® lav-dosis skanner i brug på vores afdeling. EOS skanneren har i tidligere studier vist sig at bruge markant færre røntgenstråler end andre røntgenapparater og alligevel samtidig at kunne levere røntgenbilleder af høj kvalitet.

Målene med denne PhD afhandling var at undersøge EOS skanneren i forhold til hvilken mængde af røntgenstråler den eksponerer vores patienter for, og at belyse mulighederne for at optimere lav dosis protokollerne yderligere. Et yderligere mål var at undersøge og belyse brugen af røntgenstråler i forbindelse med undersøgelse og behandling af skoliosepatienter på vores afdeling. Herunder almindelig røntgen, EOS, intraoperativ røntgengennemlysning og CT, samt evt. supplerende billeddiagnostiske undersøgelser, og sammenligne dette med litteraturen. Endelig, at undersøge muligheden for at udvikle en metode til at nedsætte den tid der bruges på at foretage

præcis organ dosis monitorering med thermoluminescente røntgen dosimetre (TLD tabletter).

Afhandlingen bygger på fem videnskabelige studier, tre af disse er blevet publiceret i anerkendte peer reviewede internationale tidsskrifter, de to sidste er indsendt til bedømmelse og afventer review. I studie I undersøgte og belyste vi som de første absorberet organdosis og helkropsdosis ved brug af den nye EOS "micro-dose" lav dosis protokol. Vi bekræftede fabrikantens postulat om at en helkropsskanning i to plan resulterede i en røntgeneksponering svarende til mindre end en uges naturlig baggrundsstråling. Øvrige fund med almindelig "standard-dose" protokol var sammenlignelige med tidligere publicerede studier.

Studierne II og III, undersøgte og fandt en måde at etablere nye dosis optimerede EOS protokoller til undersøgelse af columna totalis ("full-spine"). Dette blev opnået ved semikvantitativ billedanalyse baseret på røntgenundersøgelser af et antropomorft (menneskelignende) røntgen fantom. Resultatet blev to protokoller; i studie II, en protokol til brug ved 3D rekonstruktion af columna, og i studie III, en protokol til brug ved 2D Cobb vinkelmålinger.

Studie IV belyste den totale røntgenstråling fra almindelig røntgen (CR), EOS, O-arm CT under operationer, samt eventuelle yderligere CT skanninger foretaget i forbindelse med behandling for skoliose på vores rygcenter. Et web-baseret spørgeskema blev sendt til ni forskellige internationale rygcentre med henblik på belysning af behandlingsmønstre og procedurer for røntgenopfølgninger i forbindelse med behandling af patienter med idiopatisk skoliose (IS). Resultaterne blev sammenlignet med algoritmerne på vores center. Spørgeskemaet viste nogen grad af uoverensstemmelse klinikkerne imellem og ingen fuldstændig overholdelse af internationalt aftalte retningslinjer/ konsensus.

Studie V undersøgte muligheden for at reducere antallet af TLD tabletter som det er nødvendigt at bruge i forbindelse med organdosimetri uden at kompromittere validiteten af resultaterne. Studiet blev baseret på røntgenfantom dosimetri, med leveren som målorgan. Det blev konkluderet, at korrekt organdosimetri kan foretages ved brug af mindre end 25% af tilgængelige målepositioner.

Målene med afhandlingen er nået. Pålideligheden af vores målemetoder blev bekræftet studierne imellem, og når man sammenligner med tidligere publicerede studier. To nye lavdosis "full-spine" protokoller er klar til klinisk implementering. Ved evaluering af den totale mængde ioniserende stråling som vores patienter udsættes for i forbindelse med skoliose udredning samt behandling har vi fået et redskab til vurdering af den samlede risiko for stråleinduceret cancer for vores skoliose patienter. En metode til optimering af arbejdsgangen i forbindelse med organ- og helkropsdosimetri med TLD tabletter er blevet præsenteret.

På nuværende tidspunkt arbejder vi på en strategi for implementering af den ene eller begge af de to dosis optimerede protokoller i vores rygcenter. Redskaberne og metoderne præsenteret i denne afhandling og publiceret i internationale tidsskrifter er tilgængelige for andre centre og fremtidige forskningsprojekter.

Introduction

Ionizing radiation and medical imaging

The type of radiation emitted by medical x-ray modalities is ionizing radiation. Ionizing is radiation that carries enough energy to induce the release of electrons from a molecule or an atom(1). When tissue is under the influence of ionizing radiation, energy is released and might cause changes in surrounding tissues, causing tissue damage, and possible detrimental effects. Radiation detriment is a way to quantify cancer incidence, mortality of cancer and hereditary effects as a result of ionizing radiation to the body(2). The general use of medical imaging involving ionizing radiation has been on the rise in the past decades(3), the development of better and more precise imaging modalities as well as the need and wish for more high-definition x-ray solutions have resulted in medical imaging being the second highest cause of ionizing radiation in the western world. CT scans make up the major part of the exposure coming from medical imaging. Figure 1 shows the proportional relationship between the frequency of examinations in Europe and the accumulated dose from medical imaging.

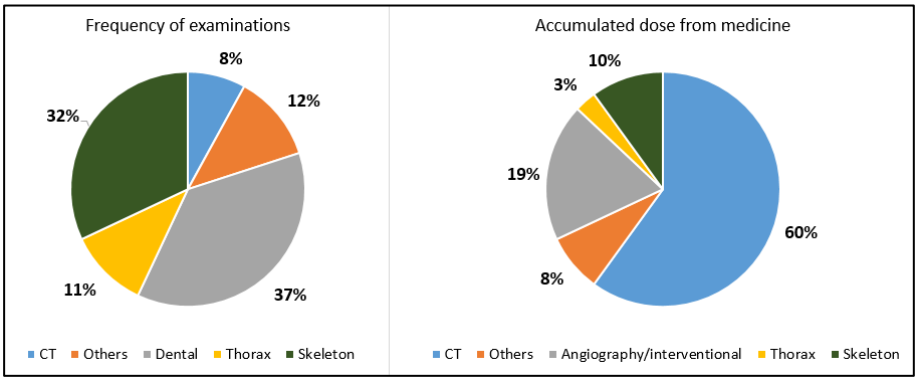

Figure 1, Euramed 2019, presented at ERPW 2019, Stockholm.

The number of fluoroscopy guided interventions, among these minimal invasive surgery of the spine have also been increasing. These methods are often faster, less invasive and less traumatic to the patients resulting in faster recovery. However, most of these methods require extensive use of x-ray imaging (fluoroscopy or CT). Furthermore, in spinal surgery there has bend a trend towards the increased use of intraoperative CT-based navigation for safe instrumentation of the spine(4).

A Swiss study (5) found that the average annual exposure from medical imaging per capita was 1.2 mSv. The worldwide average natural background radiation has been

estimated at 2.4 mSv (range 1-10)(6), in Denmark the background radiation from natural causes is estimated at 3 mSv per year and approx. 1 mSv from medical diagnostics ((7).

Health effects from radiation

Adverse health effects from radiation can be divided into two categories; deterministic effects and stochastic effects.

Deterministic health effects

The deterministic effects occur when an immediate dose exposure exceeds the threshold for acute tissue damage, eg. skin reddening, burns, organ failure, sterility, cataract, hypothyroidism, etc. Table 1 illustrates examples of threshold levels for deterministic tissue damages from radiation. Doses below thresholds cause no deterministic effects.

Table 1, Deterministic Health Effects

Examples of thresholds of occurrences for various Effects

Organ or tissue	Dose in less than two days, Gy.	Type of effect	Time of occurrence
Whole body (bone marrow)	1	Death	1-2 months
Skin	3	Rubor	1-4 weeks
	6	Burn	2-3 weeks
	4	Temporary hair loss	2 to 3 weeks
Thyroid	5	Hypothyroidism	1st-several years
Eyes	2	Cataract	6months – several years
Gonads	3	Permanent sterility	Weeks

Sources: ICRP report 118(8) and the International Atomic Energy Agency (IAEA).

Stochastic health effects

Stochastic health effects from radiation are changes and damage to cells, occurring by chance and often with a latency of many decades. The stochastic risk from radiation is believed to have no lower threshold of dose, and the risk of adverse health effects to be proportional with amount of dose absorbed to the human body(2). The most important health effect from ionizing radiation is cancer. The Linear-Non-Threshold model (LNT) is the most commonly used way to depict the assumed proportional relationship between absorbed radiation dose and the risk of cancer. Figure 2 shows the LNT model as well as other theoretic models for health risks from exposure to low-dose radiation.

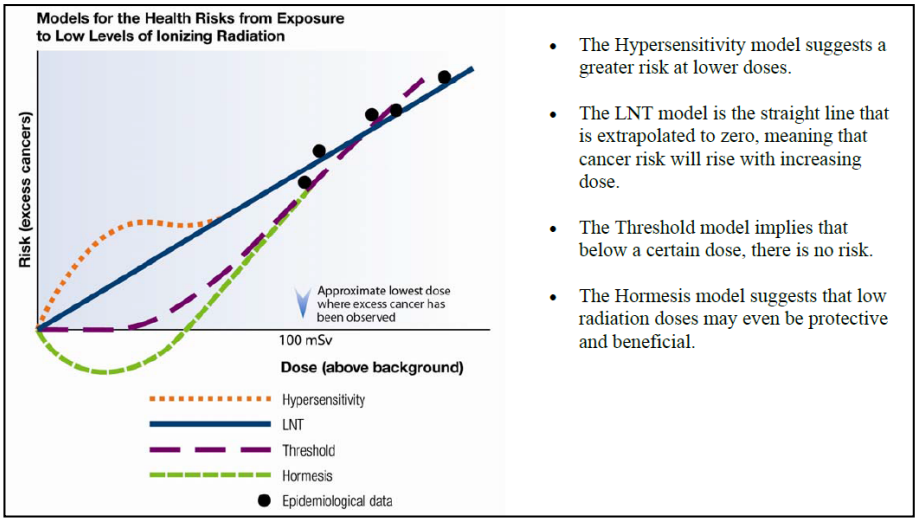

*Figure 2, Linear-Non-Threshold model (**blue line**) and other theoretic models for risk assessment in relation to radiation dose. Canadian Nuclear Safety Commission fact-sheet(2013)*(80)

Potential risk from low-dose radiation

In medicine risk is the probability of an adverse outcome. Modern risk estimates for an irradiated population are derived from the atom bomb survivor studies. The atom bomb survivor studies have reported an increased risk of cancer among people exposed to ionizing radiation(9,10), and found a direct correlation between the amount of radiation an individual is exposed to and the risk of developing cancer. The LNT currently is the most widely used model used to estimate the risk from low-dose ionizing radiation, and is recommended by the United Nations Scientific Committee on the Effects of Atomic Radiation (UNSCEAR), the International Commission on Radiation Protection (ICRP) and the National Council on Radiation Protection and

Measurement (NCRP) (2,6,11). As described above this model assumes direct proportional relationship between the amount of radiation dose absorbed and the derived risk of radiation induced cancer.

How to quantify risk

One way to describe the risk of adverse health effects posed by ionizing radiation is the term effective dose. According to the ICRP publication 103(2), effective dose is a theoretic measure, representing the full-body stochastic risk, the risk of developing cancer as the result of full-body or partial radiation exposure to the body. Effective dose is expressed in miliSieverts (mSv) and is calculated based on the summed tissue equivalent dose for all organs of the body. The absorbed radiation dose in tissue is expressed in Gray (Gy), 1Gy = 1 joule/kilogram (J kg^{-1}). The unit for effective dose is the same as for absorbed dose, J kg^{-1}, and it is expressed in (mSv)(2). For medical x-rays 1 Gy = 1 Sievert.

When a population group of one million people are exposed to one Sievert, it is theorized that 50 people will die prematurely as a cause of radiation-induced cancer ICRP(2). This means that a typical computed tomography scan of 10 mSv will result in a radiation-induced premature death in one out of 2000 scans. One premature death in 2000 scans might not seem a lot, but in 2015 alone, 919.500 CT scans were performed in Denmark (12). This would theoretically result in 460 premature deaths for one year of CT scans in Denmark. The lifetime attributable cancer risk based on 15mSv has been previously been reported to be 0.08-0.17% (13).

Scoliosis

Idiopathic scoliosis (IS) is a three-dimensional (3D) deformity of the spine, defined by a 2D Cobb angle of more than 10 degrees. It usually develops in childhood and early adolescence, the prevalence of IS in childhood has been reported to be anywhere from 2% to 5.2%(14,15) with a female to male ratio of approx. 5:1(15). The first assessments, continuous monitoring of potential curve progression as well as intraoperative imaging in case of surgery result in repeated radiographic imaging of these patients, and subsequent high cumulative levels of absorbed radiation. In a cohort study by Ronckers et al(16) more than 4,000 patients diagnosed with scoliosis in childhood were exposed to numerous x-rays during the course of assessment and treatment and followed for more than 40 years. The standard mortality rate of dying from breast cancer for this group of patients was 1.68 (95% CI: 1.38–2.02) compared with the background population(16). In a more recent study looking at adverse health effects 26 years after exposure to follow-up x-rays for scoliosis, an increased risk of endometrial cancer was found(17).

Especially the risk for children and young adults is of concern, as these patients are thought to be more susceptible to ionizing radiation. This group of patients have a longer life expectancy and thus more time to develop adverse effects to radiation exposure(8). The latency after exposure to radiation before cancer develops often is

one or more decades(6,18,19). The gold standard for radiographic imaging is the upright coronal plane, posterior-anterior (PA) and the sagittal plane, lateral full-spine x-ray film(20,21). Previously coronal plane imaging was performed in the anteroposterior (AP) plane. However, x-ray dosimetry showed radiosensitive organs received a 20-50 percent higher dose in AP than in PA plane(22,23). The most radiosensitive organs such as the breasts, thyroid glands and gonads are all exposed during scoliosis radiographic examination. By PA positioning, the radiation to these organs are to some extent reduced. One study showed 8 times more radiation to the breasts and 4 times more to the thyroid glands when comparing AP with PA projections(24). CT scans comprise the majority(5) of all diagnostic imaging involving ionizing radiation. The radiation dose emitted from single x-rays is much lower, but still not negligible. Dose reports for full-spine radiography range from 0.5mSv-3.5mSv(25–27). Scoliosis patients, in particular, are subjected to numerous x-rays, thus, often receiving high levels of accumulated doses of ionizing radiation even when not counting CT. A typical course of monitoring and treatment for scoliosis includes coronal and lateral full-spine images every 3-6 months from the time of diagnosis until spinal maturity or until a curve in need of surgical treatment is reached. Previous studies(17,24,28,29) report that a typical scoliotic patient receives approx. 15-20 full-spine x-rays. With a range from less than 5 to more than 50 x-rays, and an average accumulated dose of 5.4-15mSv(13,24,30). Even though non-ionizing imaging methods such as MRI and ultrasound have evolved and make up a substantial amount of all diagnostic procedures, ionizing radiation still makes up the vast majority of diagnostic imaging procedures(31). For the monitoring of scoliosis and other spinal deformities there are few alternatives to radiographic imaging involving ionizing radiation.

Keeping exposure of ionizing radiation from medical imaging low

As of now there is no known lower threshold to the amount of radiation which might cause adverse health effects such as cancer. It is of great importance for clinicians to be aware of the potential detrimental effects from ionizing radiation and only use medical imaging when there is a just cause, as per the ALARA (As Low as Reasonable Achievable) principle(32). The benefit of exposure needs to exceed the risk of detriment(2).

Dose optimization

Much effort has been put into lowering the radiation dose to our patients as per the ALARA principle, still providing high quality imaging for optimal treatment and assessment. Ways of keeping dose at a minimum are numerous and often very logical. Optimization of radiation dose from medically induced exposures can be subdivided into a number of principles, such as: reducing the numbers of radiographic exposures, reducing the time of exposure, minimizing the field of exposure, using diagnostic reference levels (DRL) to optimize radiographic protocols, continuous education of users, modernizing x-ray equipment and developing new modalities. None of these

principles are able to stand completely alone, and most often a number of principles are combined, evaluated and improved.

Dosimetry

Dosimetry is the cornerstone of radiation dose evaluation and dose optimization. Modern dosimetry encompass a variety of methods spanning in vivo and in vitro measurements. Dosimetry can be made externally both as in vivo or in vitro measurements as well as ambient measurements and animal measures. Internal in vivo dosimetry is often very technically demanding and the most commonly used methods are either phantom based dosimetry, the mathematical method using the Monte Carlo PCXMC method(33) or a combination of different methods. State of the art information on absorbed radiation dose is achieved by anthropomorphic phantom dosimetry. This method uses internal x-ray dosimeters in a human like x-ray phantom imitating the human body. By summing measured tissue equivalent doses from different organs within the phantom a full-body absorbed dose can be estimated in terms of effective dose. A different way of estimating effective dose is by the use of the PCXMC mathematical phantom in combination with measured skin entrance doses. Both methods are approved by the ICRP(2), but it is our belief that phantom dosimetry imitates better in vivo measurements than PCXMC, thus one of the main aims of this thesis was to evaluate different x-ray modalities and settings in two humanlike anthropomorphic phantoms.

The EOS Low-dose slot-scanning system

The promises from the industry of new imaging systems with lower radiation dose and higher image quality are plenty. One such system is the EOS (EOS®-imaging, Paris, France) biplanar slot-scanning system. The EOS system is based on a new revolutionary gaseous particle detector with a multi-wire proportional chamber, invented by Professor George Charpak in 1992, and for which he received the Noble Prize in Physics(34). The multi-wire proportional chamber is ultrasensitive and as a result less x-rays are needed for detection, and the patients are subsequently exposed to less radiation. The EOS uses stereo-radiography which allows for simultaneous coronal plane and sagittal plane full-body images in weight bearing position. The EOS can be used for spine as well as pelvic and lower limb radiographic evaluations. At our spine department we use the EOS for full-spine imaging and full-body postural assessment. The system provides information on spine deformities in a classical 2D perception, but also offers a 3D reconstruction option which allows for viewing deformities in a 3D perspective as well. The 3D reconstruction option is semi-automated and has been clinically validated(35). Image quality had prior to this study been reported to be comparable to existing x-ray systems, some in favor of EOS (26,36), some in favor of conventional radiology (CR)(37).

Reduced dose with the EOS and gaps of knowledge

Reports on dose exposure with the EOS system prior to this study were already

numerous(26,36–41), reporting anywhere from 2 to more than 40 times reduced dose compared with conventional x-ray systems. The system comes with a standard low-dose setting and a newer micro-dose option the latter has been claimed by the manufacturer to emit less radiation than one week of natural background radiation of 63µSv (EOS-imaging, figure 3).

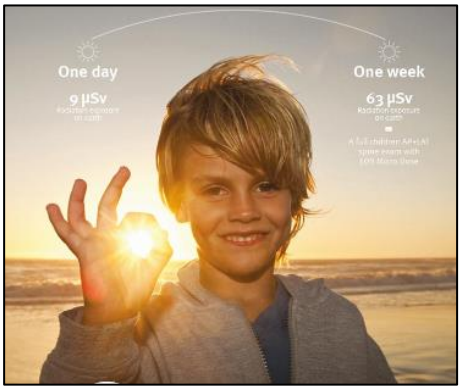

Figure 3, EOS-imaging product folder, claiming that one full-spine biplanar scan is less than one week of natural background exposure.

However, most reports were based on skin surface entrance dose differences, mathematical PCXMC phantoms and claims by manufacturer (26,34,36–38,41,42). Few studies had looked at organ doses and effective doses based on anthropomorphic phantom dosimetry(40,43). Damet et al (2014)(40) looked at organ dose and effective dose for EOS standard-dose protocol and compared with CR. They only used a fraction (54-58) out of more than 296 available dosimeter locations, theoretically compromising the validity of their results as mean organ dose values could vary significantly depending chosen dosimeter placements. No reports based on anthropomorphic phantom dosimetry had been made on the new EOS micro-dose protocol. The aim of Study I was to investigate the EOS micro-dose protocol with regards to organ dose and effective dose in order to verify claims by manufacturer as well as compare with organ dose and effective dose reports based on the PCXMC method. Furthermore, Standard-dose measurements and CR measurements were performed to compare with previous reports.

A further question was whether the micro-dose protocol could be even further reduced which was investigated in studies II and III. Could it be possible to reduce dose even further than this very low dose micro-dose protocol and still obtain images with sufficient quality to treat and diagnose patients correctly. If indeed possible, doses would be so low that barely any radiation risk would be associated with this imaging.

Total accumulated dose from all x-ray modalities

In order to estimate the magnitude of radiation dose exposure and the subsequent potential risk of detrimental effects, an overview of total accumulated dose from all x-ray modalities is needed. Cumulative doses based on routine CR and fluoroscopy on scoliotic patients undergoing routine assessment and treatment for scoliosis has been reported in a number of studies(13,16–19). Reports on the mean frequency and total number of full-spine radiographs range approx. from 10 to more than

20(16,17,19). However, no reports on total cumulative dose from CR, EOS intraoperative fluoroscopy/ or CT existed prior to this thesis. Study IV aimed at making an overall assessment of total cumulative dose from all modalities in a historic cohort of patients treated for scoliosis at our institution.

Time spend on dosimetry and validity of measurement certainty

The experiences of studies I and III illustrated the great time expenditure and questions towards validity and certainty of previously reported results(40,42) were raised. Based on these considerations a methodological study, Study V, was conducted in order to look at the possibility of estimating mean organ dose from a reduced number of dosimeters, thus reducing time on organ dosimetry. Another aim was to validate measurement certainties of studies I and III. There is as of now no gold standards within this field and the method was experimental.

Aims and Hypotheses

Aims Studies I-V

The aims of this PhD thesis was, as described in the summary of this thesis, to investigate the EOS biplanar low-dose scanner (EOS® -imaging, Paris, France), investigating radiation dose exposure and full-body radiation dose absorption from current standard dose protocol as well as the new micro-dose protocol (Study I). Studies II and III aimed at establishing and clinically validating new optimized EOS low-dose protocols. The aim of Study IV was to illustrate the total accumulated radiation dose, from all modalities, that a typical scoliosis patient receives during a full treatment or monitoring cycle at our institution. The fifth and final study aimed to evaluate different factors influencing organ dosimetry and to develop a method that could potentially reduce the time spent on precise phantom organ dosimetry, using TLDs.

Hypotheses

Study I

It was hypothesized that organ dose measurements and effective dose estimations from micro-dose exposure to anthropomorphic phantoms could be obtained by an improved version of a previously published method.

Study II

It was hypothesized that the radiation dose delivered to patients by the already low dose micro-dose protocol could be reduced even further without compromising reliability of 3D reconstructions of the spine.

Study III

It was hypothesized that the radiation dose delivered to patients by the already low dose micro-dose protocol could be reduced even further without compromising reliability of coronal plane 2D Cobb angle measurements.

Study IV

It was hypothesized that the magnitude of absorbed radiation dose varies greatly depending on radiographic follow-up protocols, and that variation of radiographic follow-up algorithms for idiopathic scoliosis exists among different spine centers.

Study V

It was hypothesized that a method for determining optimal placement of thermoluminescent dosimeters (TLDs) as well as optimal numbers of TLDs could be obtained, allowing for precise repeated and time efficient monitoring of organ doses within an anthropomorphic phantom.

Materials and Methods

Design

The five studies of this thesis spanned over a variety of designs all centered around ways to report and investigate radiation dose from full-spine imaging as well as exploring ways of influencing the amount of radiation dose used. The first study was a comparative and descriptive study with a focus on first dose report on a new EOS scan protocol as well as comparing new and repeated results with existing literature. The second and third studies were prospective clinical validation studies with technical notes, using image quality analysis to develop new scan protocols and subsequently validate these protocols in a clinical prospective manner. The fourth study was a retrospective cohort study describing total accumulated radiation dose to patients undergoing treatment for scoliosis at our institution and in conjunction with this an internet based survey for expert opinions/trends on scoliosis treatment and radiographic follow-up for comparison with own institution. The fifth, a methodological study, using advanced statistic modelling and phantom dosimetry to evaluate the position and minimum number of TLDs needed for accurate liver organ dose measurements within an anthropomorphic phantom, aiming at reducing time spent on organ and full-body dosimetry.

Ethical considerations

All studies involving patients and identifiable human data were conducted according to the Declaration of Helsinki 1975 (8^{th} revision2013)(44) on ethical principles for medical research involving human subjects.

Studies I and V did not involve patients or patient data and no ethical approval was needed.

Studies II and III were conducted at a pediatric center in Paris, France. Ethical approval was obtained from the Local Ethical Health Committee.

Study IV involved access to patient files, all data was handled according to Danish law, and an approval to conduct the study as well as storing of data was obtained by the North Denmark Region, project registration number (2019-76). Registration at the national data protection agency is no longer required. The North Denmark Region Committee on Health Research Ethics was informed of the study and confirmed that the project did not have to be submitted to the above committee.

Study populations

Study I

The "population" consisted of two humanlike CIRS-ATOM anthropomorphic dosimetry phantoms(45) (Computerized Reference System, Inc. Norfolk, VA, USA). A pediatric phantom resembling a five year-old child, type 705-D, and an adult female phantom representing an adolescent female, type 702-D.

Anthropomorphic means humanlike and both phantoms are architectured to resemble the human body with dosimetry options within 21 anatomically placed inner organs as well as the full skeleton. Each phantom consists of tissue equivalent epoxy resins with aged matched density for: average soft tissue, average bone, average lung, average brain and average breast tissues. The phantoms are divided into a number of 25mm thick axial sections, within each section are organ specific dosimetry locations/holes each with a vertical cylinder shaped tissue equivalent plug. Thermoluminescent (TLD) dosimeters (described later in the text) can be fitted within these cylinders for organ dosimetry. Owing to the tissue specific structures of the phantoms, the phantoms also have a high grade of image quality control properties. Figure 4 shows the pediatric and the female adult phantoms in the EOS scanner and the resulting biplane images.

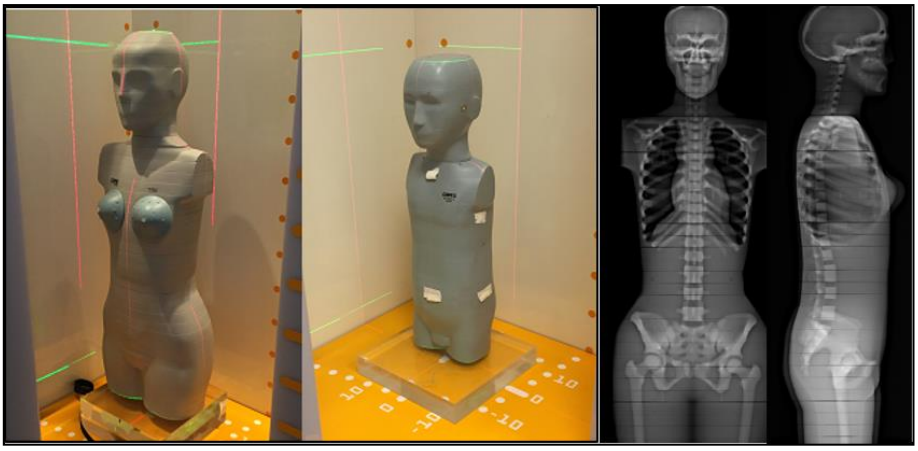

Figure 4, The pediatric phantom and the female adult phantom in the EOS scanner and subsequent two-plane imaging result(female adult).

Figure 5 shows a section of the same phantom and the numbered 5 mm locations for the placement of tissue equivalent cylinders and dosimeters as well as larger holes and plugs intended for image quality control of the lung and soft tissue of the abdomen.

Figure 5, the adult female phantom in the scanner and disassembled, illustrating examples of different phantom slices and placement of inner organs.

Studies II and III

Phantom: The pediatric phantom described in study I was used for semi-quantitative image analysis and dosimetry.

Pilot group: Four children, in the ages of 5-10 years of age, attending regular scheduled follow-up full-spine radiographic controls were offered micro-dose imaging and different reduced micro-dose imaging instead of regular EOS standard-dose imaging. Patients were informed about the study in both written and oral manner, and accepted to take part in the study. Parents of the children signed a written form of consent.

Validation group, Study II: A consecutive cohort of 18 children, 12 years of age or younger, all were scheduled for routine radiographic follow-up of their scoliosis at the outpatient clinic with EOS biplanar imaging. Written and oral information regarding the project was provided and a written form of consent was signed by parents.

Validation group, Study III: A consecutive cohort **(a cohort different from study II)** of 23 children, 12 years of age or younger, was included in the same manner as the study population of study II.

Figure 6, A 10 year-old child undergoing pilot images for study 3. To the left "Nano-dose" to the right micro-dose illustrating a 6-fold dose difference during full-spine radiography.

Study IV

All patients 18 years of age or younger within the North Denmark Region[1] in the years 2013-2016 who were undergoing assessment, treatment or routine follow-up for idiopathic scoliosis (IS). Patients were identified from International Classification of Diseases (ICD) coding within the North Denmark region hospital registries. All patients with neuromuscular disorders, mentally retarded or suffering from other severe conditions were excluded. Final inclusions were 61 patients. Hospital records, medical charts and the PACS (Picture archiving system) were scrutinized for data on radiographic imaging, length and type of treatment.

Study V

The female phantom described in study I.

Outcome parameters

The overall outcome parameter throughout the papers constituting this thesis is the quantification of radiation dose in terms of **effective dose**. Effective dose is a theoretical parameter developed by the International Commission on Radiation Protection (ICRP)(2) combining measured radiation doses in organs with specific tissue-weights based on empirical and theoretic data to define the full-body stochastic health risk, the risk of cancer induction by exposure to ionizing radiation.

Effective dose can be used to compare dose outputs from different x-ray modalities and is an important measure for dose optimization. By retrospectively collecting data

[1] (North Denmark Region, population size 2016; 585,000)

from previous medical imaging using ionizing radiation effective dose can be estimated, and an evaluation of prior and current magnitude of dose exposure and absorbed cumulative radiation dose can be evaluated and quantified. Figure 7 illustrates how effective dose is calculated.

Figure 7

Calculating Effective Dose

Effective dose (E), $\boldsymbol{E = \sum w_T H_T}$

The sum all organ equivalent doses (H_T), multiplied by specific organ tissue weights(w_T)

Primary outcome measures

Study I, primary outcome measures were quantification of radiation dose based on phantom dosimetry and subsequent evaluation of organ doses and derived effective doses.

Studies II and III, one outcome measure was quantification and optimization of radiation during development of reduced-dose radiation protocols with regards to effective dose.

Study II, a second outcome measure was intra- and inter observer reliability in terms of variation from the mean in order to quantify uncertainty of 3D reconstruction of the spine in relation to current international standards.

Study III, a second outcome measure was intra- and inter observer reliability in terms of variation from the mean in order to quantify uncertainty of Cobb Angle measurements in relation to current international standards.

Study IV. One outcome measure was the quantification of absorbed dose magnitude in terms of effective dose based on retrospectively collected data on x-ray history in a retrospective cohort of scoliosis patients. A second outcome measure was the objective proportional relationship between spine centers in trends of radiographic assessment of scoliotic patients.

Study V. One outcome measure in study V was in terms of possibility of reaching correct mean organ dose from dose measurements and statistical modelling, with a reduced number of TLDs. This was shown by regression coefficients and graphical illustrations as well as logical testing. There is as of now no gold standards within this field and the method is experimental.

A second outcome measure was the illustration of decreased sensibility of TLD dosimeters used for organ dose dosimetry in terms of decreasing magnitude of counts absorbed in the dosimeters over time.

Organ Dosimetry

Phantoms

Anthropomorphic phantom organ dosimetry is the measurement of absorbed radiation dose within human-like phantoms. The phantoms described above, were used for organ dosimetry and calculations of mean organ doses as well as effective doses.

The female adolescent phantom holds 294 internal dosimeter positions including 40 located within the breasts. All dosimeter positions were used in study I. For study V only the 28 liver specific positions were used.

The pediatric phantom holds 180 internal dosimeter positions. All dosimeter positions were used for the full-body absorbed dose evaluations of studies I and III.

On the surface of both phantoms, symmetrically placed TLDs allowed for measurement of skin entrance and skin exit doses. The physical dimensions of the phantoms are summarized in Table 2.

Table 2, Physical dimensions of anthropomorphic phantoms used in the thesis

Description	Height	Weight	Thorax dimensions
Adolescent female	160 cm	55 kg	20 cm x 25 cm
Pediatric 5 year-old	110 cm	19 kg	14 cm x 17 cm

Dosimeters

For the use of dose measurements, thermoluminescent (TLD) dosimeters of the MCP-N type was used (MCP-N, Krakow, Poland). The MCP-N TLD is a solid lithium-fluoride dosimeter covered with magnesium, copper and phosphorus, also commonly referred to as a LiF-Mg,Cu,P dosimeter. The MCP-N is highly sensitive dosimeter and is well suited to use for low-dose imaging owing to a very low detection threshold(46,47). The basic function of the dosimeters is to absorb radiation dose by trapping electrons. The absorbed electrons are released when the TLD is heated in a

TLD-reader and translated into radiation dose in terms of mSv. The Rados RE-2000 reader (RadPro International GmbH, Wermelskirchen, Germany) was used in the studies involving dosimetry. Before each exposure of TLDs they need to be reset and calibrated. Resetting TLDs to "zero-value" (the emptying of TLDs) is done by annealing (heating in an oven to release all captured electrons). The reset TLDs are then read in the TLD reader for zero-values. The mean zero value is calculated and recorded. All TLDs are subsequently exposed to a known radioactive source, in this case a strontium-90 source placed within an irradiator. The irradiator, IR-2000 (RadPro International GmbH, Wermelskirchen, Germany) was used. After irradiation by the known radiation source the TLDs need to be read (measured) again in the TLD reader. Calibration reference is measured and a mean calibration value is calculated from all TLDs read. Now, the TLDs are ready for installment in the phantom. Once exposed to an x-ray source the EOS, CR or another modality, the procedure is done reversely. All TLDs are removed from the phantom, installed in cassettes and cassette-magazines. Mean zero values of the TLDs, mean reference dose calibration values are typed into the TLD reader software and the TLDs can now be read by the TLD reader and absorbed doses read out. The process of preparing TLDs for exposure, installing into phantom, scanning phantom, removing TLDs in correct order by installing them into numbered cassettes and reading out doses takes in excess of 24 hours of continuous work, for one phantom exposed in one position. This is not counting the time of transport between hospital and x-ray lab, and not counting the time of subsequent calculations of mean organ doses and calculations into effective dose. The work needs to be done in partial darkness as the TLDs are light sensitive collect false "radiation" if exposed to light. Figure 8 shows the dosimetry lab setup.

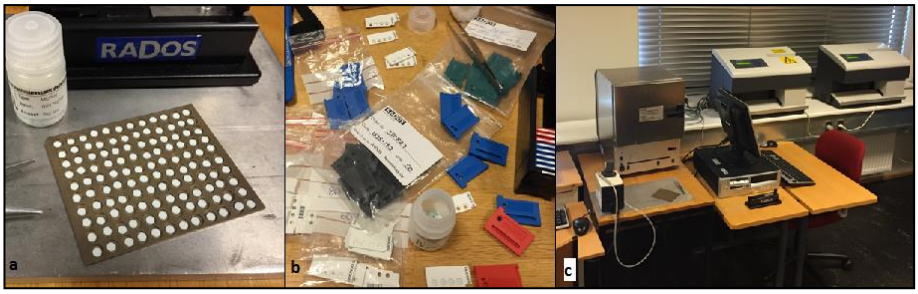

Figure 8, (a) TLDs, (b) cassettes and magazine, (c) from left; annealing oven (TLDO. PTW, Freiburg Germany), irradiator (IR-2000) and reader (Re-2000)

Imaging systems

EOS

The EOS® (EOS-imaging, Paris, France) biplanar slotscanning system was used for dose exposures in studies I-III and V and used as reference for dose calculations in study IV. The EOS scanner is a low-dose slot-scanning system that has been developed in order to acquire high quality imaging at very low doses(34,38).

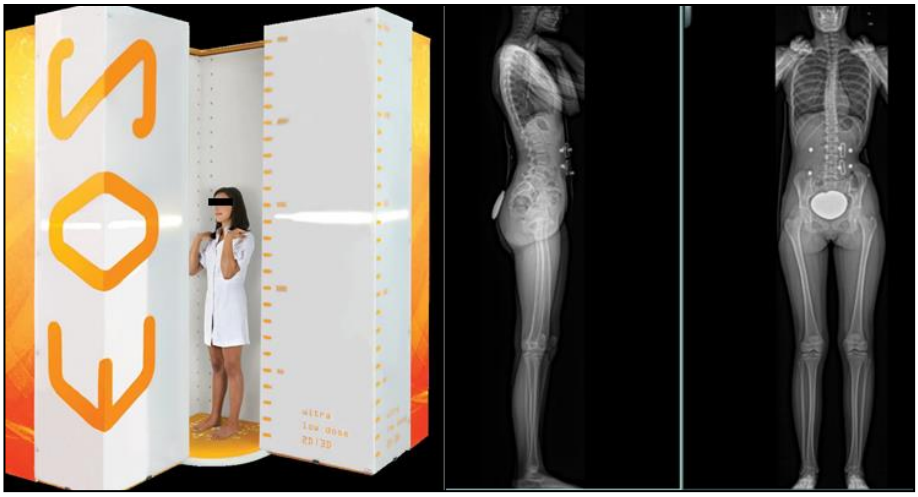

Figure 9. Left, patient in EOS scanner (Reproduction of figure(left) with permission of EOS-imaging). Right, the resulting two-plane image after a full-body scan with standard-dose settings.

The EOS scanner uses two orthogonal x-ray beams scanning the patient vertically in a time span of 8-20 seconds, while yielding simultaneously a coronal and lateral image. The images are made in weight bearing position and the patient is placed in the scanner as shown in figure 9 in either anteroposterior-lateral (APL) or posterior-anterior-lateral (PAL) positioning. Figure 10, illustrates the direction of the field of scan in relation to the EOS and the patient.

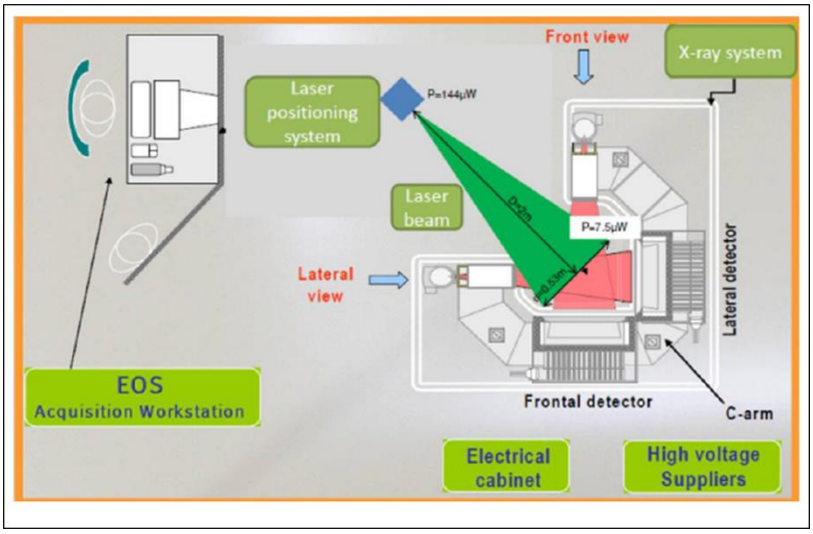

Figure 10, Direction of scan fields of the EOS biplanar scanner (reproduction of figure with the permission of EOS-imaging)

The EOS scanner can be used for full-spine radiography to assess postural balance. Some other uses are evaluation of pelvic parameters and evaluation limb length discrepancies. The EOS scanner comes with a 3D option for semi-automated reconstruction of the spine.

Conventional digital radiology (CR)
A conventional digital radiology system (Siemens Ysio Max, Malvern, PA, USA) was used for in-house exposure of phantoms for comparisons of absorbed doses in study I.

Exposure of phantoms for dose measurements

Study I

full-spine imaging was performed in PAL and APL for both phantoms in both the EOS scanner and with the CR system.

EOS

The phantoms were scanned 20 times before measurements of dose and normalization into one scan by dividing by the number of scans a method described by Damet et al (2014)(40) in order to achieve sufficient dose for measurements.

CR

The phantoms were subjected to standard default scoliosis protocols for a child and an adolescent. Imaging was performed as a pair of scan-cycles, first five scans in AP or PA and then five scans from lateral right side of the phantom, the less radiosensitive side(22,23). Figure 11 shows the pediatric phantom in the Siemens conventional x-ray modality (Siemens Ysio Max).

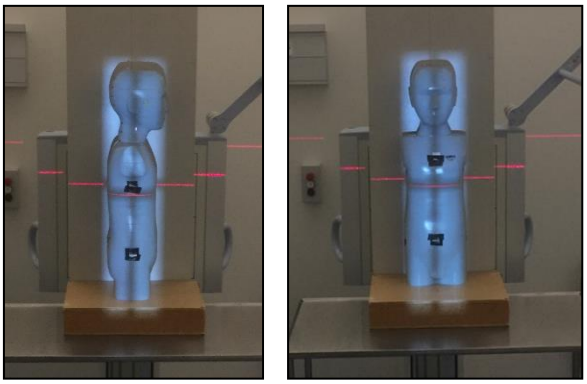

Figure 11. The 5 year-old pediatric phantom undergoing CR with the Siemens Ysio Max System. Left in lateral positioning. Right in AP positioning.

Study III

Five consecutive EOS nano-dose scans were performed in APL and normalized into one scan in order to compare with theoretical dose reduction.

Study V

The female phantom was exposed in three different positions: APL and at an axial rotation of 10 degrees either clockwise or counterclockwise in relation to APL positioning. Five consecutive EOS standard-dose scans were performed, at seven different occasions, for each of the three positions. Each occasion of five scans was normalized into one scan similarly to study III.

Calculation of organ dose

Calculation of mean organ doses was done by adding all individual TLD measures from within one organ after subtraction of mean ambient background dose and dividing by the number of scans: : $\widehat{D}_{organ} = \frac{1}{n.o.}\sum_{i=1}^{n.o.}\frac{d_i - \bar{d}_a}{n}$

Where mean ambient $\bar{d}_a$ was calculated as the mean of four non-exposed TLDs that were calibrated and read out along with the number (n.o.) of TLDs used for organ dose measurements.

Establishing reduced dose protocols in studies II and III

In order to establish new reduced dose protocols in studies II and III, semi quantitative image analysis was based on a number of phantom images conducted at a consecutive number of images with decreased dose settings. The EOS settings of current (mA) and speed of scan was changed either by decreasing the current or increasing scan speed, or both of the latter two. The current and speed settings are both directly proportional to the magnitude of radiation dose. When decreasing current by 50% the resulting radiation dose is 50% lower and by increasing speed by 50% radiation dose decreases by 50%.

Considerations taken when the reduced-dose protocols were defined: Objective measures were used to determine the minimum dose that yielded acceptable image quality. The definition was inherently subjective, since only one observer was implicated, but efforts were taken to make it as objectively as possible.

Semi-quantitative images analysis: The actual semi-quantitative image analysis consisted of a scale from 1-5, the main investigator performed a series of blinded grading of sections of each phantom in different exposure settings (APL, PAL or axial rotation imitating scoliosis), shown in random order. 1= very good, 2=good, 3 acceptable, 4= poor, 5=very poor. The images were graded against visibility of different anatomical landmarks and the possibility of making out vertebral endplates, depending on whether it being for the 3D reconstruction or the 2D Cobb angle use. The grading was not one of the main results of the study, just a necessary intermediate step. The four best settings according to the semi-quantitative analysis were used in vivo for pilot imaging on a group of four children. Figure 12 shows examples of images used for grading. The preliminary in vivo pilot measurements confirmed the readability of the x-rays before clinical application to the prospective cohort.

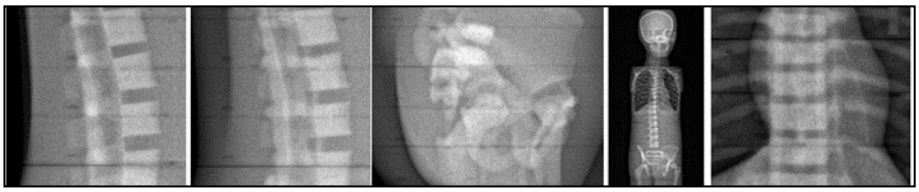

Figure 12. Examples of images used for grading (images have been resized to fit this page)

3D Reconstruction

3D reconstruction with the EOS system is a validated semi-automated feature(35) that comes with the EOS system and allows for reconstruction of the spine as well as generation of a report where important spine parameters are presented. The reconstruction is performed by trained/ certified operators, recognizing and adjusting a semi-automated "frame" for each vertebra of the spine. Figure 13 shows 3D reconstruction of a spine and the result. Two 3D reconstructions were done for each patient by each of the three operators over a three week time span.

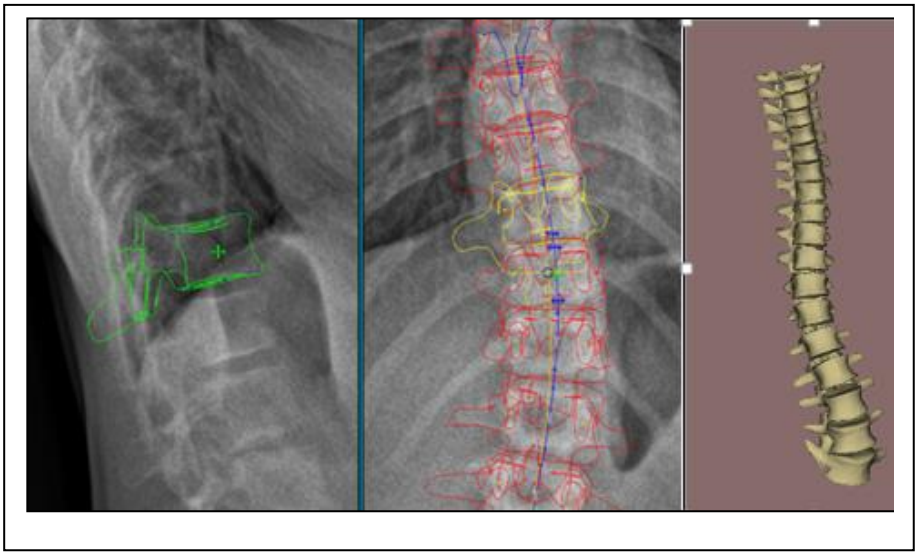

Figure 13. Reconstruction of the spine, using semi-automated technique.

2D Cobb angle measurements

Nano-dose protocol the protocol with the lowest dose of the latter was chosen for 2D Cobb angle measurements. The Cobb angle(48) is a widely accepted measure for 2D curve magnitude in scoliosis. The angle is measured between the upper endplate and the lower endplate of two vertebrae at the extremes of a scoliotic curve. Measurements, one at a time were done in random order, three times for each patient by each of five operators over a two week period of time.

Study IV, Conducting an evaluation of cumulative radiation dose

A retrospective cohort study was conducted. Patients were included as described in study population. Patient medical journals as well as PACS were scrutinized for information on magnitude and type of x-rays to which patients were exposed. Radiation dose in means of effective dose was calculated for all patients. For EOS and CR, reference values from study I was used. For the intraoperative CT scanner, the O-arm, the radiation dose for 3D scans was calculated based on Dose Length Product (DLP) multiplied by conversion-factors. For the 2D fluoroscopy option of the O-arm, Dose Area Product (DAP) was used in conjunction with conversion factors to calculate effective dose.

Both the radiation calculation for 3D and 2D were in accordance with The Danish National Board of Health, Institute of Radiation Protection(49).

A survey study on trends in scoliotic management

A questionnaire was sent out to nine international orthopedic spine centers. Each center with a background population of more than one million people. Questions were asked on treatment of idiopathic scoliosis and radiographic follow-up. Results were gathered and proportional relations were evaluated.

Statistics

Study I

To model statistical data negative binomial regression was used. In order to bypass the need of multiple phantom dosimetry, Bootstrap statistics(50) was used to gain valid 95% confidence intervals, by using random sampling and theoretical calculations of organ dose values to assign uncertainties.

Study II and III

For the comparison of variability from the mean, 95% confidence intervals were calculated as two times the standard deviation from the mean according to the ISO-

5725 standard. Correlations between study II and previously published data(26,35) were analyzed with Spearman's rank coefficient at a significance level set at 0.05.

Study IV

Only basic descriptive analysis was used, illustrating mean and median values.

Study V

Analyses of the relationship between rotation of phantom, dose absorption and TLD placement was performed along with 95% confidence intervals. Among other methods, generalized mixed effect linear modelling(51,52) was used as described in study V. Simple mean values and confidence intervals were used for description of the TLD sensitivity evaluation.

Results

Study I

First reports on organ doses and effective dose from the EOS micro-dose protocol was reported. Full-spine phantom imaging was performed in a pediatric and an adolescent phantom with EOS micro-dose and EOS standard-dose protocols and CR is illustrated in figure 14.

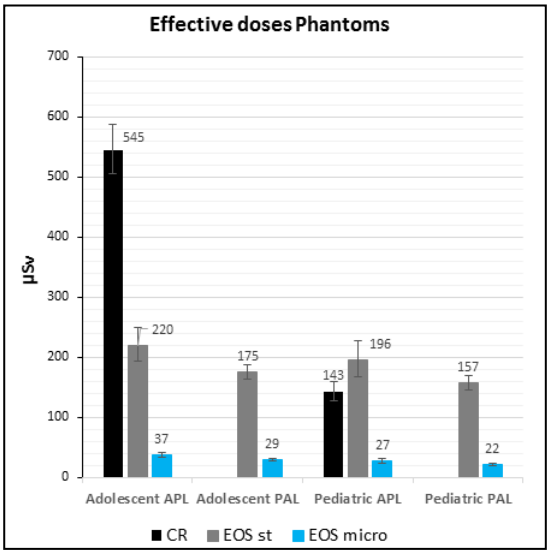

Figure 14 (study I(81)*)*

It was confirmed that one micro-dose full-spine scan, as claimed by EOS®-imaging, was less than one week of normal back-ground radiation from nature. The effective dose from one micro-dose scan ranged from 22-27 µSv depending on positioning and age, one week of mean worldwide natural background dose approx. 46 µSv(6).

The dose reduction for micro-dose versus standard-dose protocol was approx. 6-fold The dose reduction for micro-dose versus CR was 5-fold for the pediatric phantom and 17-fold for the adolescent phantom. There was an increase of effective dose of 38% when using the EOS standard-dose compared with in-house pediatric CR protocol. Most organ doses were lower in EOS PAL positioning, by approx. 21%, and

a 29% reduction of mean breast dose. Mean dose to the left breast was reduced 5.5-fold from 403 µSv to 73 µSv, mean organ dose to the right breast was increased by 33%. A few organs received a higher dose in PA. For instance, liver dose was increased by 22% (258 µSv versus 211 µSv) for the adolescent phantom and liver dose was increased by 76% (230 µSv versus 131 µSv)for the pediatric phantom.

Studies II and III

Based on semi-quantitative image analyses of phantom images and subsequent in vivo pilot imaging, two dose-optimized protocols were established and clinically validated. Table 3 shows the comparison of doses between exposures of protocols.

Table 3, Doses for default EOS scan protocols and the two optimized protocols of studies II and III

Protocol	Nano-dose	Reduced Micro-dose	Micro-dose	Standard-dose
DAP* mGy.cm^2	16	41	97	593

*Dose Area Product for the pediatric phantom

Study II

The reduced micro-dose protocol established for 3D reconstruction, yielded less than half that of already validated micro-dose protocol, and more than 10-fold less than the standard-dose protocol. 15 children with a mean age of 11 years(8-12) were included. A total of 180 3D reconstructions were performed by the three operators. Intra- and inter observer reliability was comparable and in many ways as good as already validated micro-dose for 3D reconstruction. In table 4 some of the results of the 3D

3D Parameter Results

	T1-T12 kyphosis	L1-S1 Lordosis	Cobb angle	Pelvic Incidence	Sacral Slope	PelvicTilt
Micro	6.6	5.1	3.8	3.7	3.7	2.7
Nano	6.6	5.8	5.4	5.4	4.6	3.6
Ilharreborde et al 2016 Micro	7.1	7.9	5.4	7.8	7.0	1.9
Humbert et al 2009 Standard	5.5	4.1	3.8	3.4	3.0	1.4

Table 4, Inter-operator reproducibility, variations from the mean (Presented at ICEOS 2017, San Diego CA)

reconstructions have been listed and compared with previous studies. The average duration of one 3D reconstruction was approx. 9 minutes (range 6-21).

Study III

A cohort of 23 consecutive children was included and underwent full-spine biplanar imaging with micro-dose and nano-dose protocols. Mean age was 11 years (9-12). Dose reduction of the nano-dose protocol was as illustrated in table 4, 37-fold reduced compared with standard dose and 6-fold reduced compared with micro-dose protocol. A total of 630 Cobb angle measurements were performed over a time span of two weeks. Reproducibility for both protocols was good. The Bland Altman plot illustrated a variation from the mean within internationally accepted standards of ≤5 degrees of deviation from the mean, figures 15 and 16. Results for the nano-dose protocol were not significantly inferior to the micro-dose protocol.

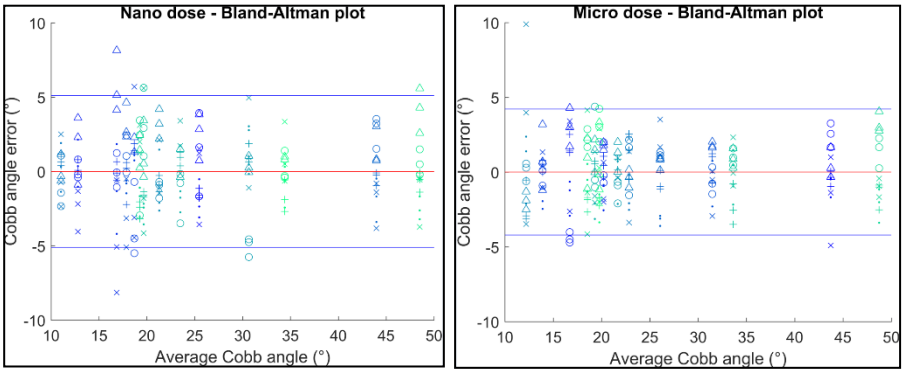

Figures 15 and 16. Interobserver reproducability of Cobb angle measurements for Nano-dose and Micro-dose protocols.(study III)

Study IV

An overview of total accumulated full-body absorbed radiation dose for the scoliosis patients who were at some point of their treatment and radiographic follow-up at Aalborg University hospital in the years 2013-2016. The impact and differences of different radiographic systems are shown in table 5.

The patients who received one or two ancillary CT scans (eg. Control, PET-CT, etc) had their cumulative absorbed radiation from all causes doubled. Intraoperative accumulated radiation dose could be as low as a total of 1.393mSv, for 2 low-dose O-arm, intraoperative scans of 70kV/20mA (each scan 0.461mSv) and 26 seconds of 2D O-arm fluoroscopy (0.427mSv). The highest accumulated intraoperative dose for one patient was 12.297mSv. The result of three high dose

default intraoperative scans of 120kV/40mA (each scan 3.319mSv) and 58 seconds of 2D fluoroscopy (2.338mSv).

Table 5, Radiation exposure (Study IV)

	Conservative group[1] (Median and range)	Surgery group (Median and range)
Conventional spine X-rays (CR) number[2] / radiation dose	4 (0-20)/1.1mSv(0-5.5)	14.5 (2-57)/4.1mSv(0.6-15.5)
Biplanar EOS imaging Number[2] / radiation dose	2 (0-17)/ 0.58mSv(0-2.4)	10.5 (0-26)/ 1.3mSv(0-3.1)
O-arm 3d scans Number/ dose		2(1-4)/ 3.8mSv(0.9-10.0)
O-arm 2D fluoroscopy time in seconds/ dose		33.7(20.3-136.0)/ 0.9mSv(0.4-3.5)
Radiation dose combined (CR, EOS, O-arm)	1.1mSv(0.2-7.2)	10.3mSv(3.8-20.4)
Additional CT and PET-CT[3]	0	1(1-2)
Radiation dose	0	11.9mSv(0.6-20.1)
Total radiation dose all modalities	1.1mSv(0.2-7.2)	10.8mSv(3.8-35.9)

[1]Braced and observational
[2]Total number of coronal and lateral images
[3]A total of 6 patients had additional imaging owing to various reasons explained in the results section.

The lowest radiation dose exposure observed for a posterior spinal fusion (PSF) of 10 levels comprising 2 low-dose scans of each 0.461mSv, and 26 seconds of intraoperative fluoroscopy, was 1.393mSv. The highest intraoperative exposure during one PSF of 11 levels was almost 10- fold higher comprising 3 high-dose scans of each 3.319mSv and a total of 58 seconds of fluoroscopy. The patient receiving the highest dose of Intraoperative fluoroscopy from one intraoperative procedure received (2.425mSv) from 88 seconds. The Scan dose for this patient was 4.600mSv from 1 high-dose scan and one low-dose scan.

Study V

At 21 different occasions, a total of 105 EOS standard-dose scans in PA, were performed on a female anthropomorphic phantom in order to evaluate absorbed liver mean organ dose. No statistical significant differences of mean organ doses were observed as illustrated in Figure 17.

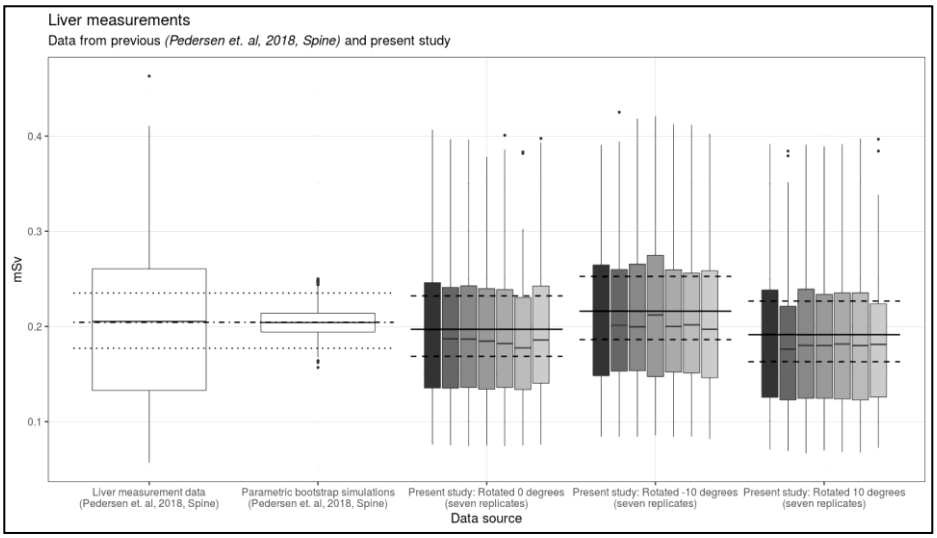

Figure 17(study V). Distribution of absorbed liver organ dose for three different axial rotational as well as liver doses previously measured and published by same authors(81)*(Study I).*

Table 3. The number of TLDs in a subset in relation to possible combinations and acceptable combinations yielding a "true" mean dose.

No. TLDs	Combinations	Acceptable combinations	1/Ratio[a]
1	28	2	0.071
2	378	25	0.066
3	3276	314	0.096
4	20475	2240	0.109
5	98280	11486	0.117
6	376740	46218	0.123
7	1184040	151884	0.128
8	3108105	413259	0.133

[a]The probability of an acceptable combination

Table 6(study V)

Table 6 illustrates the inverse relationship between rising numbers of TLDs in susbsets smaller than the total of 28 possible TLD locations (used to calculate the "true" mean organ dose) and the probability of reaching an acceptable combination by chance only.

For the for subsets of 5-6 TLDs picked by logical symmetrical selection mean organ dose values were within 95% CI of “true” organ dose in 23 out of 24 cases.

TLD tablet sensitivity decreased by almost 11% over the 21 radiation cycles of each five scans. Figure 18 shows the decline in sensitivity over time for measured reference doses prior to phantom imaging.

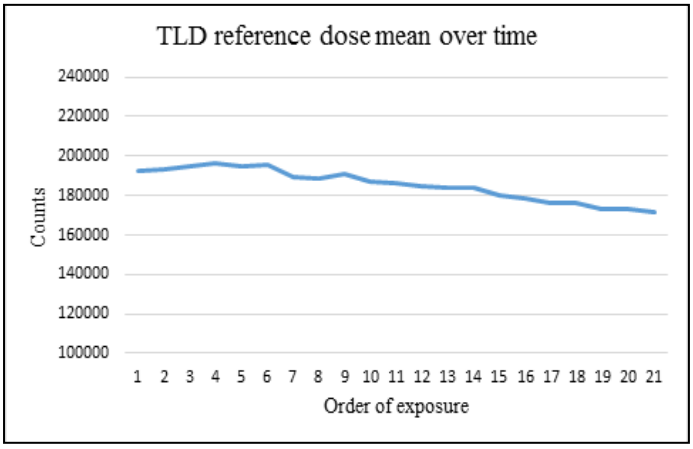

Figure 18 (Study V)

No decrease in measured mean liver organ dose within each group of the three axial positions comprising 7 out of 21 organ dose measurements was observed (all TLDs were calibrated against reference doses chronologically and measured prior to installment and dose exposure in the phantom)

Discussion

The aim of this thesis was to provide novel information on the EOS scanner, reproduce and further develop previously reported methods and compare our results (study I) with published data. An investigation into establishing even more reduced-dose protocols with the EOS and the clinical validation of these was undertaken (Studies II and III). A total overview of accumulated dose to IS patients treated at our institution and a comparison with a number of international spine centers and current consensus guidelines for radiographic follow-up was performed (study IV). An investigation of how to optimize time spent on reliable phantom dosimetry was performed (study V). The combination of the above studies founded the basis for an evaluation and quantification of absorbed radiation dose and associated risk to the human body in relation to spinal imaging using ionizing radiation and ways to influence this by means of dose optimization.

Dose optimization

As described throughout this thesis, there are many ways to reduce radiation dose to patients. The most simple way is to eliminate exposure or reduce the number of x-rays. In order to do so it is necessary to know what is the exact need of a particular investigation, is it indeed needed, and secondly how often is it needed. This of course depends on the natural course of a given disease and differs from one disorder to another, and from one patient to another. In studies I-IV different reduced dose protocols were evaluated.

Study I
Main findings

The main findings of study I included a first phantom based organ dose and effective dose evaluation of the commercially available and clinically validated micro-dose protocol(26,41). An approx. 6-fold reduction of dose compared with the EOS standard-dose protocol was documented, and manufacturer claims of radiation dose exposure of less than one week of natural background-dose from one full-spine biplanar scan were verified. Results on micro-dose exposure were in line with other reports based on skin entrance dose and mathematical phantoms(26,53,54). However, the results of an award winning paper of Hui et al(39) were not in line with these results. We redid their calculations and recognized a methodological error resulting in a supplementary addendum to their paper(55).

Results of organ doses and effective doses using standard-dose protocol were comparable with previous reports based on phantom dosimetry and computerized models(24,40,42,43).

When comparing EOS standard-dose with CR for the adolescent phantom an expected dose reduction of more than 50% was observed. Unexpectedly, we found a 38% increase of total absorbed dose for the 5 year-old phantom. The reason for this was speculated to be a combination of optimized CR equipment in combination with a low-dose scoliosis protocol for the CR system. Renewed CR exposures and measurements of effective dose for the pediatric phantom yielded same results. One study of effective dose from CR for full-spine imaging reported similar results for 5 to 7 –year old children(27).

Both for the adolescent phantom and the pediatric phantom effective doses from CR were lower than diagnostic reference levels (DRLs) generally listed as 1-3.5 mSv(26,56–58). However, other authors(13,24,40) found very similar results for full-spine imaging of adults. When reporting on dose differences between different modalities it is crucial to be sure to state exactly what is being reported. The 45-fold reduction of dose from micro-dose vs CR as reported by Ilharreborde et al(2016)(26) is true when comparing with reference levels of 3.5 mSv for AP and Lateral x-ray, but very different from the 0.40-0.55 mSv as measured in study I and other more recent studies(13,24,40,58). As long as there is no universal DRL, the different proportional relation from each paper must always be taken into consideration.

Strengths and Limitations

The method for measuring full-body absorbed dose in the phantoms was similar to the method used by Damet et al (2014)(40), however, in order to strengthen the validity of measurements we used all available dosimeter locations for dose assessment. Damet et al used less than 25% of available locations. The method was limited in study I by the low number of measurements done for each phantom position, thus, bootstrap statistics(50) was used to strengthen the validity of uncertainty intervals, expressed as 95% CI. Repeated measurements of mean liver organ dose were performed in study V, and dose values were found to be almost identical; 204μSv (95% CI: 173-238) vs 197μSv (95% CI: 169-232) in study V. The observations supported our assumptions of estimating correct uncertainty values when advanced bootstrapping was used.

Conclusion and clinical context

As a conclusion study I corroborated the fact that micro-dose protocol is currently the commercially available full-spine x-ray protocol exposing patients to the least amount of radiation. This is well in line with the current efforts to develop safe and precise diagnostic modalities to our patients. Patients and clinicians can be reassured that undergoing micro-dose full-spine radiographic assessment poses no proven risk and is no different from a few days of natural background radiation.

Studies II and III

Even with the EOS micro-dose being the most low dose option for full-spine radiography, still no lower level for which radiation dose could be harmful to the body has been defined. The micro-dose protocol had previously been clinically validated for both standard 2D images and for 3D reconstruction(26,35,53,54,59,60), and the question was raised whether it would be possible to reduce dose even further and still produce reliable Cobb angle measurements as well as 3D reconstruction. Two reduced micro-dose protocols were established and prospectively clinically validated.

Study II resulted in a clinically validated protocol for 3D reconstruction of the spine, with a dose reduction of 58% compared with micro-dose protocol.

Study III resulted in a clinically validated "nano-dose" protocol for 2D Cobb angle measurements, exposing patients to $1/6^{th}$ (a dose reduction of 83%) the dose of the micro-dose protocol. A dose less than one day of natural background radiation(6). The variability of interobserver and intraobserver of Cobb angle measurements were within previously published standards(61,62).

Strengths and Limitations

Both the reduced micro-dose (study II) as well as the micro-dose protocol were found to be inferior to standard dose for both 2D and 3D parameters as illustrated in study II. However, results for the new protocol showed that it was comparable to micro-dose 3D reconstruction and better than micro-dose "fast 3D"(26) reconstruction and thus could replace the micro-dose protocol for standard monitoring and 3D reconstruction of patients with mild to moderate scoliosis. Standard dose would still be the choice for most precise reconstruction and for evaluation of 3D parameters preceding surgery.

The nano-dose protocol was not significantly inferior to the micro-dose protocol for coronal plane Cobb angle measurements, with minimal variability from the mean as illustrated in the results. Similarly to the reduced micro-dose protocol of study II, the nano-dose protocol was clinically validated in a prospective manner. Five observers instead of usually two or three observers provided additional strength to the interobserver analysis.

For both studies obese patients and patients with implants were excluded, and thus neither protocol was validated for these patients. The general population is getting increasingly obese, and reduced radiation doses and obesity often do not correlate well, which was observed during the validation process of study III. The relatively small number of patients in both studies (study II (15) and study III (21)) might lead to falsely reduced variability towards the mean. Seven out of 21 children in study III had a mean Cobb angle below 10 degrees, these were analyzed separately as it would

be expected that inter- and intraobserver variability of these patients would be lower than for actual scoliotic curves.

There seems to be no reason why not to apply these protocols in cases where micro-dose generally applies, for 3D reconstruction of the spine or coronal plane Cobb angle assessment. Patients and just as important parents of children to be examined can rest assured that the potential harm from these protocols is close to zero.

Conclusions and Clinical Context

Reducing the amount of radiation dose is possible as shown in studies II and III. Results of both reduced micro-dose protocols were comparable to previously published standards for conventional radiology as well as micro-dose protocol, readily applicable to existing systems and ready for use in non-obese patients.

Study IV

An overview of the magnitude of cumulative dose from ionizing radiation in patients treated for IS at our institution was performed. As expected patients who underwent surgery received much higher cumulative doses than those treated conservatively. This study was the first study to report total cumulative doses from all modalities including: CR, EOS, intraoperative CT and fluoroscopy as well as ancillary CT scans. The magnitude of x-ray examinations was comparable to literature(13,16,17,28,29,63). Dose evaluations confirmed the theoretical reduction of doses when using EOS for monitoring, as well as reduced dose protocols for intraoperative CT scans for navigation. Just one ancillary CT scan was found to increase total absorbed radiation dose two-fold, reminding us of the importance of the right indication and the impact of such examinations.

Results of a survey forwarded to 9 international high-volume spine centers showed trends of treatment and radiographic follow-up. There was no strict adherence to published international guidelines(20,64,65). Reasons for not adhering to consensus guidelines are various, and could be the result of clinical setup, habits, ignorance or possibly a lack of confidence in the correctness of outlined standards. For patients with scoliotic disorders the effort of Establishing and updating international guidelines for the use of radiographic follow up for patients with scoliosis is an ongoing process. By Introducing international standards for radiographic follow-up, the risk of every center making up their own clinical practice and potentially exposing patients to unnecessary imaging is restricted. However, one has to remember that

consensus reports are based on expert opinions and not always hard evidence and need to be continuously updated along with the development of equipment and procedures.

Strengths and Limitations

The quantification of exposure was reported as both absorbed dose, and numbers and types radiographic procedures for CR, EOS, O-arm CT and ancillary CT. This allows for future research on the same topic to be compared with our results, even in the case of change of conversion factors, tissue weighting factors or the case of different DRLs, etc. The limited size of the historic cohort of patients studied did not allow for statistical analysis of possible correlations.

Conclusion and Clinical Context

When adhering to clinically validated low-dose protocols and consensus guidelines for radiographic monitoring and perioperative imaging, radiation dose can be kept low. In fact the total cumulative dose from repeated full-spine follow-up EOS imaging using standard dose for semiannual imaging for 10 years and 2 low-dose intraoperative CT scans, as defined by Petersen et al (2012)(66) will amount to approx. 3-4 mSv, not much different from one year of natural background radiation.

Study V

Results of study V showed that mean liver doses and uncertainties in AP positioning corresponded very well with the results of study I (figures 1.X and 5.1), and thus supported the assumptions made on uncertainties using bootstrap statistics previously in study I.

The results of study V showed that handling time of liver organ dose measurements can be reduced by at least 75%, compared with full organ dosimetry, without compromising certainty of results. Damet et al (2014-2018)(40,67,68) used only a fraction (<25%) of available dosimeters in their studies of the EOS and O-arm investigating organ doses and effective doses based on anthropomorphic phantom dosimetry. For instance, for liver organ dose measurements only 2 to 5 out of 28 possible locations were used. The authors did not state how this number of dosimeters was chosen, or which considerations were made before choosing specific locations for dosimeters. However, the probability that their measurements were significantly different from the "true mean" of all 28 dosimeters is likely, according to study V.

To our knowledge, study V is the only study to have conducted repeated measurements with the same TLDs in the same locations for anthropomorphic phantom dosimetry over time. During the course of repeated radiation cycles from 1 to 21, the mean sensitivity of the dosimeters dropped by almost 11%, corresponding

with findings of Poirier et al(69). This did not affect the reliability of measurements significantly, but showed the importance of continuous calibration of TLDs before dose measurements, and the importance of not to mix batches of TLDs. The exact reason for this drop of sensitivity is not known, but several causes have been discussed previously(69–71), and has been listed in study V.

Strength, limitations and considerations of design

The path to reaching the correct statistical analysis and methods for study V was challenging and time consuming. We did test if empirically chosen subsets could reach correct mean dose. Dose means from subsets of TLDs placed logically in relation to the particular x-ray source were compared with total dose mean and reached an acceptable result, as was in fact shown by "empirical selection" of subsets in study V. However, this method would not have had the same statistical strength unless for instance a large number of independently chosen subsets were applied by preferably more than one observer as an interobserver study.

The results on reduced handling time and possibility of applying less TLDs when performing dosimetry applies to a particular ATOM dosimetry phantom used in a particular EOS scanner, and the direction of incoming x-rays specific to the EOS scanner. However, the statistical model using the same phantom or other phantoms can be applied to other x-ray modalities.

Future work and clinical implications

The method used in study V provides a tool at hand for future investigators in the field of organ dosimetry, and the option to apply this approach for future research and development is present.

Confounding and limiting factors of dose absorption and causality

We still do not know the most precise ways of obtaining dose estimates from absorbed radiation dose from within the body. Neither do we have a full understanding of the implications of dose magnitude and distribution within the tissues of the human body.

Dosimetry is often problematic or impossible especially when internal dosimetry is considered. Methods are not always intercomparable, owing to a number of reasons such as different methodology, imprecise measurements, etc.

The presence of different noxas from the surrounding environment or in relation to occupational exposure, or life style factors such as smoking and drinking influence the risk of protracting cancer and might act as confounders when trying to evaluate the risk from radiation itself. Unknown epigenetic factors, the presence of predisposing disorders or disease entities as mentioned by Oakley et al (30), might again pose further risk of confounding. An example of this could be the correlation between the increased mortality from breast cancer and the number of x-rays to which patients were subjected in the studies of Ronckers et al (16,72)and Simony et al(17). We don't know if there might be a higher prevalence of breast cancer among scoliotic females exposed to x-rays as a consequence of their underlying disease entity compared with the background population.

Large prospective studies are to be undertaken in order to find a clear causality between low-dose radiation and the risk of cancer. The difficulty in finding correct suitable controls and monitoring of exposed population would pose great challenges. The fact that the lifetime risk of dying from cancer has been estimated to approx. 20-30% makes it difficult to detect a potential increased risk of 0.17% from a dose of 10 mSv(73). Thus, it remains very difficult to prove a specific pathology to be caused by radiation as many diseases are already relatively common.

Dose optimization controversies and risk evaluation

Risk calculations on the adverse effects of radiation are calculated based on "black boxes" as a lot of information is indeed not accessible. Epidemiologic data from historic cohorts such as the atom bomb survivor studies(9,10,74,75) and cohorts of patients followed over time support the fact that there is a correlation between the magnitude of absorbed radiation dose and the risk of detrimental effects. The risk estimates in this thesis are based on effective dose and the assumption of direct proportionality of absorbed dose and the resulting risk of detrimental effects in accordance with the LNT and the recommendations of the ICRP(2).

Not everyone agrees with the assumptions of the direct proportional relationship between doses and risk and the extrapolation to include very doses and no lower dose threshold. Some contenders of the LNT, argue that there is no risk when exposed to occasional full-spine images, since the doses are way below any dose ever proven to cause harm and that the body's own repair mechanisms will have repaired any radiation induced cell damage before the individual being subjected to new low dose radiation(30,76,77).

The whole issue of risk of risk from low dose radiation and dose optimization is an ongoing topic of big dispute(12,30,73,77–79). So, are we hunting ghosts when trying to dose optimize and avoid potential radiation induced cancers? Siegel et al(77) believe so. They claim that the greatest risks to patients are posed by doctors striving to reduce dose, while risking to provide patients with inadequate imaging, thus possibly missing important pathological signs and diagnoses. The same authors, however, state that care must be taken to avoid unnecessary radiation!

Even though, the LNT has been disputed and questioned in recent times, there is so far no viable alternative to this model(73), and it is still recommended by the ICRP, UNSCEAR, IAEA and NCRP. It is out of the scope of this thesis to decide for or against the model for estimation of risk as a result of low dose radiation. Still, as of today there is no known lower threshold of dose which might potentially cause cancer, and until this is proven, we have be considerate and avoid all unnecessary radiation exposure to our patients. It is the obligation of all researchers and clinicians to be aware of the potential risk from radiation, to be prudent, appreciate precaution and act as per the ALARA principle as long as we have no clear evidence for or against the risk posed by the ionized radiation used in medical imaging and treatment.

Conclusion

The aims of the overall thesis were met. A thorough investigation into the current dose exposure from the EOS low-dose scanner was conducted, and methods to reduce radiation dose even further were established and clinically validated. Results of exposure from micro-dose protocol as well as exposure from reduced dose protocols relayed novel information and underlined the very low dose subjected to patients from these modalities. The methods used for estimation of dose and levels of uncertainty were confirmed within the studies and when compared with literature. An evaluation of absorbed radiation dose from all x-ray modalities used at our department for the treatment of scoliosis was conducted. This evaluation illustrated the dispersal of radiation dose amongst patients treated for idiopathic scoliosis, allowing us to estimate risks from ionizing radiation for this group of patients. A method was proposed to reduce time spent on organ dosimetry without compromising certainty of organ dose estimations.

Suggestions for Future Research

The studies of this thesis have been conducted in a manner of transparency allowing for other researchers to scrutinize results and methods, and if needed the reproduction of studies.

Currently a strategy of how to implement one or both reduced-dose protocols is being worked out at our institution. A prospective study evaluating the future results of these protocols would be mandatory. Research into to the challenges of the increasing obesity of the population and consequences for image quality and absorbed dose would be areas of interest.

Tools and methods for reducing time on organ and whole body dosimetry were presented for one organ. Future studies applying same or similar methods to other organs or all organs of anthropomorphic phantoms are imminent.

We have evaluated both individual organ dose and full body absorbed doses. Future research areas of interest is the correlation between specific dose to one organ in relation to full-body absorbed dose.

Risk was assessed in terms of effective dose. A different way of evaluating risk from ionizing radiation could be contemplated to be in terms of years potentially lost life (YPLL). YPLL is another way to evaluate the risk of dying from radiologically induced cancer. Based on the principles of study IV a study describing the consequences of continuous radiological examinations in spine patients in terms of YPLL could be proposed.

References

1. Erickson B. U.S. environmental protection agency. Today's Chem Work [Internet]. 1999 [cited 2019 Oct 8];(Suppl). Available from: https://web.archive.org/web/20150212174819/http://www.epa.gov/radiation/understand/ionize_nonionize.html

2. The International Commission on Radiological Protection. The 2007 Recommendations of the International Commission on Radiological Protection. ICRP Publication 103. Ann ICRP. 2007;37(2–4).

3. Thomas KE. CT utilization--trends and developments beyond the United States' borders. Pediatr Radiol [Internet]. 2011 Sep [cited 2011 Nov 20];41 Suppl 2:562–6. Available from: http://www.ncbi.nlm.nih.gov/pubmed/21847739

4. Helm PA, Teichman R, Hartmann SL, Simon D. Spinal Navigation and Imaging : History , Trends , and Future. IEEE Trans Med Imaging. 2015;34(8):1738–46.

5. Samara ET, Aroua A, Bochud FO, Ott B, Theiler T, Treier R, et al. Paper EXPOSURE OF THE SWISS POPULATION BY MEDICAL X-RAYS : 2008 REVIEW. 2012;(May 2011):263–70.

6. UNSCEAR. SOURCES AND EFFECTS OF IONIZING RADIATION United Nations Scientific Committee on the Effects of Atomic Radiation. Vol. I. 2010. 156 p.

7. Sundhedsstyrrelsen. Straaledoser, Ioniserende stråling [Internet]. [cited 2019 Oct 10]. Available from: https://www.sst.dk/da/Viden/Straaling/Fakta/Straaledoser

8. Clement CH, Stewart FA, Akleyev A V., Hauer-Jensen M, Hendry JH, Kleiman NJ, et al. ICRP publication 118: ICRP Statement on Tissue Reactions and Early and Late Effects of Radiation in Normal Tissues and Organs Ã¢â‚¬â€ Threshold Doses for Tissue Reactions in a Radiation Protection Context. Ann ICRP. 2012;41(1–2):1–322.

9. Shimizu Y, Mabuchi K, DL P, Shigematsu I. - Mortality study of atomic-bomb survivors: implications for assessment of. Cancer Surv. 1996;27(1):325–38.

10. Grant EJ, Brenner A, Sugiyama H, Sakata R, Sadakane A, Utada M, et

al. Solid Cancer Incidence among the Life Span Study of Atomic Bomb Survivors: 1958–2009. Radiat Res [Internet]. 2017;187(5):513–37. Available from: http://www.bioone.org/doi/10.1667/RR14492.1

11. Upton AC, Adelstein SJ, Hall EJ, Brenner DJ, Clifton KH, Finch SC, et al. Evaluation of the linear-nonthreshold dose-response model for ionizing radiation. NCRP Rep. 2001;(136).

12. Statista I, Floor 55 Broad Street; 30th, New York N 10004, States U. Statista.pdf [Internet]. Available from: https://www.statista.com/statistics/609088/computed-tomography-scan-examinations-in-denmark/

13. Law M, Ma W-K, Lau D, Chan E, Yip L, Lam W. Cumulative radiation exposure and associated cancer risk estimates for scoliosis patients: Impact of repetitive full spine radiography. Eur J Radiol [Internet]. 2016;85(3):625–8. Available from: http://www.sciencedirect.com/science/article/pii/S0720048X15302163

14. Konieczny MR, Senyurt H, Krauspe R. Epidemiology of adolescent idiopathic scoliosis. J Child Orthop. 2013;7(1):3–9.

15. Willner S, Udén A. A prospective prevalence study of scoliosis in southern Sweden. Acta Orthop. 1982;53(2):233–7.

16. Doody MM, Ronckers CM, Land CE, Miller JS, Stovall M, Lonstein JE, et al. Cancer mortality among women frequently exposed to radiographic examinations for spinal disorders. Radiat Res. 2010;174(1):83–90.

17. A. S, S.B. C, K.E. J, L.Y. C. Incidence of cancer and infertility, in patients treated for adolescent idiopathic scoliosis 25 years prior. Eur Spine J. 2015;24(6 SUPPL. 1):S740.

18. Pace N, Ricci L, Negrini S. A comparison approach to explain risks related to X-ray imaging for scoliosis, 2012 SOSORT award winner. Scoliosis [Internet]. 2013;8(1):11. Available from: http://www.pubmedcentral.nih.gov/articlerender.fcgi?artid=3710473&tool=pmcentrez&rendertype=abstract

19. Levy AR, Goldberg MS, Mayo NE, Hanley JA, Poitras B. Reducing the Lifetime Risk of Cancer From Spinal Radiographs Among People With

Adolescent Idiopathic Scoliosis. Spine (Phila Pa 1976). 1996;21(13):1540–7.

20. Knott P, Pappo E, Cameron M, Demauroy J, Rivard C, Kotwicki T, et al. SOSORT 2012 consensus paper: reducing x-ray exposure in pediatric patients with scoliosis The epidemiology of x-ray exposure in pediatric patients with spinal deformity. 2014;1–9.

21. Bettany-Saltikov J, Turnbull D, Ng SY, Webb R. Management of Spinal Deformities and Evidence of Treatment Effectiveness. Open Orthop J. 2018;11(1):1521–47.

22. Ben-Shlomo A, Bartal G, Mosseri M, Avraham B, Leitner Y, Shabat S. Effective dose reduction in spine radiographic imaging by choosing the less radiation-sensitive side of the body. Spine J. 2016;16(4):558–63.

23. Chaparian A, Kanani A, Baghbanian M. Reduction of radiation risks in patients undergoing some X-ray examinations by using optimal projections: A Monte Carlo program-based mathematical calculation. J Med Phys [Internet]. 2014;39(1):32–9. Available from: http://www.pubmedcentral.nih.gov/articlerender.fcgi?artid=3931225&tool=pmcentrez&rendertype=abstract%5Cnhttp://www.ncbi.nlm.nih.gov/pubmed/24600170%5Cnhttp://www.pubmedcentral.nih.gov/articlerender.fcgi?artid=PMC3931225

24. Luo TD, Stans AA, Schueler BA, Larson AN. Cumulative radiation exposure with EOS imaging compared with standard spine radiographs. Spine Deform [Internet]. 2015;3(2):144–50. Available from: http://dx.doi.org/10.1016/j.jspd.2014.09.049

25. Sundhedsstyrrelsen. Vejledning om patientdoser og referencedoser for røntgenundersøgelser [Internet]. 2012. Available from: https://www.sst.dk/-/media/Udgivelser/2012/Vejledning-om-patientdoser-og-referencedoser-for-røntgenundersøgelser.ashx

26. Ilharreborde B, Ferrero E, Alison M, Mazda K. EOS microdose protocol for the radiological follow-up of adolescent idiopathic scoliosis. Eur Spine J. 2016;25(2):526–31.

27. Gialousis G, Yiakoumakis EN, Makri TK, Papadoupoulou D, Karlatira M, Karaiskos P, et al. Comparison of dose from radiological examination for scoliosis in children among two pediatric hospitals

by Monte Carlo simulation. Heal Phys [Internet]. 2008;94(5):471–8. Available from: http://www.ncbi.nlm.nih.gov/pubmed/18403968

28. Law M, Ma WK, Chan E, Lau D, Mui C, Cheung K, et al. Evaluation of cumulative effective dose and cancer risk from repetitive full spine imaging using EOS system: Impact to adolescent patients of different populations. Eur J Radiol. 2017;96(September):1–5.

29. Presciutti SM, Karukanda T, Lee M. Management decisions for adolescent idiopathic scoliosis significantly affect patient radiation exposure. Spine J [Internet]. 2014;14(9):1984–90. Available from: http://dx.doi.org/10.1016/j.spinee.2013.11.055

30. Oakley PA, Ehsani NN, Harrison DE. The Scoliosis Quandary: Are Radiation Exposures From Repeated X-Rays Harmful? Dose-Response [Internet]. 2019;17(2):155932581985281. Available from: http://journals.sagepub.com/doi/10.1177/1559325819852810

31. Gottfried K-LD, Penn G. Radiation in Medicine: A Need for Regulatory Reform. Vol. 328, The national academies. 1996. 0–309 p.

32. Strauss KJ, Kaste SC. ALARA in Pediatric Interventional and Fluoroscopic Imaging: Striving to Keep Radiation Doses as Low as Possible During Fluoroscopy of Pediatric Patients-A White Paper Executive Summary. J Am Coll Radiol. 2006;3(9):686–8.

33. Tapiovaara M ST. A Monte Carlo program for calculating patient doses in medical x-ray examinations (2nd Ed.). STUK -A231Radiation Nucl Saf Auth [Internet]. 2008;2(November):1–13. Available from: https://www.julkari.fi/bitstream/handle/10024/124342/stuk-a231.pdf?sequence=1

34. Melhem E, Assi A, El Rachkidi R, Ghanem I. EOS(®) biplanar X-ray imaging: concept, developments, benefits, and limitations. J Child Orthop [Internet]. 2016 Feb 16 [cited 2016 Feb 21];10(1):1–14. Available from: http://www.scopus.com/inward/record.url?eid=2-s2.0-84958794308&partnerID=tZOtx3y1

35. Humbert L, De Guise JA, Aubert B, Godbout B, Skalli W. 3D reconstruction of the spine from biplanar X-rays using parametric models based on transversal and longitudinal inferences. Med Eng Phys. 2009;31(6):681–7.

36. Yvert M, Diallo A, Bessou P, Rehel J-L, Lhomme E, Chateil J-F. Radiography of scoliosis: Comparative dose levels and image quality between a dynamic flat-panel detector and a slot-scanning device (EOS system). Diagn Interv Imaging [Internet]. 2015; Available from: http://linkinghub.elsevier.com/retrieve/pii/S221156841500234X

37. Kalifa G, Charpak Y, Maccia C, Fery-Lemonnier E, Bloch J, Boussard JM, et al. Evaluation of a new low-dose digital X-ray device: First dosimetric and clinical results in children. Pediatr Radiol. 1998;28(7):557–61.

38. Deschênes S, Charron G, Beaudoin G, Labelle H, Dubois J, Miron M-C, et al. Diagnostic imaging of spinal deformities: reducing patients radiation dose with a new slot-scanning X-ray imager. Spine (Phila Pa 1976). 2010;35(9):989–94.

39. Hui SCN, Pialasse J-P, Wong JYH, Lam T, Ng BKW, Cheng JCY, et al. Radiation dose of digital radiography (DR) versus micro-dose x-ray (EOS) on patients with adolescent idiopathic scoliosis: 2016 SOSORT-IRSSD "John Sevastic Award" Winner in Imaging Research. Scoliosis Spinal Disord. 2016;11(1):46.

40. Damet J, Fournier P, Monnin P, Ceroni D, Zand T, Verdun FR, et al. Occupational and patient exposure as well as image quality for full spine examinations with the EOS imaging system Occupational and patient exposure as well as image quality for full spine examinations with the EOS imaging system. Med Phys. 2014;063901.

41. Newton PO, Khandwala Y, Bartley CE, Reighard FG, Bastrom TP, Yaszay B. New EOS Imaging Protocol Allows a Substantial Reduction in Radiation Exposure for Scoliosis Patients. Spine Deform [Internet]. 2016 Mar [cited 2016 Mar 15];4(2):138–44. Available from: http://www.sciencedirect.com/science/article/pii/S2212134X15002312

42. Clavel AH, Thevenard-Berger P, Verdun FR, Létang JM, Darbon A. Organ radiation exposure with EOS: GATE simulations versus TLD measurements. 2016;9783:978352. Available from: http://proceedings.spiedigitallibrary.org/proceeding.aspx?doi=10.1117/12.2217097

43. Branchini M, del Vecchio A, Gigliotti CR, Loria A, Zerbi A, Calandrino

R. Organ doses and lifetime attributable risk evaluations for scoliosis examinations of adolescent patients with the EOS imaging system. Radiol Medica. 2018;123(4):305–13.

44. Kong H, West S. WMA Declaration of Helsinki- Ethical Principles. World Med Assoc. 2013;(June 1964):29–32.

45. Dose WB, Dose O, Radiation T. ATOM Dosimetry Phantoms [Internet]. 2013. Available from: http://www.cirsinc.com/file/Products/701_706/701 706 DS 080715(1).pdf

46. Kolotilin V V., Hokhrekov VI, Tarasova LM, Zakhriapin SB. A high sensitivity LiFMg,Cu,P thermoluminescent dosimeter. Int J Radiat Appl Instrumentation Part. 1993;21(1):169–71.

47. González PR, Furetta C, Azorín J. Comparison of the TL responses of two different preparations of LiF:Mg,Cu,P irradiated by photons of various energies. Appl Radiat Isot. 2007;65(3):341–4.

48. Cobb JR. Outline for the study of scoliosis. The American Academy of Orthopedic Surgeons Instructional Course Lectures. Vol. 5. Ann Arbor, MI: Edwards; 1948. 1948;1948.

49. Sundhedsstyrelsen. CT Referencedoser [Internet]. Indsamling og vurdering af patientdoser ved CT - © Sundhedsstyrelsen, 2015. 2015. Available from: http://sundhedsstyrelsen.dk/da/udgivelser/2015/~/media/5FFD019 14F8A430A8407C9B46D94AA6E.ashx

50. Haukoos JS, Lewis RJ. Advanced statistics: Bootstrapping confidence intervals for statistics with “difficult” distributions. Acad Emerg Med. 2005;12(4):360–5.

51. Goeman JJ. L1 penalized estimation in the Cox proportional hazards model. Biometrical J. 2010;52(1):70–84.

52. Schielzeth H, Nakagawa S. Nested by design: Model fitting and interpretation in a mixed model era. Methods Ecol Evol. 2013;4(1):14–24.

53. Morel B, Moueddeb S, Blondiaux E, Richard S, Bachy M, Vialle R, et al. Dose, image quality and spine modeling assessment of biplanar EOS micro-dose radiographs for the follow-up of in-brace adolescent

idiopathic scoliosis patients. Eur Spine J [Internet]. 2018;27(5):1082–8. Available from: https://doi.org/10.1007/s00586-018-5464-9

54. Law M, Ma WK, Lau D, Cheung K, Ip J, Yip L, et al. Cumulative effective dose and cancer risk for pediatric population in repetitive full spine follow-up imaging: How micro dose is the EOS microdose protocol? Eur J Radiol [Internet]. 2018;101(February):87–91. Available from: https://doi.org/10.1016/j.ejrad.2018.02.015

55. Hui SCN, Chu WCW. Supplementary Addendum to "Radiation dose of digital radiography (DR) versus micro-dose x-ray (EOS) on patients with adolescent idiopathic scoliosis: 2016 SOSORT- IRSSD 'John Sevastic Award' Winner in Imaging Research." Scoliosis Spinal Disord. 2018;13(1):1–2.

56. Sundhedsstyrrelsen. Referencedoser for røntgenundersøgelse af columna lumbalis. 2017; Available from: https://www.sst.dk/da/udgivelser/2017/referencedoser-for-roentgenundersoegelse-af-columna-lumbalis-kiropraktor

57. Public Health England. UK National Diagnostic Reference Levels (NDRLs) from 19 August 2019 [Internet]. 2019 [cited 2019 Nov 14]. Available from: https://www.gov.uk/government/publications/diagnostic-radiology-national-diagnostic-reference-levels-ndrls/ndrl

58. Mogaadi M, Ben Omrane L, Hammou A. Effective dose for scoliosispatients undergoing full spine radiography. Radiat Prot Dosimetry. 2012;149(3):297–303.

59. Ilharreborde B, Steffen JS, Nectoux E, Vital JM, Mazda K, Skalli W, et al. Angle Measurement Reproducibility Using EOSThree-Dimensional Reconstructions in Adolescent Idiopathic Scoliosis Treated by Posterior Instrumentation. Spine (Phila Pa 1976) [Internet]. 2011;36(20):E1306–13. Available from: http://content.wkhealth.com/linkback/openurl?sid=WKPTLP:landingpage&an=00007632-201109150-00018

60. Bagheri A, Liu XC, Tassone C, Thometz J, Tarima S. Reliability of Three-Dimensional Spinal Modeling of Patients With Idiopathic Scoliosis Using EOS System. Spine Deform [Internet]. 2018;6(3):207–12. Available from: https://doi.org/10.1016/j.jspd.2017.09.055

61. Langensiepen S, Semler O, Sobottke R, Fricke O, Franklin J, Schönau E, et al. Measuring procedures to determine the Cobb angle in idiopathic scoliosis: A systematic review. Eur Spine J. 2013;22(11):2360–71.

62. Papaliodis D, Bonanni P, Roberts T, Hesham K, Richardson N, Cheney R, et al. Computer Assisted Cobb Angle Measurements: A novel algorithm. Int J Spine Surg [Internet]. 2017;11(3):167–72. Available from: http://ijssurgery.com/10.14444/4021

63. S. G, E. K, J. L, P. C, M. E. Are routine postoperative radiographs necessary during the first year after posterior spinal fusion for idiopathic scoliosis? A retrospective cohort analysis of implant failure and surgery revision rates. J Pediatr Orthop [Internet]. 2014;35(1):33–8. Available from: http://ovidsp.ovid.com/ovidweb.cgi?T=JS&NEWS=N&PAGE=toc&SEARCH=01241398-201007000-00000.kc&LINKTYPE=asBody&LINKPOS=1&D=yrovft%5Cnhttp://ovidsp.ovid.com/ovidweb.cgi?T=JS&PAGE=reference&D=emed13&NEWS=N&AN=2014975271%5Cnhttp://ovidsp.ovid.com/ovidweb.cgi?T=J

64. de Kleuver M, Lewis SJ, Germscheid NM, Kamper SJ, Alanay A, Berven SH, et al. Optimal surgical care for adolescent idiopathic scoliosis: an international consensus. Eur Spine J. 2014;23(12):2603–18.

65. Fletcher ND, Glotzbecker MP, Marks M, Newton PO. Development of Consensus-Based Best Practice Guidelines for Postoperative Care Following Posterior Spinal Fusion for Adolescent Idiopathic Scoliosis. Spine (Phila Pa 1976). 2017;42(9):E547–54.

66. Petersen AG, Eiskjær S, Kaspersen J. Dose optimisation for intraoperative cone-beam flat-detector CT in paediatric spinal surgery. Pediatr Radiol. 2012;42(8):965–73.

67. Prod'homme M, Sans-Merce M, Pitteloud N, Damet J, Lascombes P. Intraoperative 2D C-arm and 3D O-arm in children: a comparative phantom study. J Child Orthop [Internet]. 2018;12(5):550–7. Available from: https://online.boneandjoint.org.uk/doi/10.1302/1863-2548.12.180016

68. Pitteloud N, Gamulin A, Barea C, Damet J, Racloz G, Sans-Merce M. Radiation exposure using the O-arm®surgical imaging system. Eur Spine J. 2017;26(3):651–7.

69. Poirier Y, Kuznetsova S, Villarreal-Barajas JE. Characterization of nanoDot optically stimulated luminescence detectors and high-sensitivity MCP-N thermoluminescent detectors in the 40-300 kVp energy range. Med Phys. 2018;45(1):402–13.

70. Lüpke M, Goblet F, Polivka B, Seifert H. Sensitivity loss of Lif: Mg,Cu,P thermoluminescence dosemeters caused by oven annealing. Radiat Prot Dosimetry. 2006;121(2):195–201.

71. Piters TM, Bos AJJ. Influence of the Cooling Rate on Repeatability of LiF:Mg,Cu,P Thermoluminescent Chips. Radiat Prot Dosimetry. 1990;33(1–4):91–4.

72. Doody MM, Lonstein JE, Stovall M, Hacker DG, Luckyanov N, Land CE. Breast cancer mortality after diagnostic radiography: findings from the U.S. Scoliosis Cohort Study. Spine (Phila Pa 1976). 2000;25(16):2052–63.

73. Weber W, Zanzonico P. The controversial linear no-Threshold model. J Nucl Med. 2017;58(1):7–8.

74. Ozasa K, Shimizu Y, Suyama A, Kasagi F, Soda M, Grant EJ. Studies of the Mortality of Atomic Bomb Survivors , Report 14 , 1950 – 2003 : An Overview of Cancer and Noncancer Diseases. Radiat Res [Internet]. 2012;243(3):229–43. Available from: http://www.ncbi.nlm.nih.gov/pubmed/22171960

75. Pierce DA, Preston DL. Radiation-related cancer risks at low doses among atomic bomb survivors. Radiat Res [Internet]. 2000;154(2):178–86. Available from: http://www.ncbi.nlm.nih.gov/pubmed/10931690

76. Rithidech KN. Health Benefits of Exposure to Low-dose Radiation. Health Phys [Internet]. 2016;110(3):293–5. Available from: http://content.wkhealth.com/linkback/openurl?sid=WKPTLP:landingpage&an=00004032-201603000-00015

77. Siegel JA, Sacks B, Pennington CW, Welsh JS. Dose Optimization to Minimize Radiation Risk for Children Undergoing CT and Nuclear

Medicine Imaging Is Misguided and Detrimental. J Nucl Med [Internet]. 2017;58(6):865–8. Available from: http://jnm.snmjournals.org/lookup/doi/10.2967/jnumed.117.195263

78. Siegel JA, Pennington CW, Sacks B. Subjecting radiologic imaging to the linear no-Threshold hypothesis: A non sequitur of non-Trivial proportion. J Nucl Med. 2017;58(1):1–6.

79. Tubiana M, Aurengo A. Dose-effect relationship and estimation of the carcinogenic effects of low doses of ionising radiation: The Joint Report of the Académie des Sciences (Paris) and of the Académie Nationale de Médecine. Int J Low Radiat. 2006;2(3–4):135–53.

80. Cnsc-ccsn. Linear-Non-Threshold Model Fact Sheet [Internet]. 2013 [cited 2019 Nov 20]. Available from: https://nuclearsafety.gc.ca/eng/resources/health/linear-non-threshold-model/index.cfm

81. Pedersen PH, Petersen AG, Østgaard SE, Tvedebrink T, Eiskjær SP. EOS Micro-dose Protocol: First Full-spine Radiation Dose Measurements in Anthropomorphic Phantoms and Comparisons with EOS Standard-dose and Conventional Digital Radiology. Spine (Phila Pa 1976). 2018;43(22):E1313–21.

Appendices, Papers I-V

Spine

SPINE Volume 43, Number 22, pp E1313–E1321
© 2018 Wolters Kluwer Health, Inc. All rights reserved.

DEFORMITY

EOS Micro-dose Protocol: First Full-spine Radiation Dose Measurements in Anthropomorphic Phantoms and Comparisons with EOS Standard-dose and Conventional Digital Radiology

Peter Heide Pedersen, MD,* Asger Greval Petersen, MSc, MPE,† Svend Erik Østgaard, MD, PhD,* Torben Tvedebrink, PhD,‡ and Søren P. Eiskjær, MD*

Study Design. A comparative study of radiation dose measured in anthropomorphic phantoms.

Objectives. The aim of this study was to first report the first organ dose and effective dose measurements in anthropomorphic phantoms using the new EOS imaging micro-dose protocol in full-spine examinations, and to compare these measurements of radiation dose to measurements in the EOS standard-dose protocol and conventional digital radiology (CR).

Summary of Background Data. Few studies evaluating organ dose and effective dose for the EOS low-dose scanner exist, and mainly for the standard-dose protocol. To the best of our knowledge, no studies of effective dose based on anthropomorphic phantom measurements exist for the new micro-dose protocol.

Methods. Two anthropomorphic phantoms, representing a 5-year-old (pediatric) and a 15-year-old (adolescent). The phantoms were exposed to EOS micro-dose and standard-dose protocols during full-spine imaging. Additionally, CR in scoliosis settings was performed. For all modalities, organ doses were measured and effective doses were calculated using thermoluminescent dosimeters.

Results. We found a 17-fold reduction (94%) of effective dose in micro-dose protocol compared with our CR system in the adolescent phantom. Micro-dose versus standard-dose protocol, showed a 6-fold reduction (83%), and for standard-dose versus our CR system a 2.8-fold reduction (64%) reduction of effective dose was observed.

For the pediatric phantom, a 5-fold reduction (81%) of effective dose in micro-dose protocol compared to our CR system was observed. Micro-dose versus standard-dose protocol, showed a seven-fold (86%) reduction. However, we observed an increase in absorbed dose of 38% when comparing the EOS standard-dose protocol with our CR system.

Conclusion. The EOS imaging micro-dose option exposes patients to lower radiation doses than any currently available modality for full-spine examination. Expected reduction of dose was established for the adolescent phantom when comparing CR and standard-dose protocol. However, no reduction of effective dose with EOS standard-dose protocol compared to our reference CR system was observed in the pediatric phantom.

Key words: anthropomorphic phantoms, cancer risk, cumulative dose, effective dose, EOS stereo-radiography, full-spine radiography, low-dose, micro-dose, organ dose, phantom dosimetry, radiation dose, scoliosis, slot-scanning system.

Level of Evidence: N/A

Spine 2018;43:E1313–E1321

From the *Department of Orthopedic Surgery, Aalborg Universitetshospital, Aalborg, Denmark; †Region Nordjylland, Røntgenfysik, Denmark; and ‡Department of Mathematical Sciences, Aalborg University, Aalborg, Denmark.

Acknowledgment date: October 27, 2017. First revision date: March 7, 2018. Acceptance date: April 10, 2018.

The device(s)/drug(s) is/are FDA-approved or approved by corresponding national agency for this indication.

No funds were received in support of this work.

No relevant financial activities outside the submitted work.

Address correspondence and reprint requests to Peter Heide Pedersen, MD, Ortopædkirurgisk Afdeling, Aalborg Universitetshospital, Hobrovej 18–22, 9000 Aalborg, Denmark; E-mail: php@rn.dk

DOI: 10.1097/BRS.0000000000002696

Adequate radiological imaging is required for the assessment and treatment of spinal deformity. Patients are frequently exposed to numerous radiographs, during diagnosis and treatment, whether conservative or surgical, and follow-up. The higher the total absorbed radiation dose, the higher is the risk of developing radiation-induced cancer. The atom bomb survivor studies[1] show a direct correlation between the total absorbed radiation dose and the risk of developing cancer. Especially

Copyright © 2018 Wolters Kluwer Health, Inc. Unauthorized reproduction of this article is prohibited.

children are at risk, as the stochastic damage caused by ionizing radiation often has a latency period of one or more decades before developing into cancer.[2] A large cohort study[3] showed a 68% increase in mortality, with a standard mortality ratio of 1.68 from breast cancer amongst a cohort of 5573 scoliosis patients followed for >40 years after being diagnosed and exposed to frequent radiographic examinations. Furthermore, a recent study indicated an increased risk of endometrial cancer amongst scoliosis patients as well.[4] To address this challenge, much effort has gone into optimizing radiologic equipment and finding alternatives to keep radiation dose as low as possible to decrease the risk of radiation-induced cancer while maintaining adequate image quality, commonly referred to as the ALARA principle (as low as reasonable achievable).[5]

The EOS low-dose imaging system (EOS imaging, Paris, France) has been developed to produce high-quality images at low radiation doses.[6] We have been using the EOS scanner for full-spine examinations at our institution, since the fall of 2014. The EOS scanner uses a bi-planar slot-scanning technology, which has been described in detail elsewhere.[7–10] The original version of the system had a standard low-dose protocol. Lately, a micro-dose protocol with even lower dose imaging has become an option. EOS standard-dose setting has mainly been evaluated with regards to skin entrance dose;[7,9,11] however, only a few studies have evaluated organ dose and full-body absorbed dose (effective dose).[10–12]

The micro-dose protocol has so far mainly been evaluated in terms of image quality, although an up to 45-fold reduction of absorbed radiation dose compared to CR has been stated;[13] a recent study reported effective dose estimates, based on the Monte Carlo dose-simulation program (PCXMC)[14] using a mathematical phantom. The micro-dose protocol has previously been reported to provide the clinician with images comparable to CR.[13,15]

The dual aim of our study was to report the first-ever organ dose and effective dose measurements in anthropomorphic phantoms using the EOS micro-dose protocol, and to compare our results to measurements in the EOS standard-dose protocol and CR.

MATERIALS AND METHODS

Phantom Exposure

Two clinically validated anthropomorphic CIRS-ATOM phantoms (Computerized Imaging Reference System, Inc. Norfolk, VA),[16] a female adult (representing an adolescent), and a pediatric were used. ATOM dosimetry phantoms have been designed to explore organ dose and effective dose, they consist of tissue equivalent epoxy resins and hold dosimeter locations specific to 21 inner organs.

Each phantom was positioned in the upright position within the EOS scanner (Figure 1). Full spine biplane radiological examinations were performed in two positions: anterior-posterior-lateral (APL) and posterior-anterior-lateral (PAL). Left lateral side of the phantom facing x-ray source in the APL position and right lateral side in PAL. Vertical collimation with a laser positioning system was done in order to ascertain identical scan fields.

The micro-dose protocol shown in Table 1 differs from the standard-dose protocol by featuring increased cobber (Cu) filtration, decreased x-ray tube voltage (kV), and optimized image processing.

As previously described by *Damet et al*,[10] 20 consecutive scans were performed in each position to accumulate sufficient dose for measurements of the absorbed dose. The doses measured for each position were normalized into single examinations, and are listed as such in tables and figures. Measurements were done similarly for full-spine posterior-anterior (PA) and anterior-posterior (AP), and subsequently, lateral (LAT) positions in CR (Siemens Ysio Max, Malvern,

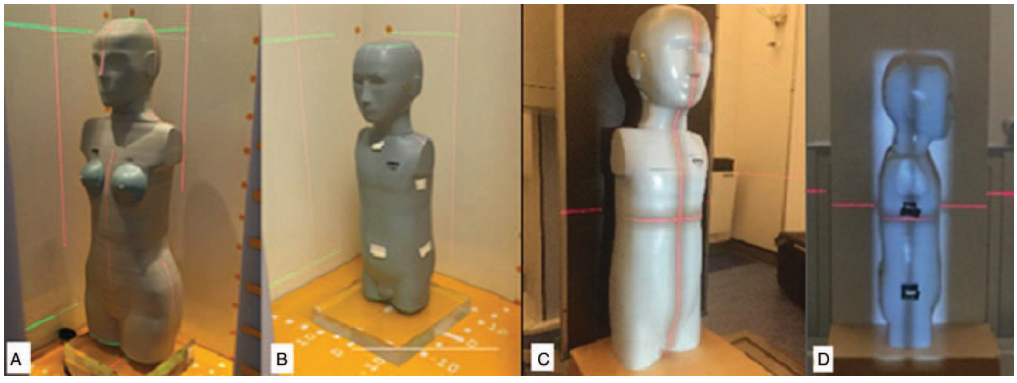

Figure 1. (A), Female phantom (representing an adolescent) in the EOS stereo-radiography scanner. Anterior-posterior-lateral (APL) position (frontal and lateral images are acquired simultaneously). **(B)**, Child phantom (representing a 5-year-old) in EOS scanner in APL position. **(C,D)**, Child phantom in the conventional digital radiology system in AP and lateral position (frontal and lateral images are acquired independently).

Copyright © 2018 Wolters Kluwer Health, Inc. Unauthorized reproduction of this article is prohibited.

TABLE 1. EOS Scan Parameters

Protocols	Female Pediatric Phantom Standard-dose	Female Pediatric Phantom Micro-dose	Female Adolescent Phantom Standard-dose	Female Adolescent Phantom Micro-dose
Morphotype	Small	Small	Medium	Medium
Scan speed	4	3	4	4
Anterior x-ray tube				
kV	83	60	90	65
mA	200	80	250	80
DAP ($mGycm^2$)	200	27	437	65
Lateral x-ray tube				
kV	102	80	105	90
mA	200	80	250	80
DAP ($mGycm^2$)	340	60	648	151

DAP indicates dose area product.

PA., USA), with CR long cassette wall stand, imaging parameters used are shown in Table 2. For CR LAT exposures, the right lateral side of the phantoms faced the x-ray-source according to in-house scoliosis protocol.

Dosimetry

Thermoluminescent dosimeters (TLD) (MCP-N, Krakow, Poland) were used for dosimetry. MCP-N dosimeters have a threshold of detecting radiation that is 200 times lower than more commonly used TLD-100 dosimeters.

Each TLD was placed within the phantoms at organ-specific positions and table-listed depths; eight dosimeters were placed on skin surfaces. All available internal dosimeter locations were used. The total of measuring points was in the range 184 (pediatric phantom) to 298(adolescent phantom). For calibration and dose readings, Rados IR-2000 irradiator and the Rados RE-2000 reader (RadPro International GmbH, Wermelskirchen, Germany) were used. Mean organ doses were measured, and effective doses were calculated as described in previous studies.[10,17]

TABLE 2. CR Scoliosis Parameters (Siemens Ysio Max)

CR Scoliosis Protocols*	Pediatric Phantom	Female Adolescent Phantom
Anterior exposure		
kV	85	96
mAs	10	40
DAP ($mGycm^2$)	120	1510
Lateral exposure†		
kV	90	102
mAs	16	63
DAP ($mGycm^2$)	190	1470

DAP indicates dose area product.
**Standard scoliosis protocols for 2- to 10-year olds and for adults, used at our institution.*
†Right lateral.

$$\text{Effective dose (E)}, E = \sum w_T H_T$$

represents the full-body stochastic health risk, which is the probability of cancer induction and genetic effects, from any partial radiation of the body. Effective dose is measured in milisieverts (mSv), and according to the International Commission on Radiological Protection(ICRP) publication 103,[5] calculated by summing the equivalent dose of each organ (H_T), which for x-ray radiation is equal to the average absorbed radiation dose for each organ, multiplied by a tissue-specific weighting(W_T) factor.

Statistical Methods

Radiation dose was visualized by $\log_{10}$-transforming measurement data to compare standard-dose and micro-dose. Furthermore, this reduced variability of data observed because of the underlying proportionality in mean and variance. We used a negative binominal regression method in order to statistically model data. Data observation was used to identify the expected additive structure in mean for the radiation dose, that is, the only interaction terms were between organs and the position of the phantom relative to the source (APL/PAL). From the statistical model, expected tissue/organ levels were estimated for the two directions (APL/PAL) with an additive term due to different dose protocols. Based on the estimated model parameters and associated standard errors, the ratio of absorbed dose was compared between CR, micro-dose, and standard dose. The estimated absorbed dose was evaluated using the estimated model parameters and tissue factors from predetermined positions. The associated 95% confidence intervals were evaluated using parametric bootstrap similar to the mean estimate.[18] This parametric bootstrap was used to assess how the uncertainty in parameter estimates was manifested in the absorbed dose. Main results have been expressed with 95% confidence intervals.

Copyright © 2018 Wolters Kluwer Health, Inc. Unauthorized reproduction of this article is prohibited.

RESULTS

Final Inclusions

Adolescent Phantom

All 290 internal TLD positions were available for TLD placement, so were eight dosimeters placed on skin surfaces around the phantom. A few dosimeters were lost during dosimetry; one to six of a total of 298 equal to 0.3% to 2% of the dosimeters were used for calculating effective dose.

Pediatric Phantom

A total of 176 of 180 internal TLD positions were available for placement of dosimeters. Four positions lost were because of image quality insert cylinders. An additional eight dosimeters were placed on the surface of the phantoms for skin dose measurements. In most positions and exposure-protocols, a few dosimeters were lost during read-outs, either because they were broken or had fallen out. The number of lost dosimeters ranged from zero to two per exposure position, equal to 0 to 1% of the dosimeters used for calculating effective doses. Dosimeter readings from the three positions representing prostate and testes have not been included in the results; the phantoms represented females.

Effective Doses

Figure 2 provides an overview of effective doses for both phantoms and exposure positions, including CR.

Adolescent Phantom

We observed a 17-fold reduction (94%) of absorbed dose in micro-dose settings compared to measured dose absorbed with CR. Effective dose for PAL full spine, bi-planar, radiographic examination with the micro-dose protocol was 29 μSv (27–31); the corresponding dose for CR PA-LAT was 491 μSv (456–531). A six-fold reduction (83%) of effective dose was observed when comparing micro-dose with standard dose protocol. A 2.8-fold (64%) reduction of effective dose reduction was observed when comparing standard dose protocol with our CR system in PA-LAT.

Pediatric Phantom

Effective dose for PAL full spine, bi-planar radiographic examination with the micro-dose protocol was 22 μSv (20–23); the corresponding dose for CR PA-LAT was 114 μSv (104–127); this is equivalent to a five-fold reduction, (81%) of absorbed dose. A seven-fold reduction (86%) of effective dose was observed when comparing micro-dose with standard-dose protocol. However, there was an increase in absorbed dose of 38% when the EOS standard dose settings were compared with our CR system in PA-LAT.

Organ Doses

Figures 3 to 6 demonstrate organ doses with micro-dose and standard-dose protocols for both phantoms, and show PAL/APL relations. For most organs, doses were lower in PAL than in APL. Effective doses in PAL compared with APL were reduced by an average of 21% (20%–22%) for the phantoms in both standard and micro-dose protocols. The adolescent mean organ dose to the breasts was reduced by 29% in PAL; this reduction was solely on the left breast where dose was reduced from 403 to 73 μSv, a 5.5-fold reduction, whereas the right breast dose was increased from 216 to 287 μSv, a 33% increase in dose.

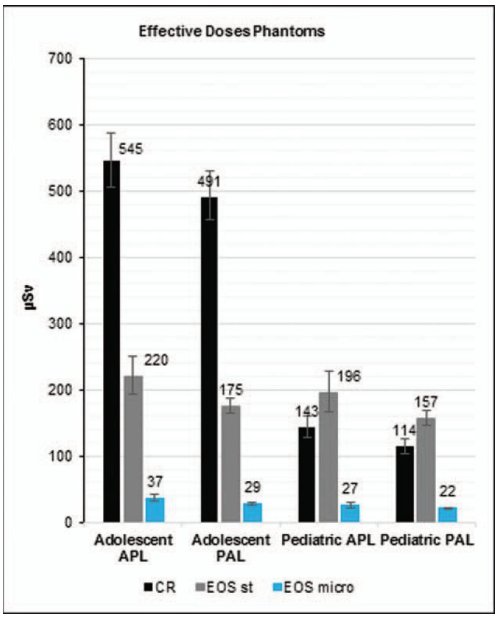

Figure 2. Effective doses for anthropomorphic phantoms with different imaging protocols. APL indicates anterior-posterior + lateral exposure; CR, conventional digital radiology, scoliosis protocol; EOS st, EOS standard-dose protocol; EOS micro, EOS micro-dose protocol; PAL, posterior-anterior + lateral exposure. Error bars represent 95% confidence intervals.

DISCUSSION

To the best of our knowledge, the present study reports the first, anthropomorphic phantom-based, measurements of effective dose and organ dose using the EOS micro-dose protocol. We showed a significant reduction of absorbed doses using the micro-dose setting compared with a conventional system and to EOS standard-dose settings as summarized in Figure 2. We confirmed the manufacturer's claim that the micro-dose scan delivers radiation equal to <1 week of natural background radiation; viz. the mean weekly exposure is 46 μSv.[19] This finding corroborates that radiographic full-spine examinations can be performed without exposing the patient to more than very low amounts of ionizing radiation.

By presenting organ dose measurements in a micro-dose protocol and calculating the effective dose, we contribute to the ongoing evaluation of the risk of tissue detriment and death from radiation-induced cancer. With an average

Copyright © 2018 Wolters Kluwer Health, Inc. Unauthorized reproduction of this article is prohibited.

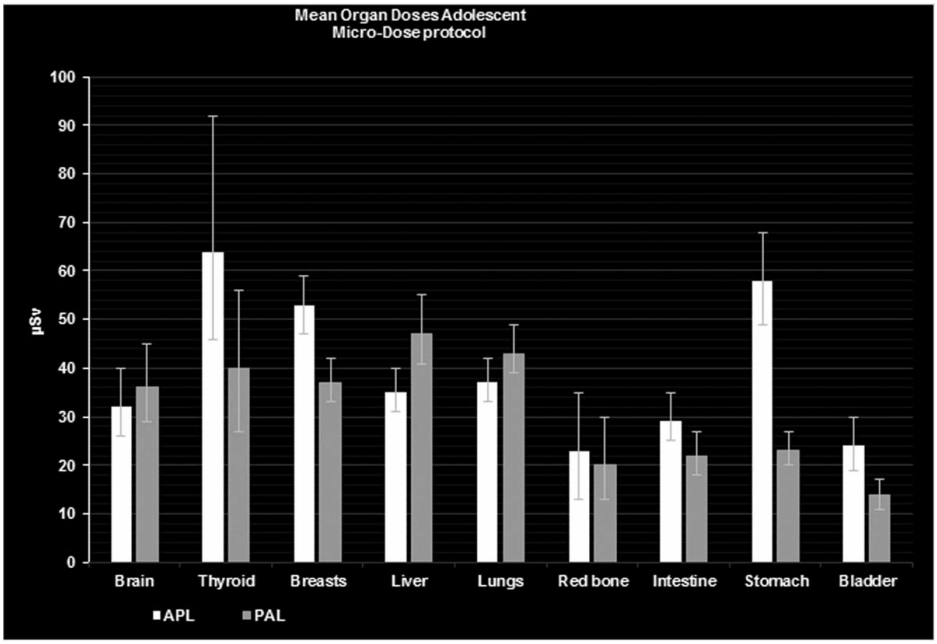

Figure 3. Mean organ doses in APL and PAL with micro-dose protocol, for the adolescent phantom. Error bars represent 95% confidence intervals. APL indicates anterior-posterior + lateral exposure; PAL, posterior-anterior + lateral exposure.

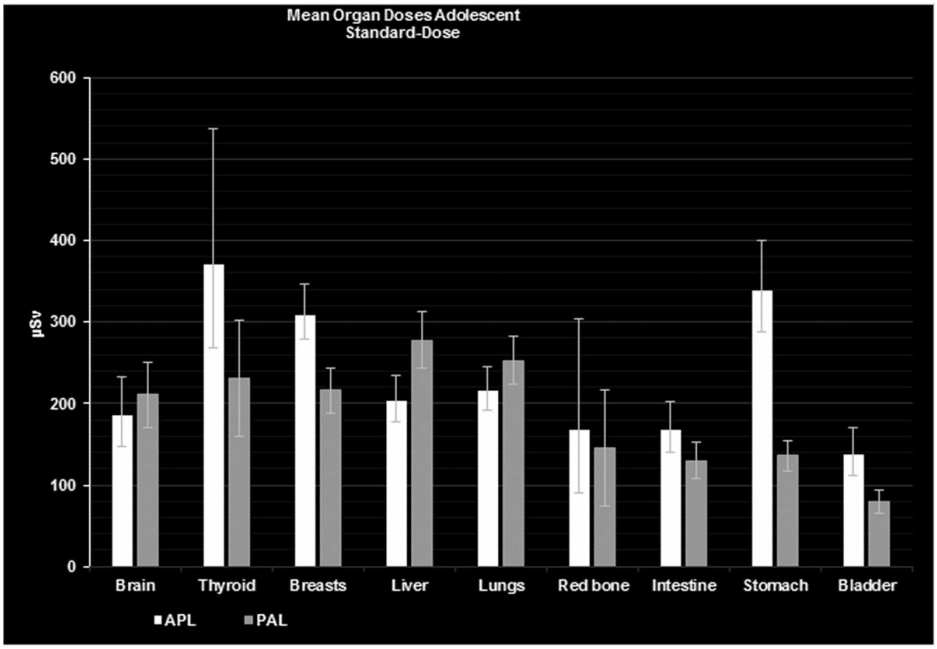

Figure 4. Mean organ doses in APL and PAL with standard-dose protocol, for the adolescent phantom. Error bars represent 95% confidence intervals. APL indicates anterior-posterior + lateral exposure; PAL, posterior-anterior + lateral exposure.

Copyright © 2018 Wolters Kluwer Health, Inc. Unauthorized reproduction of this article is prohibited.

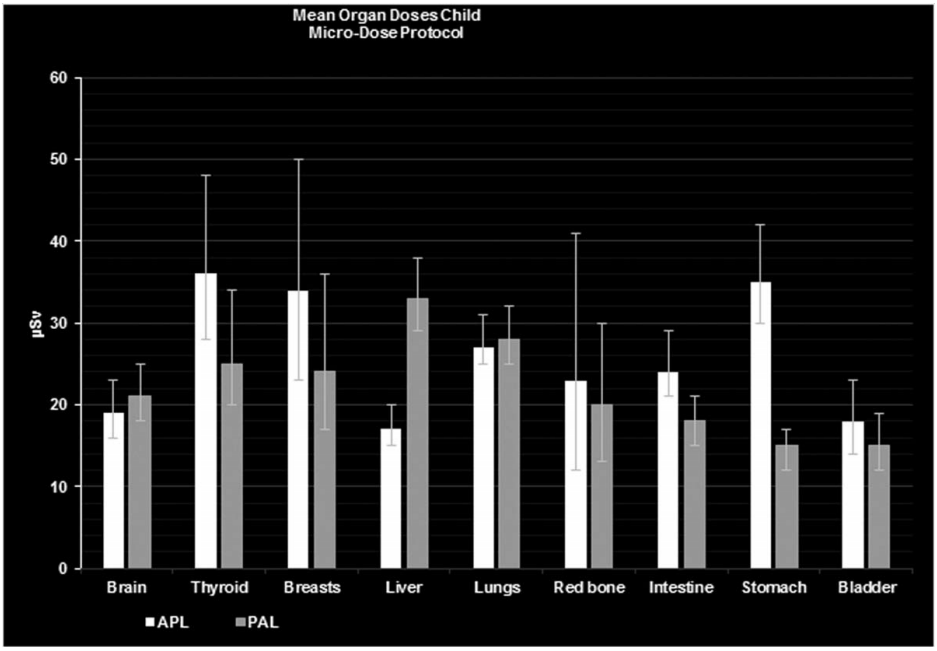

Figure 5. Mean organ doses in APL and PAL with micro-dose protocol, for the child phantom. Error bars represent 95% confidence intervals. APL indicates anterior-posterior + lateral exposure; PAL, posterior-anterior + lateral exposure.

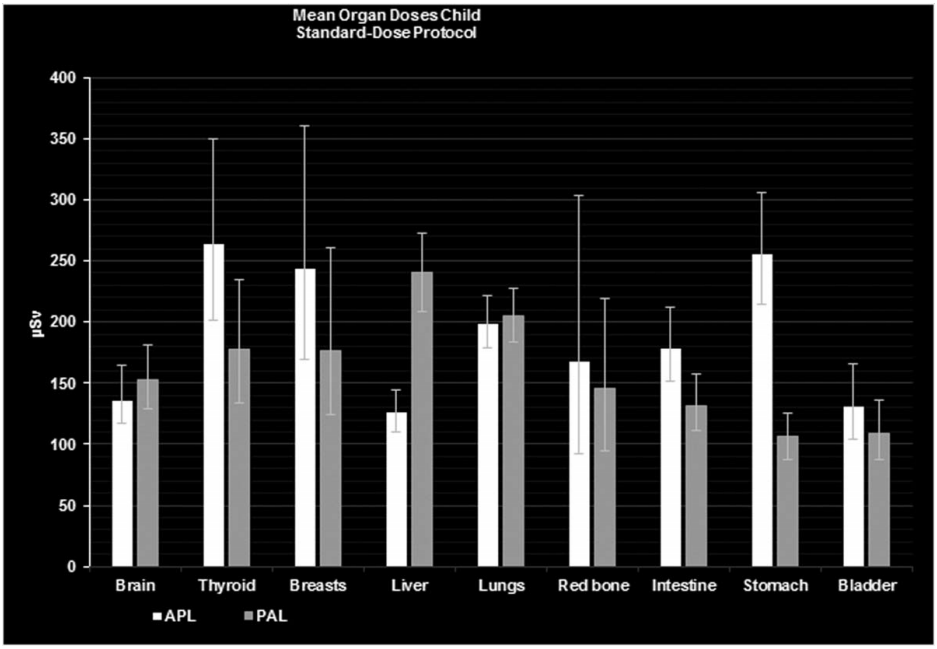

Figure 6. Mean organ doses in APL and PAL with standard-dose protocol, for the child phantom. Error bars represent 95% confidence intervals. APL indicates anterior-posterior + lateral exposure; PAL, posterior-anterior + lateral exposure.

Copyright © 2018 Wolters Kluwer Health, Inc. Unauthorized reproduction of this article is prohibited.

world-wide annual effective dose of 2.4 mSv (range1–10) per capita[19] from natural background exposure, a full-spine examination with micro-dose protocol and an effective dose of 22–37 μSv represents a very low dose. Two annual full-spine examinations with micro-dose protocol for 25 consecutive years would yield an accumulated effective dose <2 mSv, which is equivalent to <1 year of natural background exposure. Hence, the EOS micro-dose option offers full-spine imaging at an almost negligent radiation level. A recent study[13] reports a 45-fold dose reduction with the micro-dose protocol compared with CR. This is, in fact, true if one was to compare to the dose delivered in conventional scoliosis full-spine examinations where radiation doses have been reported to reach around 3.5 mSv.[13,20] As shown by our study, the CR dose with modern equipment used for AP-LAT spine imaging reached 0.545 mSv in the adolescent phantom. Damet *et al*[10] found a comparable figure of 0.450 mSv for full-spine AP-LAT full-spine. Compared with our CR reference for PA-LAT full-spine doses, the micro-dose protocol offers a 17-fold reduction, which is still a marked reduction, but not in the means of 45-fold reduction. The radiation doses from modern systems have been much reduced,[3,21] and it seems that some reference guidelines for full-spine effective doses need to be updated or reconsidered as far as the description of the dose reduction afforded by new systems is concerned.

Interestingly, in the pediatric phantom, our standard-dose protocol showed no dose reduction compared with our reference CR. The child CR measurements were repeated and yielded same results. However, the PA-LAT CR dose of 114 μSv (104–127) for the pediatric phantom was not far from the 150 μSv for 4- to 7-year olds, reported by Gialousis *et al*.[21] Some of the explanation for the low-dose for the small-child CR is likely attributable to conventional imaging optimization. Furthermore, we used a reduced-dose scoliosis protocol with right lateral exposure. Radiation exposure of the lees radiation-sensitive right lateral side has been reported to reduce lateral effective dose by up to 28% for children.[22] For the adolescent phantom, we observed an effective dose reduction with EOS standard dose compared with CR, which is consistent with previous reports.[10,11] Our EOS standard-dose results for both phantoms are consistent with most reports.[10–12] Table 3 shows previously reported doses compared with the doses of the present study. Hui *et al*[14] reported an effective dose of 2.6 μSv for AP micro-dose projection, much lower than doses reported by any other study. We were surprised by this very low measure and have redone the calculations based on reported values. We found an effective dose of 3.1 μSv if we included the inherent aluminum filter of the EOS scanner in dose calculations, DAP values were used. If instead calculating effective dose from reported entrance skin dose, the effective dose was 5.2 μSv. The calculated values are closer to previously reported values but still very low. The exact reason is not known.

Organ doses to most organs were lower in PAL than in APL. Previous studies have documented that obtaining radiographs in the PA position decreases the amount of absorbed dose in most radiosensitive organs, and thus the effective dose.[12,22,23] By measuring organ dose in both APL and PAL, we were able to illustrate the dose divergence in the two positions for the EOS. The mean dose reduction in PAL *versus* APL was 21%. A 29% mean dose reduction to the breasts was observed in the adolescent phantom. This is consistent with findings of Luo *et al*,[11] when including lateral dose. The reported eight-fold reduction did not include lateral dose.[11] The EOS PAL position should be favored as a means of reducing the previously reported elevated risk of breast cancer. Historically, different methods have been applied for assessing organ dose and effective dose in the EOS scanner. Initially skin-entrance dose was described in comparisons of TLD measurements on skin surfaces with EOS and CR, and to calculate effective dose with the PCXMC method.[24] Clavel *et al*[12] used GATE organ volume simulation with PCXMC to compare with TLD dose measurements. Damet *et al*[10] reported organ dose and effective dose for the EOS standard protocol, based on measurements in anthropomorphic phantoms. The anthropomorphic phantoms provided us with a model closely mimicking the in vivo situation in terms of the anatomical placement of organs and tissue-equivalent materials. The setting allowed us to calculate patient organ doses and effective doses after direct exposure to dosimeters.

A limitation of the method used is the fact that measurements were based on 20 consecutive scans in each position and normalized to one scan, instead of making a number of individual scans and measurements. Damet *et al*[10] used only a fraction of available dosimeter placements (<25%) within the phantoms. Using only some of the predetermined dosimeter locations allows for considerable variations of dose

TABLE 3. Previous Studies on Radiation Dose in EOS APL Standard-dose Protocol

	Breasts, Mean, mSv	Thyroid, Mean, mSv	Ovaries Maen, mSv	Effective dose, mSv
Damet *et al*, 2014[10] (adult phantom)*	0.45	0.30	0.13	0.290
Luo *et al*, 2015[11] (PCXMC, adult)	0.33	0.35	0.17	0.240
Present study (adult phantom)*	0.31	0.37	0.09	0.220

APL indicates anterior-posterior + lateral exposure.
**Female adult phantom representing an adolescent.*

Copyright © 2018 Wolters Kluwer Health, Inc. Unauthorized reproduction of this article is prohibited.

measurements. For instance, four of 28 TLD locations were used in the liver for the adolescent phantom allowing for >20,000 possible combinations!.

We chose to strengthen our study, by using all internal dosimeter locations. This allowed us to evaluate more precisely the mean absorbed dose within each organ. Furthermore, to address the uncertainties inherent in any studies within this area, we performed negative binomial regression analysis as described above. This model provided a more flexible framework for count data interpretation, than the Poisson regression, in the case of potential overdispersion, which was the case in this study.

Even with new low-dose imaging, we still have to keep focusing on ALARA, keeping the radiation dose as low as possible. The mean annual absorbed dose of ionizing radiation from medical causes is on the rise. Currently, the annual absorbed dose is estimated at 1.2 mSv.[25] So far, no lower threshold for the amount of ionizing radiation causing tissue damage, and potentially radiation-induced cancer has been established.[1] Still, we need to devote efforts to keeping the risk from radiation-induced cancer from full-spine examinations lower than previously reported levels;[3,26] and we need to continuously work towards minimizing the total radiation dose to which we expose our patients.

➢ Key Points

- ❑ This study presents first phantom measurements of organ dose, and effective dose calculations, with the EOS micro-dose protocol in full spine examinations.
- ❑ Radiation dose exposure from EOS micro-dose protocol was six to seven times less than the EOS standard-dose protocol.
- ❑ Effective dose with EOS micro-dose protocol was reduced 17-fold for the adolescent and five-fold for the pediatric phantom compared with CR.
- ❑ This study confirmed the fact that one EOS micro-dose full-spine examination corresponds to <1 week of natural background radiation.
- ❑ Our results also showed that the EOS standard-dose protocol for full-spine examinations does not always offer lower radiation dose exposure than modern CR in small children.

Acknowledgments

The authors acknowledge the valuable support of University College Nordjylland (Radiografskolen), Selma Lagerløfs Vej 2, 9220 Aalborg Ø, Denmark, providing access to TLD irradiator and dose reader along with technical support.

References

1. Ozasa K, Shimizu Y, Suyama A, et al. Studies of the mortality of atomic bomb survivors, report 14, 1950– 2003: an overview of cancer and noncancer diseases. *Radiat Res* 2012;243:229–43.
2. Pace N, Ricci L, Negrini S. A comparison approach to explain risks related to X-ray imaging for scoliosis, 2012 SOSORT award winner. *Scoliosis* 2013;8:11.
3. Doody MM, Ronckers CM, Land CE, et al. Cancer mortality among women frequently exposed to radiographic examinations for spinal disorders. *Radiat Res* 2010;174:83–90.
4. A S, SB C, KE J, et al. Incidence of cancer and infertility, in patients treated for adolescent idiopathic scoliosis 25 years prior. *Eur Spine J* 2015;24:S740.
5. The International Commission on Radiological Protection. The 2007 Recommendations of the International Commission on Radiological Protection. ICRP Publication 103. *Ann ICRP*;37.
6. Melhem E, Assi A, El Rachkidi R, et al. EOS(®) biplanar X-ray imaging: concept, developments, benefits, and limitations. *J Child Orthop* 2016;10:1–14.
7. Deschênes S, Charron G, Beaudoin G, et al. Diagnostic imaging of spinal deformities: reducing patients radiation dose with a new slot-scanning X-ray imager. *Spine (Phila Pa 1976)* 2010;35:989–94.
8. Yvert M, Diallo A, Bessou P, et al. Radiography of scoliosis: comparative dose levels and image quality between a dynamic flat-panel detector and a slot-scanning device (EOS system). *Diagn Interv Imaging* 2010;96:1177–88.
9. Kalifa G, Charpak Y, Maccia C, et al. Evaluation of a new low-dose digital X-ray device: first dosimetric and clinical results in children. *Pediatr Radiol* 1998;28:557–61.
10. Damet J, Fournier P, Monnin P, et al. Occupational and patient exposure as well as image quality for full spine examinations with the EOS imaging system Occupational and patient exposure as well as image quality for full spine examinations with the EOS imaging system. *Med Phys;63901* 2014;41:063901.
11. Luo TD, Stans AA, Schueler BA, et al. Cumulative radiation exposure with EOS imaging compared with standard spine radiographs. *Spine Deform* 2015;3:144–50.
12. Clavel AH, Thevenard-Berger P, Verdun FR, et al. Organ radiation exposure with EOS: GATE simulations versus TLD measurements. *J Med Imaging* 2016;9783:978352.
13. Ilharreborde B, Ferrero E, Alison M, et al. EOS microdose protocol for the radiological follow-up of adolescent idiopathic scoliosis. *Eur Spine J* 2016;25:526–31.
14. Hui SCN, Pialasse J-P, Wong JYH, et al. Radiation dose of digital radiography (DR) versus micro-dose x-ray (EOS) on patients with adolescent idiopathic scoliosis: 2016 SOSORT- IRSSD "John Sevastic Award" Winner in Imaging Research. *Scoliosis Spinal Disord* 2016;11:46.
15. Newton PO, Khandwala Y, Bartley CE, et al. New EOS imaging protocol allows a substantial reduction in radiation exposure for scoliosis patients. *Spine Deform* 2016;4:138–44.
16. Body W, Organ D. Therapeutic D. ATOM dosimetry phantoms size and age related dose calculations features. 2013. Available at: http://www.cirsinc.com/file/Products/701_706/701%20706%20ATOM%20PB%20110615.pdf. Accessed Occtober 26, 2017.
17. Fujii K, Akahane K, Miyazaki O, et al. Evaluation of organ doses in CT examinations with an infant anthropomorphic phantom. *Radiat Prot Dosimetry* 2011;147:151–5.
18. Haukoos JS, Lewis RJ. Advanced statistics: bootstrapping confidence intervals for statistics with "difficult" distributions. *Acad Emerg Med* 2005;12:360–5.
19. United Nations Committee on the Effects of Atomic Radiation. *Sources and Effects of Ionizing Radiation. UNSCEAR 2008 Report to the General Assembley with scientific annexes*. Vol 1. 2010.
20. Mogaadi M, Ben Omrane L, Hammou A. Effective dose for scoliosispatients undergoing full spine radiography. *Radiat Prot Dosimetry* 2012;149:297–303.
21. Gialousis G, Yiakoumakis EN, Makri TK, et al. Comparison of dose from radiological examination for scoliosis in children among two pediatric hospitals by Monte Carlo simulation. *Heal Phys* 2008;94:471–8.

Copyright © 2018 Wolters Kluwer Health, Inc. Unauthorized reproduction of this article is prohibited.

22. Ben-Shlomo A, Bartal G, Mosseri M, et al. Effective dose reduction in spine radiographic imaging by choosing the less radiation-sensitive side of the body. *Spine J* 2015;16: 558–63.
23. Chaparian A, Kanani A, Baghbanian M. Reduction of radiation risks in patients undergoing some X-ray examinations by using optimal projections: A Monte Carlo program-based mathematical calculation. *J Med Phys* 2014;39:32–9.
24. Servomaa a, Tapiovaara M. Organ dose calculation in medical X ray examinations by the program PCXMC. *Radiat Prot Dosimetry* 1998;80:213–9.
25. Samara ET, Aroua A, Bochud FO, et al. Paper exposure of the Swiss population by medical x-rays: 2008 review. *Health phys* 2012;102:263–70.
26. Doody MM, Lonstein JE, Stovall M, et al. Breast cancer mortality after diagnostic radiography: findings from the U.S. Scoliosis Cohort Study. *Spine (Phila Pa 1976)* 2000;25:2052–63.

Copyright © 2018 Wolters Kluwer Health, Inc. Unauthorized reproduction of this article is prohibited.

European Radiology (2019) 29:1874–1881
https://doi.org/10.1007/s00330-018-5749-8

MUSCULOSKELETAL

A reduced micro-dose protocol for 3D reconstruction of the spine in children with scoliosis: results of a phantom-based and clinically validated study using stereo-radiography

Peter H. Pedersen[1,2,3] · Claudio Vergari[2] · Abdulmajeed Alzakri[2,4] · Raphaël Vialle[3] · Wafa Skalli[2]

Received: 23 May 2018 / Revised: 16 August 2018 / Accepted: 10 September 2018 / Published online: 22 October 2018
© European Society of Radiology 2018

Abstract

Purpose The aim of this study was to validate the reproducibility of 3D reconstructions of the spine using a new reduced micro-dose protocol.

Methods First, semi-quantitative image analysis was performed using an anthropomorphic child phantom undergoing low-dose biplanar radiography. This analysis was used to establish a "lowest dose" allowing for acceptable visibility of spinal landmarks. Subsequently, a group of 18 scoliotic children, 12 years of age or younger, underwent full-spine biplanar radiography with both micro-dose and the newly defined reduced micro-dose. An intra- and inter-observer reliability study of 3D reconstructions of the spine was performed according to the International Organization for Standardization (ISO)-5725 standard, with three operators.

Results The reduced micro-dose setting corresponded to a theoretical reduction of radiation dose exposure of approximately 58%. In vivo results showed acceptable intra- and inter-observer reliability (for instance, 3.8° uncertainty on Cobb angle), comparable to previous studies on 3D spine reconstruction reliability and reproducibility based on stereo-radiography.

Conclusion A new reduced micro-dose protocol offered reliable 3D reconstructions of the spine in patients with mild scoliosis. However, the quality of 3D reconstructions from both reduced micro-dose and micro-dose was inferior to standard-dose protocol on most parameters. Standard-dose protocol remains the option of choice for most accurate assessment and 3D reconstruction of the spine. Still, this new protocol offers a preliminary screening option and a follow-up tool for children with mild scoliosis yielding extremely low radiation and could replace micro-dose protocol for these patients.

Key Points

- *We investigated the reliability of 3D reconstructions of the spine based on a new stereo-radiography protocol reducing radiation dose by 58% compared with established micro-dose imaging protocol.*
- *The new reduced micro-dose protocol offers a reproducible preliminary screening option and a follow-up tool in the necessarily frequent repeat imaging of children with mild scoliosis yielding extremely low radiation and could replace existing micro-dose protocol for these patients.*
- *EOS standard-dose protocol remains the option of choice for exact radiographic assessment of scoliosis, offering more exact 3D reproducibility of the spine compared to both micro-dose and the new reduced micro-dose protocols.*

Keywords Three-dimensional imaging · Scoliosis · Radiation dosage · Radiography · Reproducibility of results

✉ Peter H. Pedersen
php@rn.dk

[1] Orthopedic Department, University Hospital of Aalborg, Hobrovej 18-22, 9000 Aalborg, Denmark

[2] Arts et Metiers ParisTech, LBM/Institut de Biomecanique Humaine Georges Charpak, 151 bd de l'Hopital, 75013 Paris, France

[3] Department of Pediatrics, Sorbonne Université, APHP Paris, 26 avenue du Dr Arnold Netter, 75012 Paris, France

[4] Orthopedic Department, College of Medicine, King Saud University, Riyadh, Saudi Arabia

Abbreviations

AIS	Adolescent idiopathic scoliosis
ALARA	As low as reasonable achievable
AVR	Apical vertebra rotation
DAP	Dose area product
IAR	Intra vertebral rotation
ISO	International organization for standardization
PAL	Posterior-anterior-lateral positioning
PT	Pelvic tilt
TI	Torsional index of the spine

Introduction

The evaluation of 3D spine deformity in scoliosis is challenging and optimally requires comprehension and use of 3D clinical parameters [1, 2]. The correct interpretation of spinal deformities is mandatory to define the optimal treatment strategy for the patients. Different methods for 3D evaluations have been used and evaluated [3], and reconstruction based on stereo-radiography is a commonly used method. Several studies have investigated the possibility of predicting progression of scoliosis based on 3D parameters [1, 2, 4–6], since predicting scoliosis progression at an early stage would be of paramount importance. Apical vertebra rotation (AVR), torsional index of the spine (TI), and intra-vertebral rotation (IAR) have been proven significant parameters in determining progression in mild scoliosis (Cobb angle < 25° [2, 4]). In the recent 20 years, a lot of effort has gone into defining the "gold standard" for 3D parameters, and to apply these for effective and easy-to-use tools in daily clinical life [3].

The repeated use of X-ray imaging needed for scoliotic patient follow-up has been of concern in recent years. Ionizing radiation has been associated with a potential risk of developing radiation-induced cancer in scoliotic patients [7–10]. Children have a long life expectancy and are thought to be especially sensitive to long-term stochastic effects from ionizing radiation. Thus, it is of great importance taking steps towards using methods reducing the radiation exposure to our patients. The best approach of course would be to define robust methods of early detection of progressive scoliosis and more efficient methods of treatment in order to limit the number of radiographic exams needed for follow-up. However, although promising results have been reported in the literature, such methods are still not validated or widespread [4, 6, 11]. The second-best approach is to reduce the ionizing radiation delivered by the radiological exam.

EOS® low-dose stereo-radiography (EOS Imaging) is an imaging system that allows for high-quality imaging at a radiation dose lower than most conventional systems [5, 8, 12], adhering to the ALARA dose-optimization principle of keeping dose as low as reasonably achievable [13]. 3D reconstruction from EOS imaging stereo-radiography has been described in several previous studies [4, 14–17]. Good reliability on 3D parameters has been reported for both standard-dose and micro-dose protocols [14, 15, 17]. Ilharreborde et al [15, 17] looked at both standard-dose and micro-dose protocols with regard to intra- and inter-observer reproducibility. Results were satisfactory for both modalities and a significant reduction of dose compared with the original standard-dose protocol was described. We hypothesized that the radiation dose delivered to the patient could be reduced even further without compromising reliability of 3D reconstructions. The aim of the present study was to investigate the possibility of reducing the dose of the established micro-dose protocol retaining the possibility of trustworthy 3D reconstructions from the EOS imaging stereo-radiography.

Materials and methods

Defining the reduced micro-dose protocol

The minimal dose judged to yield sufficient image quality for recognition of anatomical landmarks was defined by imaging a clinically validated ATOM dosimetry child phantom (CIRS, Computerized Imaging Reference System, Inc.) [18]. Figure 1 shows the phantom in posterior-anterior-lateral (PAL) positioning within an EOS scanner. Radiographic expositions were made with sequentially lower dose settings. Radiation dose exposure from the EOS micro-dose protocol was reduced by decreasing the current, milliamps (mA), and the scan speed. Both parameters are directly proportional to radiation dose: a 25% decrease of mA reduces exposure by 25%. A change of scan speed from speed 4 to speed 3 likewise results in a reduction of radiation dose by 25%. An experienced surgeon rated image quality with a semi-quantitative approach: phantom images were cut in regions of interest (lumbar, thoracic and full body, in frontal and lateral views) and anonymized, so the surgeon could blindly grade them, in a random order of region and quality. A score from 1 to 5 was assigned to each image by the surgeon (1 = optimal, 5 = unacceptable), and all images were scored twice. A cumulative score was calculated for each dose and plotted against dose. A sharp increase of image quality was noticed at 28 mGy.cm^2 (50 mA and 60 kV for frontal imaging and 50 mA and 80 kV for lateral imaging, with a scan speed of 2): although the score increase was not statistically significant, this cutoff value was chosen. Preliminary in vivo measurement confirmed the readability of the X-rays with these settings.

Theoretic dose reductions were calculated from proportional differences of dose area product (DAP) values between the standard-dose, micro-dose, and reduced micro-dose protocols (Table 1).

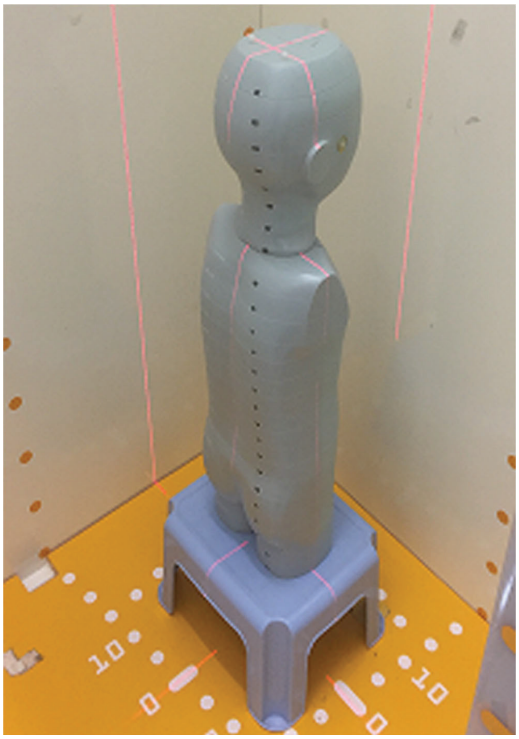

Fig. 1 The anthropomorphic phantom, representing a 5-year-old child, placed in posterior-anterior-lateral positioning within the EOS scanner

Table 1 Scan protocols and resulting DAP values for the 5-year-old anthropomorphic phantom

EOS scan protocols			
Protocols Morphotype	Reduced micro-dose Small	Micro-dose Small	Standard-dose Small
Scan speed	2	3	4
Anterior X-ray tube			
kV[a]	60	60	83
mA[b]	50	80	200
DAP[c] (mGy.cm^2)	13	30	222
Lateral X-ray tube			
kV	80	80	102
mA	50	80	200
DAP (mGy.cm^2)	28	67	371
Total DAP values (mGy.cm^2)[d]	41	97	593

Radiographic exposures undertaken with posterior-anterior-lateral stereographic biplanar imaging

[a] Kilovolts

[b] Milliamps

[c] DAP = dose area product for a child phantom representing a 5-year-old at phantom height of 72 cm

[d] Anterior + lateral DAP values

Inclusions

The local ethics review board approved of the study design and methods. A consecutive group of 18 children, 12 years of age or younger, planned for routine clinical and radiological investigation of scoliosis were offered micro-dose and reduced micro-dose images instead of one standard-dose image. An informed consent was obtained for each patient prior to imaging. Images with both protocols were obtained at the same radiological session, one after the other, no more than 2 min apart. This method allowed for direct comparison of 3D parameter reproducibility between the two modalities. Exclusion criteria were severe obesity, previous spine surgery with implants, and mal-positioning of the patients.

3D reconstructions

A validated method of 3D reconstruction of the spine from EOS 2D biplane images was used [14]. Patient data and acquisition settings were blinded and reconstructions took place in random order. Three operators, all trained within 3D reconstructions, did two reconstructions for each obtained image. One operator determined, for each patient, the levels of junctional and apical vertebrae for each scoliotic curve. Table 2 lists the 3D parameters investigated. Figure 2 illustrates 3D reconstruction images using the reduced micro-dose protocol.

Statistics

Intra- and inter-operator reproducibility were determined according to the ISO 5725-2:1994 standard, in terms of standard deviation. Bland-Altman plots were used to observe measurement agreement. Results were compared with previously published data on 3D reconstruction based on stereo-radiography and micro-dose [14, 17]. Correlations were analyzed with Spearman's rank coefficient; significance was set at 0.05.

Results

The reduced micro-dose protocol corresponds to a theoretical reduction of radiation exposure of approximately 58% and 93% compared with micro-dose and standard-dose protocols, respectively. Table 1 shows the three scan settings and DAP values for the child phantom.

Preliminary in vivo images with the new reduced micro-dose setting allowed sufficient quality for 3D reconstruction.

Fig. 2 Examples of 3D reconstruction from reduced micro-dose protocol, coronal and lateral views

Figure 3 illustrates an example of micro-dose and reduced micro-dose full-spine imaging.

A group of 18 consecutive children going for routine clinical investigation for scoliosis were then assessed with both micro-dose and reduced micro-dose imaging. Three children were excluded; two were carrying braces during imaging, one had an abnormal number of vertebrae (14 thoracic vertebrae). The remaining 15 children were included in the study. The mean age was 10.7 years (range 4–12), gender distribution amongst the included patients: four males and 11 females. Mean reconstruction time was 10 min (range 6–21 min) for the micro-dose and 9 min (range 5–16 min) for the reduced micro-dose. Reconstruction time was not correlated with Cobb angle (i.e., with scoliosis severity, $p > 0.05$).

Reproducibility

A total of 180 3D reconstructions were made (15 patients × 2 modalities × 3 operators × 2 occurrences). 3D reconstructions were possible for all patients, and key anatomical landmarks needed for 3D reconstructions were visible for patients in both protocols. However, for both protocols, mostly the reduced micro-dose group, spinous processes were in some cases

Table 2 The different 3D parameters investigated

3D parameters investigated									
3D parameters	Cobb angle	T1-T12 kyphosis	T4-T12 kyphosis	L1-S1 lordosis	AVR	TI	Pelvic incidence	Sacral slope	Pelvic tilt

AVR apical vertebra rotation, *TI* torsional index of the spine

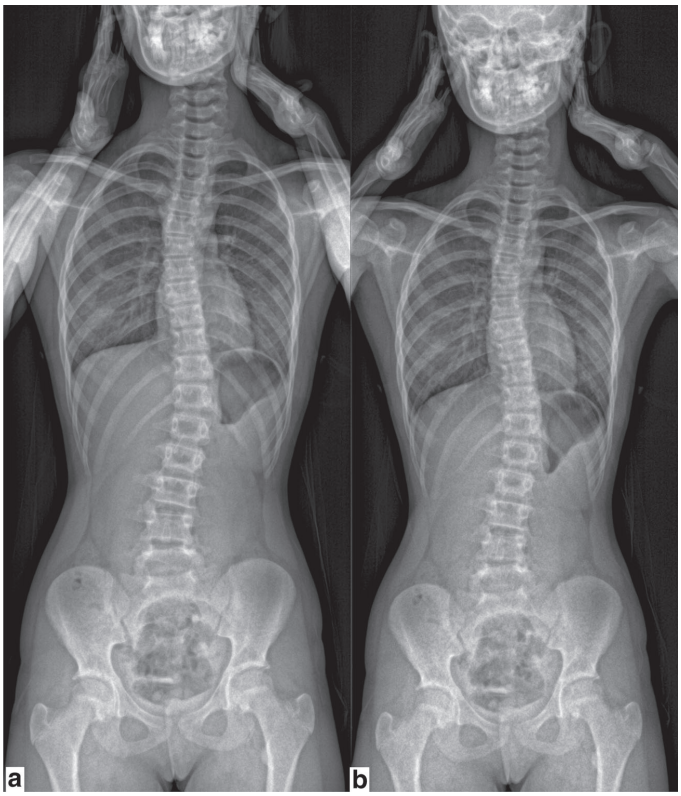

Fig. 3 **a** Coronal full-spine image in EOS scanner using micro-dose protocol. **b** Coronal full-spine image in EOS scanner using reduced micro-dose protocol

difficult to visualize because of increased vertebral rotation. Other anatomical landmarks such as vertebral endplates and pedicles were not affected to the same degree. Tables 3 and 4 show results on 3D repeatability and reproducibility along with results from previously published papers. Both micro-dose and reduced micro-dose showed good reproducibility; however, 3D reconstruction from standard-dose as demonstrated by Humbert et al 2009 [14] remained superior. Reproducibility between micro-dose and reduced micro-dose within this study was better for the micro-dose protocol. The highest degree of variability was on AVR and kyphosis parameters. Table 4 shows that reduced micro-dose was better

Table 3 Intra-operator repeatability of clinical parameters, in terms of standard deviation of uncertainty, obtained in the current study and compared with existing literature. All parameters are expressed in degrees

Intra-operator repeatability, variability from the mean										
Studies, mean Cobb angle	Protocol	Main Cobb angle	T1-T12 kyphosis	T4-T12 kyphosis	L1-S lordosis	AVR	Torsion	Pelvic incidence	Sacral slope	Pelvic tilt
Current study 16.1° (range 0.2–39)	Reduced micro-dose	4.3	5.3	4.7	4.6	4.7	4.7	4.3	3.2	2.6
	Micro-dose	2.4	5.3	4.0	3.5	5.3	3.5	3.1	2.6	2.7
Ilharreborde et al 2016 24.8° (range 4.6–64.7)	Micro-dose	3.6	4.8	4.5	5.8	–	–	5.2	5.2	1.3
Ilharreborde et al 2011 62° ± 11*	Standard-dose	4.8	5.9	4.4	5.1	5.3	–	4.6	4.3	1.0

*Standard deviation

Table 4 Inter-operator reproducibility of clinical parameters, in terms of standard deviation of uncertainty, obtained in the current study and compared with existing literature. All parameters are expressed in degrees

Inter-operator reproducibility, variability from the mean										
Studies, mean Cobb angle	Protocol	Main Cobb angle	T1-T12 kyphosis	T4-T12 kyphosis	L1-S lordosis	AVR	TI	Pelvic incidence	Sacral slope	Pelvic tilt
Current study 16.1° (range 0.2–39)	Reduced micro-dose	5.4	6.6	6.0	5.8	7.5	6.0	5.4	4.6	3.6
	Micro-dose	3.8	6.6	4.6	5.1	6.6	4.8	3.7	3.7	2.7
Ilharreborde et al 2016 24.8° (range 4.6–64.7)	Micro-dose	5.4	7.1	5.7	7.9	–	–	7.8	7.0	1.9
Ilharreborde et al 2011 62° ± 11*	Standard-dose	6.2	7.0	5.7	5.9	6.1	–	4.7	4.3	1.4
Humbert et al 2009 Mild scoliosis	Standard-dose	3.1	5.5	3.8	4.6	3.4	4.0	3.4	3.0	1.4

*Standard deviation

on all parameters except pelvic tilt (PT) and T4-T12 kyphosis, compared with Ilharreborde et al (2016) [17] "fast-spine" micro-dose reconstructions.

Discussion

The purpose of this study was to investigate and validate reproducibility of 3D reconstruction of the spine from stereoradiography with a reduced micro-dose protocol in scoliotic pediatric patients. For most 3D parameters in mild, reproducibility was comparable to previous studies [14, 15, 17]. As expected, the reduced micro-dose protocol was less reliable than standard-dose and micro-dose for some parameters. 3D transverse rotational parameter uncertainty, AVR and torsion, was higher in this study on both reduced micro-dose and micro-dose protocols than the reported values from Humbert et al (2009) [14] using standard-dose, as well as uncertainties on Cobb angle and T4-T12 kyphosis (5.4° and 6.0° in reduced micro-dose, respectively, versus 3.1° and 3.8° in the previous work). However, the reproducibility obtained using reduced micro-dose "full" 3D reconstruction was superior in all clinical parameters except for PT to the results obtained using "fast spine 5min process" (Ilharreborde 2016) using micro-dose in patients with scoliosis severity comparable to this study. Thus, the reduced micro-dose protocol offered acceptable 3D reconstruction reliability of the spine in patients with mild scoliosis. Depending on the objective of the exam, such reliability would be fine for initial screening and follow-up of scoliosis.

Limitations

The definition of minimal dose was inherently subjective, since only one surgeon was implicated in the semi-quantitative definition of the cutoff dose, but efforts were taken to make it as objectively as possible. Quantitative parameters to determine image quality were also tested (such as signal-to-noise ratio), but they tended to vary linearly with dose variations, showing no useful cutoff value. The semi-quantitative approach utilized, on the other hand, implicitly accounted for the visibility of the anatomical landmarks of interest for the interpretation of the radiographic information and it showed a cutoff value indicating that image interpretation below a certain radiation dose (28 mGy.cm^2) would suffer significantly.

A reduction of radiation dose exposure to the patients of more than 50% could be beneficial to the patients reducing potential harmful side effects to ionizing radiation considering the ALARA principle. Still, the risk benefit balance needs to always be evaluated according to the needs of a given radiological assessment. Existing EOS standard-dose protocol already offers high-quality images suitable for 3D reconstruction of the spine at a low radiation dose, as shown by Humbert et al [14]. For instance, the reduced micro-dose protocol would not be accurate enough to calculate the severity index of scoliosis progression [4] or simulate or plan surgery. Moreover, the reliability might not be accurate enough for research, where the development of algorithms and decision trees needs higher accuracy. Images obtained with reduced micro-dose were as expected of lower quality than standard-dose and micro-dose, i.e., more noisy and with less contrast. In standard-dose and micro-dose, the spinous processes are often difficult to visualize, which was generally worse for reduced micro-dose. Spinous process location is, along with pedicles, an important landmarks used to evaluate the axial orientation of the vertebra. However, pedicles were sufficiently recognizable in most patients, except one patient with severe kyphosis. This was independent of the imaging dose as it is inherent to the patient's spinal geometry; this type of patient would also have been challenging with other 2D modalities and does in

fact put a restriction on usability of 3D reconstruction from stereo-radiography. In some cases, regular CT should be advocated for.

For both modalities, T1, which is one of the landmarks needed to initialize the 3D reconstruction, was not always visible in lateral projection due to overlapping upper extremities/shoulders, although correct validated patient positioning was adopted in this work and patient malpositioning was the cause for exclusion. Nevertheless, sagittal inclination of T1 can usually be inferred by the orientations of the adjacent vertebrae. The same applies in the mid-thoracic region where there is low visibility in the lateral view because of the large body span traversed by the X-rays.

As shown above, operator time is still a limiting factor since the average 3D reconstruction time was 10 min, which is often not compatible with everyday clinical routine. A new and faster method is needed to benefit optimally from this 3D analysis method, potentially automated, to reduce user dependence [14, 15, 17]. We do not recommend this new protocol for children with implants or wearing braces as these cases were not yet investigated.

Conclusion

We propose a new reduced micro-dose protocol for 3D reconstructions based on stereo-radiography which offers reliable 3D reconstructions for preliminary screening and follow-up in children with mild scoliosis. However, standard-dose protocol remains the option of choice for most accurate assessment and 3D reconstruction. The reduced micro-dose protocol is applicable to existing EOS systems and can be taken into use for children being assessed for mild scoliosis right away and could replace micro-dose for these patients.

Funding Fondation ParisTech BiomecAM chair on subject specific modeling, with the financial support of Société Générale and Covea.

Compliance with ethical standards

Guarantor The scientific guarantor of this publication is Prof. Raphaël Vialle.

Conflict of interest Two authors of this manuscript declare relationship with the following company: EOS imaging®, Paris, France (Prof. Raphaël Vialle, consulting fees. Prof. Wafa Skalli, coinventor of the EOS system, with no personal financial benefice (royalties rewarded to research and education)).

Statistics and biometry No complex statistical methods were necessary for this paper.

Informed consent Written informed consent was obtained from all subjects (patients) in this study.

Ethical approval Institutional Review Board approval was obtained.

Methodology
- Prospective validation study with technical notes
- Multicenter study

References

1. Labelle H, Aubin CE, Jackson R, Lenke L, Newton P, Parent S (2011) Seeing the spine in 3D: how will it change what we do? J Pediatr Orthop 31:S37–S45. https://doi.org/10.1097/BPO.0b013e3181fd8801
2. Courvoisier A, Drevelle X, Dubousset J, Skalli W (2013) Transverse plane 3D analysis of mild scoliosis. Eur Spine J 22:2427–2432. https://doi.org/10.1007/s00586-013-2862-x
3. Donzelli S, Poma S, Balzarini L et al (2015) State of the art of current 3-D scoliosis classifications: a systematic review from a clinical perspective. J Neuroeng Rehabil 12:91. https://doi.org/10.1186/s12984-015-0083-8
4. Skalli W, Vergari C, Ebermeyer E et al (2017) Early detection of progressive adolescent idiopathic scoliosis. Spine (Phila Pa 1976) 42:823–830. https://doi.org/10.1097/BRS.0000000000001961
5. Deschênes S, Charron G, Beaudoin G et al (2010) Diagnostic imaging of spinal deformities: reducing patients radiation dose with a new slot-scanning X-ray imager. Spine (Phila Pa 1976) 35:989–994. https://doi.org/10.1097/BRS.0b013e3181bdcaa4
6. Nault ML, Mac-Thiong JM, Roy-Beaudry M et al (2014) Three-dimensional spinal morphology can differentiate between progressive and nonprogressive patients with adolescent idiopathic scoliosis at the initial presentation: a prospective study. Spine (Phila Pa 1976) 39:601–606. https://doi.org/10.1097/BRS.0000000000000284
7. Levy AR, Goldberg MS, Mayo NE, Hanley JA, Poitras B (1996) Reducing the lifetime risk of cancer from spinal radiographs among people with adolescent idiopathic scoliosis. Spine (Phila Pa 1976) 21:1540–1547. https://doi.org/10.1097/00007632-199607010-00011
8. Law M, Ma WK, Chan E et al (2017) Evaluation of cumulative effective dose and cancer risk from repetitive full spine imaging using EOS system: impact to adolescent patients of different populations. Eur J Radiol 96:1–5. https://doi.org/10.1016/j.ejrad.2017.09.006
9. Ronckers CM, Land CE, Miller JS, Stovall M, Lonstein JE, Doody MM (2010) Cancer mortality among women frequently exposed to radiographic examinations for spinal disorders. Radiat Res 174:83–90. https://doi.org/10.1667/RR2022.1
10. Simony A, Carreon LY, Jensen KE, Christensen SB, Andersen MO (2015) Incidence of cancer and infertility, in patients treated for adolescent idiopathic scoliosis 25 years prior. Spine J 15:S112. https://doi.org/10.1016/j.spinee.2015.07.076
11. Kadoury S, Mandel W, Roy-Beaudry M, Nault ML, Parent S (2017) 3-D morphology prediction of progressive spinal deformities from probabilistic modeling of discriminant manifolds. IEEE Trans Med Imaging 36:1194–1204. https://doi.org/10.1109/TMI.2017.2657225
12. Damet J, Fournier P, Monnin P et al (2014) Occupational and patient exposure as well as image quality for full spine examinations with the EOS imaging system occupational and patient exposure as well as image quality for full spine examinations with the EOS imaging system. Med Phys. https://doi.org/10.1118/1.4873333

13. Strauss KJ, Kaste SC (2006) ALARA in pediatric interventional and fluoroscopic imaging: striving to keep radiation doses as low as possible during fluoroscopy of pediatric patients-a white paper executive summary. J Am Coll Radiol 3:686–688. https://doi.org/10.1016/j.jacr.2006.04.008
14. Humbert L, De Guise JA, Aubert B, Godbout B, Skalli W (2009) 3D reconstruction of the spine from biplanar X-rays using parametric models based on transversal and longitudinal inferences. Med Eng Phys 31:681–687. https://doi.org/10.1016/j.medengphy.2009.01.003
15. Ilharreborde B, Steffen JS, Nectoux E et al (2011) Angle measurement reproducibility using EOSThree-dimensional reconstructions in adolescent idiopathic scoliosis treated by posterior instrumentation. Spine (Phila Pa 1976) 36:E1306–E1313. https://doi.org/10.1097/BRS.0b013e3182293548
16. Courvoisier A, Ilharreborde B, Constantinou B, Aubert B, Vialle R, Skalli W (2013) Evaluation of a three-dimensional reconstruction method of the rib cage of mild scoliotic patients. Spine Deform 1:321–327
17. Ilharreborde B, Ferrero E, Alison M, Mazda K (2016) EOS microdose protocol for the radiological follow-up of adolescent idiopathic scoliosis. Eur Spine J 25:526–531. https://doi.org/10.1007/s00586-015-3960-8
18. Dose WB, Dose O, Radiation T (2013) ATOM Dosimetry Phantoms. http://www.cirsinc.com/file/Products/701_706/701%20706%20ATOM%20PB%20110615.pdf. Accessed 17 Oct 2018

PRIMARY RESEARCH

A Nano-Dose Protocol For Cobb Angle Assessment in Children With Scoliosis: Results of a Phantom-based and Clinically Validated Study

Peter H. Pedersen, MD, Claudio Vergari, PhD,† Alexia Tran, MD,‡ Fred Xavier, MD, PhD,§ Antoine Jaeger, MD,‖ Pierre Laboudie, MD,‖ Victor Housset, MD,‖ Søren P. Eiskjær, MD,* and Raphäel Vialle, MD, PhD‖*

Study design: This was a prospective validation study with technical notes.

Objective: This study aimed to validate a new ultra–low-dose full-spine protocol for reproducible Cobb angle measurements—the "nano-dose" protocol.

Summary of Background Data: Scoliosis is a 3-dimensional (3D) deformity of the spine characterized by 3D clinical parameters. Nevertheless, 2D Cobb angle remains an essential and widely used radiologic measure in clinical practice. Repeated imaging is required for the assessment and follow-up of scoliosis patients. The resultant high dose of absorbed radiation increases the potential risk of developing radiation-induced cancer in such patients. Micro-dose radiographic imaging is already available in clinical practice, but the radiation dose delivered to the patient could be further reduced.

Methods: An anthropomorphic child phantom was used to establish an ultra–low-dose protocol in the EOS Imaging System still allowing Cobb angle measurements, defined as nano-dose. A group of 23 consecutive children presenting for scoliosis assessment, 12 years of age or younger, were assessed with standard-dose or micro-dose and additional nano-dose full-spine imaging modalities. Intraobserver and interobserver reliability of determining the reliability of 2D Cobb angle measurements was performed. The dosimetry was performed in the anthropomorphic phantom to confirm theoretical radiation dose reduction.

Results: A nano-dose protocol was established for reliable Cobb angle measurements. Dose area product with this new nano-dose protocol was reduced to 5 mGy×cm^2, corresponding to one sixth of the micro-dose protocol (30 mGy×cm^2) and <1/40th of the standard-dose protocol (222 mGy×cm^2). Theoretical dose reduction, for posteroanterolateral positioning was confirmed using phantom dosimetry. Our study showed good reliability and repeatability between the 2 groups. Cobb variability was <5 degrees from the mean using 95% confidence intervals.

Conclusions: We propose a new clinically validated nano-dose protocol for routine follow-up of scoliosis patients before surgery, keeping the radiation dose at a bare minimum, while allowing for reproducible Cobb angle measurements.

(*Clin Spine Surg* 2019;00:000–000)

Scoliosis is a 3-dimensional (3D) deformity of the spine that can be characterized by 3D clinical parameters. The quantitative evaluation of scoliosis is important to follow its progression, and, when planning for conservative or surgical procedures, results in numerous radiologic examinations. High levels of cumulated absorbed radiation dose have been associated with an increased risk of cancer among these patients.[1–3] To reduce this potential danger from iatrogenic ionizing radiation, considerable research into radiation dose optimization has been ongoing. The principal aim is to keep the radiation dose at a minimum while ensuring sufficient image quality for diagnosis and treatment, as per the ALARA principle (As Low As Reasonably Achievable).[4,5] Various systems adhering to the ALARA principle exist; one such system is the EOS slot-scanner (EOS Imaging, Paris, France).[6] The EOS system yields high-quality images at radiation doses lower than conventional x-ray systems, which has been described in detail previously.[7–11] EOS standard-dose and micro-dose options are already available in clinical practice, but we hypothesized that the radiation delivered to the patient could be even further reduced, still allowing reproducible Cobb angle measurements.

The Cobb angle is the angle between the upper endplate and the lower endplate of the 2 vertebrae at the extremes of the assessed curvature. It is used to distinguish

Received for publication August 21, 2018; accepted April 19, 2019.

From the *Department of Orthopedic Surgery, University Hospital of Aalborg, Aalborg, Denmark; †Arts et Metiers ParisTech, LBM/Institut de Biomecanique Humaine Georges Charpak; ‡Department of Radiology, Armand Trousseau Hospital, Sorbonne Université, APHP Paris, Paris, France; §Department Surgery (Spine), QEII Health Sciences Centre—Halifax Infirmary, Dalhousie University, Halifax, Canada; and ‖Department of Pediatric Orthopedics, Armand Trousseau Hospital, Sorbonne Université, APHP Paris, Paris, France.

R.V. has received honoraria from EOS Imaging, Paris, France. The remaining authors declare no conflict of interest.

Reprints: Peter H. Pedersen, MD, Department of Orthopedic Surgery, University Hospital of Aalborg, Hobrovej 18-22, 9000 Aalborg, Denmark (e-mail: php@rn.dk).

Copyright © 2019 Wolters Kluwer Health, Inc. All rights reserved.

Copyright © 2019 Wolters Kluwer Health, Inc. Unauthorized reproduction of this article is prohibited.

between normal and pathologic conditions of the spine. Cobb angle can be reliably measured from a 3D reconstruction of the spine.[12] This method allows taking into account the patient's orientation relative to the imaging plane and the 3D/2D projection bias.[13] Nevertheless, 3D imaging capabilities in weight-bearing position are not yet widespread, and 2D Cobb angle remains an important and widely used radiologic measure in clinical practice. 2D Cobb angle is measured manually on a coronal x-ray by drawing intersecting perpendicular lines to the above-mentioned endplates or, more commonly, by fixing landmark points parallel to these endplates in a picture archiving and communication system (PACS), automatically calculating the Cobb angle.

Differences between computer-assisted methods and manual methods have been evaluated in several review papers with regard to variability and reproducibility.[14–17] The consensus states that a change of 5 degrees in Cobb angle over a 6-month period is consistent with a significant progression of spinal curvature. Moreover, the arbitrary limit between a "healthy" spine and a scoliotic spine is 10 degrees in the coronal plane.[17] This study aimed to determine the lowest irradiation dose (nano-dose) that would still yield a reproducible 2D Cobb angle measurement, assuming a 5-degree uncertainty as acceptable.

METHODS

First, a phantom-based study was performed to semiquantitatively define the minimal dose allowing visibility of the spine, defined as "nano-dose," as detailed below. Then, a prospective cohort of scoliosis patients was recruited to determine the reliability of 2D Cobb angle measurement with nano-dose, which was compared with the reliability obtained on the same patients with subsequent micro-dose imaging.

Establishing and Verifying Nano-Dose

Initial steps to determine the lowest possible dose, still allowing Cobb angle measurements, were undertaken on an anthropomorphic phantom representing a 5-year-old child (ATOM-CIRS; Computerized Imaging Reference System Inc., Norfolk, VA).[18] Successive reductions of scan parameters were followed by phantom imaging in posteroanterolateral (PAL) exposure. This technique is a common protocol at many institutions and is also the standard for conventional radiology of the spine. Doses were lowered by reducing the current (mA) and the scan speed, which are both directly proportional to the radiation dose. For instance, halving the current leads to a 50% diminution in the radiation dose, and an increase from scan speed 3 to scan speed 2 further reduces the radiation dose by one third.

An experienced surgeon, blinded to the imaging settings, rated the images' quality on a scale from 1 to 5. A sharp decrease in image quality was detected at dose area product (DAP) $<5\,mGy\times cm^2$ for the coronal plane (Table 1), which was retained as the target nano-dose. Clinical pilot imaging was performed on pediatric patients being assessed for suspected scoliosis, at 3 different settings around the previously selected nano-dose, to qualitatively evaluate image quality and confirm the nano-dose of $5\,mGy\times cm^2$. Table 1 shows the scan parameters for the chosen nano-dose setting and resulting reduction of DAP when applied to the phantom.

TABLE 1. EOS Scan Parameters For Nano-Dose and Micro-Dose Protocols

Acquisition Protocol	Nano-Dose	Micro-Dose	Standard-Dose
Morphotype	Small	Small	Small
Scan speed	2	3	4
Coronal plane*			
kV	60	60	83
mA	20	80	200
DAP† ($mGy\times cm^2$)	5	30	222
Lateral plane			
kV	80	80	103
mA	20	80	200
DAP† ($mGy\times cm^2$)	11	67	371

*Coronal posteroanterior positioning.
†Dose area product (DAP) (the absorbed dose multiplied by area irradiated) displayed for the pediatric phantom with a scan field height of 72 cm.

Dosimetry with thermoluminescent dosimeters was performed in the pediatric phantom with the chosen nano-dose setting to determine the absorbed radiation dose. A method previously published by Damet et al[10] was used to calculate effective dose from measured mean organ doses multiplied by organ-specific tissue weighting factors according to The International Committee on Radiological Protection (ICRP), publication 103.[4]

Inclusions

A consecutive group of 24 children going for routine full-spine imaging control of scoliosis were offered nano-dose imaging in addition to micro-dose imaging instead of routine standard-dose imaging. A predefined age limit of 12 years of age was chosen. They did not suffer from any neurological or syndromic conditions, and they were able to stand by themselves without means of external help. Patients and parents were provided with written and oral information concerning the study, and signed consent was obtained for each patient. Our local ethics committee approved the study design and protocol. The 2 sets of images were taken one after the other within 2 minutes' time. The patients were carefully instructed to remain in the same positions during acquisitions.

All the patients were included from a juvenile or early-onset idiopathic scoliosis screening or follow-up examination.

Reproducibility Assessment

Five observers took part in the study, 4 orthopedic surgeons and 1 radiologist, all with experience of measuring Cobb angles. Curves were measured at predesignated levels to make sure that the same curves were measured. The same software and technical conditions were used (Carestream PACS Carestream Health Inc., Rochester, NY). As shown in Figure 1, Cobb angle was automatically calculated when digitizing 2 segments

Copyright © 2019 Wolters Kluwer Health, Inc. All rights reserved.

Copyright © 2019 Wolters Kluwer Health, Inc. Unauthorized reproduction of this article is prohibited.

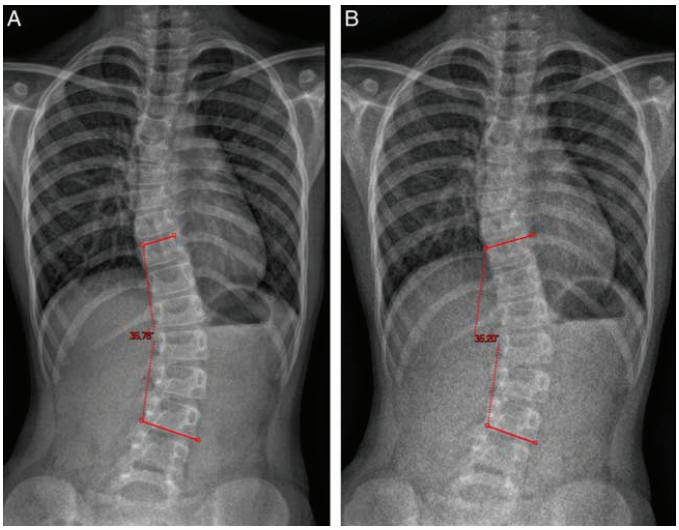

FIGURE 1. Cobb angle measurement with micro-dose (A) and Cobb angle measurement with nano-dose (B).

parallel to endplates of the vertebra at each extreme of the curve. Observers rated micro-dose and nano-dose images 3 times each in a randomized order and over a 2-week period to avoid bias.

For those patients with a 2D Cobb angle >10 degrees, intraobserver and interobserver reliability of Cobb angle measurements were assessed, according to the ISO-5725 standard, in terms of twice the SD of repeated measurements. For both radiation doses, Cobb angle limits of agreement were reported in Bland-Altman plots. Some of the patients who were imaged for the first suspicion of scoliosis, had Cobb angles <10 degrees; for these patients, the reliability of the diagnosis was estimated as the number of Cobb angle measurements being higher or lower than 10 degrees.

RESULTS

A total of 23 children with a mean age of 11 years (range, 9–12 y) underwent micro-dose and nano-dose full-spine examinations. Two patients were excluded because of artifacts due to metallic implants close to the spine, which made image quality for nano-dose unacceptable, and no further patients with implants were included. One patient was excluded before nano-dose imaging owing to severe obesity [body mass index (BMI > 30)] rendering images with the micro-dose protocol of poor quality. A total of 630 Cobb angle measurements were made, 3 measurements per observer of 2 dose levels for each of the 21 patients.

Seven patients showed an average Cobb angle <10 degrees. For these patients, 88% of the Cobb angle measurements in the micro-dose (ie, 92 measurements of 105) were consistently <10 degrees. With nano-dose, 96% of the measurements (ie, 101 of 105) were <l0 degrees.

For the remaining 14 patients with a Cobb angle >10 degrees, mean Cobb angle was 25 degrees (range, 11–49 degrees).

The intraobserver repeatability and interobserver reproducibility relative to the 2 dose levels are shown in Table 2. As expected, intraobserver repeatability was higher than interobserver reproducibility. The results showed good reliability, that is, ≤5 degrees uncertainty from the mean using 95% confidence intervals (CIs). Nano-dose and micro-dose showed the same intraoperator repeatability, whereas nano-dose was 1 degree less reproducible than micro-dose. Figures 2 and 3 illustrate Bland-Altman plots for the 2 imaging modalities, showing that measurement uncertainty did not increase with curve severity and that no systematic bias was observed.

The proportional dose reduction from micro-dose to nano-dose was 83% (ie, nano-dose was 6 times less irradiating than micro-dose). DAP values using the same collimation displayed by the EOS system have been listed in Table 1. Effective dose with the pediatric phantom in PAL exposure was 3.8 μSv (95% CI: 3.5–4.2), whereas, previously, an effective dose of 22 μSv (95% CI: 20–23) was reported for the same phantom in PAL projection using EOS micro-dose protocol and 157 μSv for standard-dose.[11]

TABLE 2. Reproducibility of Cobb Angle Measurements

Acquisition Protocol	Micro-Dose	Nano-Dose
Intraoperator reproducibility (deg.)*	3.0	3.4
Interoperator reproducibility (deg.)	4.1	5.0

*Reproducibility values are expressed as a variation from the mean (2 SD).

Copyright © 2019 Wolters Kluwer Health, Inc. All rights reserved.

Copyright © 2019 Wolters Kluwer Health, Inc. Unauthorized reproduction of this article is prohibited.

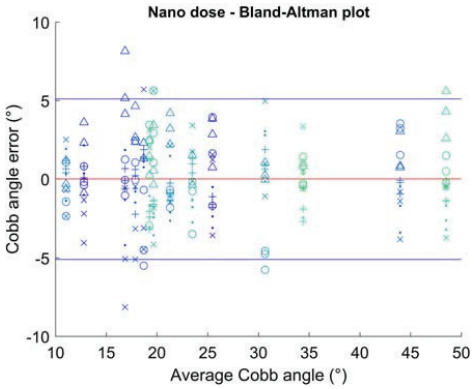

FIGURE 2. Bland-Altman plot for Cobb angle in nano-dose x-rays. Symbols represent different operators.

DISCUSSION

To the best of our knowledge, the proposed nano-dose protocol of this study offers the lowest possible dose, with existing low-dose systems allowing for reproducible Cobb angle measurements. Twenty-one consecutive patients were assessed with micro-dose and nano-dose x-rays. Repeatability and reproducibility were good and comparable between the 2 modalities. The interobserver and intraobserver variability for both micro-dose and nano-dose was well within previously published measures for conventional radiology.[14,15,17]

Radiation exposure to patients with the new nano-dose protocol was equal to an effective dose of ~3.8 μSv, that is, one sixth of the existing micro-dose protocol and roughly 40 times less than the EOS standard-dose protocol, a dose that is <1 day of natural background exposure —that is, the worldwide mean weekly exposure is estimated at ~46 μSv.[19] This protocol values safety by means of lowest possible risk of stochastic health effects from ionizing radiation and adheres to the ALARA principle by still allowing for reproducible Cobb angles.

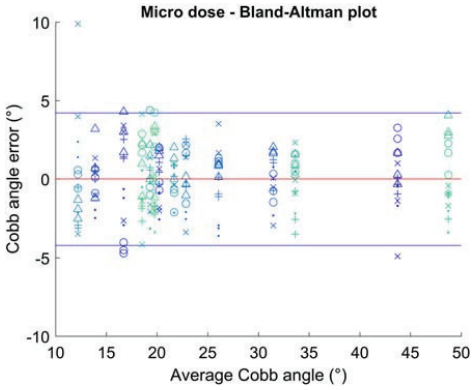

FIGURE 3. Bland-Altman plot for Cobb angle in micro-dose x-rays. Symbols represent different operators.

Limitations of this Study

The quality was as expected—worse for nano-dose images. Figure 4 shows micro-dose and nano-dose films. For some, it was difficult to identify the endplates. This occurred both with micro-dose and with nano-dose techniques, although more often for nano-dose, and would be expected to affect the reproducibility of the Cobb angles negatively, as described in previous studies. Nano-dose actually seemed more accurate toward defining no scoliosis (Cobb < 10 degrees). The reason could be that, when the endplate was not easily recognizable because of reduced image quality, observers tended to use other landmarks that remain visible, such as the pedicles, and they converge toward the same result, whereas endplate orientation is not always easily interpreted even in normal quality images.

Another limitation is the fact that repeated measurements were made on preselected end vertebrae, thus omitting variable observer identification of end vertebrae. This approach was chosen to limit the source of the uncertainty to the imaging. Moreover, lateral images were not analyzed; initial qualitative analysis of these images suggest that nano-dose should solely be used for anteroposterior or posteroanterior projection in assessing the possible progression of scoliosis in the coronal plane. Although the endplate remains visible in very mild scoliosis, the interpretation of the sagittal plane in more severe scoliosis could be questionable. Regardless of image quality, it will always be less difficult to measure Cobb angle in the coronal plane in patients with hypokyphosis or normal degrees of kyphosis, as opposed to patients with hyperkyphosis in severe scoliosis.

There is always a risk of confounding, a comparatively small number of patients might lead to falsely increased repeatability. However, the order of measurement was randomized to avoid memorization of angles, and measurements were performed by 5 observers making 3 separate measurements for each modality, decreasing the risk of falsely elevated repeatability. Having 5 observers is common practice for such a study.[15]

The results and conclusions of this study were based on children between 9 and 12 years of age, with a BMI < 26. Further research is necessary to determine whether such low dose could provide good image quality in younger children, who present incomplete mineralization of the spine, or older children who could have higher BMI.

Cobb Angle Controversy

An accurate and reproducible measure is crucial to diagnose, follow-up, and evaluate treatment of scoliosis. 2D Cobb angle is not an exact and precise measure, as has been discussed earlier. Although more sophisticated methods exist to obtain Cobb angle and other 3D parameters of the scoliotic trunk, they are not yet widespread, and 2D Cobb angle remains the most widely used

Copyright © 2019 Wolters Kluwer Health, Inc. All rights reserved.

Copyright © 2019 Wolters Kluwer Health, Inc. Unauthorized reproduction of this article is prohibited.

FIGURE 4. Micro-dose and nano-dose spine images in frontal and lateral views.

and referenced radiologic method within deformity surgery to assess curve magnitude.[17] In our daily clinical practice, Cobb angle measurement is used to assess curve progression in children and adolescents during growth. A curve magnitude progression of >5 degrees after 6 months is consistent with progressive scoliosis and may require orthotic treatment using a brace. Nevertheless, limiting the observation of scoliosis to the coronal plane might lead to missing important factors that might be related to progression, such as sagittal global alignment, unbiased vertebral axial rotations, rib cage deformity, etc. Moreover, lowering the dose too much would be against the ALARA principle: on the one hand, it would decrease the potential risk of future cancer development. In contrast, lower quality of the image might not allow the surgeon to detect specificities of the patient or localized alterations.

Dose-Optimization Controversy

In a recent paper by Siegel et al,[20] the issue of dose optimization has been taken up for revision. According to the authors, ionizing radiation from medical diagnostic equipment has not been proven to cause health risks with regard to radiation-induced cancer, and might, in fact, be dangerous to patients for not being diagnosed correctly instead. They do state that eliminating all nonclinically warranted medical diagnostic procedures is important, but claim that "the attempts to lessen fictitious risk by lowering dose in clinically warranted studies is a misapplication of the principles." However, the authors have not referred to any of the studies showing an association with increased risk of cancer mortality, for example, among scoliosis patients after repeated exposure to diagnostic x-rays.[2] Indeed, it is extremely difficult to prove direct relations between radiation exposure and cancer, but likewise difficult to prove the opposite.

Is there a need to reduce dose further, when the EOS micro-dose, which has previously been validated with regard to image quality for scoliosis assessment,[21] is already <1 week of natural background radiation and in accordance with ALARA?

The gain for the patient is a reduced potential risk of radiation-induced cancer in the long term. The potential risks are as follows: bad image quality and overevaluation or underevaluation of scoliosis severity. The former can be neglected, as long as obese patients and patients with metal implants are excluded. Moreover, even if an additional micro-dose or standard-dose EOS needs to be performed, the dose delivered by the nano-dose would still be negligible. Overevaluation could rise from large errors in Cobb angle measurements; given the present results, this can be excluded as well. Underevaluation of severity can arise from neglecting aspects other than Cobb angle that characterize a progressive phenotype: altered sagittal alignment, spinal torsion, etc.

CONCLUSIONS

Results show that reproducibility for the proposed nano-dose protocol is not significantly inferior to the micro-dose protocol for coronal plane Cobb angle assessment. The new protocol is not intended to take over first diagnostic imaging or presurgery planning, but we suggest it could be used for routine follow-up of children 12 years of age or younger, being observed for possible progression of scoliosis. The parents and patients would be assured that the protocol to the best of our knowledge poses no more risk than living daily life; thus, repeating images every 3–6 months would not pose any health risks or concerns. This protocol allows for safely repeated evaluations of potential Cobb angle progression.

ACKNOWLEDGMENTS

The authors acknowledge the valuable help from University College Nordjylland (Radiografskolen), 9220 Aalborg Ø, Denmark, for providing access to TLD irradiator

Copyright © 2019 Wolters Kluwer Health, Inc. All rights reserved.

Copyright © 2019 Wolters Kluwer Health, Inc. Unauthorized reproduction of this article is prohibited.

and dose reader along with technical support. They also thank Professor Hubert Ducou le Pointe at the Radiological Department at Sorbonne Université, Armand Trousseau Hospital, APHP Paris, France, for helping facilitate this study. The authors are grateful to the ParisTech BiomecAM chair program on subject-specific musculoskeletal modelling (with the support of ParisTech and Yves Cotrel Foundations, Société Générale, Proteor, and Covea).

REFERENCES

1. Levy AR, Goldberg MS, Mayo NE, et al. Reducing the lifetime risk of cancer from spinal radiographs among people with adolescent idiopathic scoliosis. *Spine (Phila Pa 1976)*. 1996;21: 1540–1547.
2. Doody MM, Ronckers CM, Land CE, et al. Cancer mortality among women frequently exposed to radiographic examinations for spinal disorders. *Radiat Res*. 2010;174:83–90.
3. Simony A, Christensen SB, Jensen KE, et al. Incidence of cancer and infertility, in patients treated for adolescent idiopathic scoliosis 25 years prior. *Eur Spine J*. 2015;24(suppl 1):S740.
4. The International Commission on Radiological Protection. The 2007 Recommendations of the International Commission on Radiological Protection. ICRP Publication 103. *Ann ICRP*. 2007;37:2–4.
5. Strauss KJ, Kaste SC. ALARA in pediatric interventional and fluoroscopic imaging: striving to keep radiation doses as low as possible during fluoroscopy of pediatric patients-a white paper executive summary. *J Am Coll Radiol*. 2006;3:686–688.
6. Melhem E, Assi A, El Rachkidi R, et al. EOS(®) biplanar X-ray imaging: concept, developments, benefits, and limitations. *J Child Orthop*. 2016;10:1–14.
7. Deschênes S, Charron G, Beaudoin G, et al. Diagnostic imaging of spinal deformities: reducing patients radiation dose with a new slot-scanning X-ray imager. *Spine (Phila Pa 1976)*. 2010;35: 989–994.
8. Yvert M, Diallo A, Bessou P, et al. Radiography of scoliosis: Comparative dose levels and image quality between a dynamic flat-panel detector and a slot-scanning device (EOS system). *Diagn Interv Imaging*. 2015;96:1177–1188.
9. Kalifa G, Charpak Y, Maccia C, et al. Evaluation of a new low-dose digital X-ray device: first dosimetric and clinical results in children. *Pediatr Radiol*. 1998;28:557–561.
10. Damet J, Fournier P, Monnin P, et al. Occupational and patient exposure as well as image quality for full spine examinations with the EOS imaging system. *Med Phys*. 2014;41:063901.
11. Pedersen PH, Peterson AG, Østgaard SE, et al. EOS® micro-dose protocol: first full-spine radiation dose measurements in anthropomorphic phantoms and comparisons with EOS standard-dose and conventional digital radiology. *Spine (Phila Pa 1976)*. 2018;43: E1313–E1321.
12. Humbert L, De Guise JA, Aubert B, et al. 3D reconstruction of the spine from biplanar X-rays using parametric models based on transversal and longitudinal inferences. *Med Eng Phys*. 2009;31:681–687.
13. Lechner R, Putzer D, Dammerer D, et al. Comparison of two- and three-dimensional measurement of the Cobb angle in scoliosis. *Int Orthop*. 2017;41:957–962.
14. Kuklo TR, Potter BK, Schroeder TM, et al. Comparison of manual and digital measurements in adolescent idiopathic scoliosis. *Spine (Phila Pa 1976)*. 2006;31:1240–1246.
15. Langensiepen S, Semler O, Sobottke R, et al. Measuring procedures to determine the Cobb angle in idiopathic scoliosis: a systematic review. *Eur Spine J*. 2013;22:2360–2371.
16. Vrtovec T, Pernuš F, Likar B. A review of methods for quantitative evaluation of spinal curvature. *Eur Spine J*. 2009;18:593–607.
17. Papaliodis D, Bonanni P, Roberts T, et al. Computer assisted Cobb angle measurements: a novel algorithm. *Int J Spine Surg*. 2017;11:167–172.
18. Computerized Imaging Reference Systems, Inc. Whole body dose, organ dose, therapeutic dose. ATOM Dosimetry Phantoms; 2013. Available at: http://www.cirsinc.com/wp-content/uploads/2019/05/701-706-ATOM-PB-120418.pdf. Accessed May 24, 2019.
19. United Nations Scientific Committee on the Effects of Atomic Radiation (UNSCEAR). Sources and effects of ionizing radiation; 2010.
20. Siegel JA, Sacks B, Pennington CW, et al. Dose optimization to minimize radiation risk for children undergoing CT and nuclear medicine imaging is misguided and detrimental. *J Nucl Med*. 2017;58:865–868.
21. Ilharreborde B, Ferrero E, Alison M, et al. EOS microdose protocol for the radiological follow-up of adolescent idiopathic scoliosis. *Eur Spine J*. 2016;25:526–531.

 Copyright © 2019 Wolters Kluwer Health, Inc. All rights reserved.

Copyright © 2019 Wolters Kluwer Health, Inc. Unauthorized reproduction of this article is prohibited.

Study IV

EOS, O-arm, X-Ray; what is the cumulative radiation exposure during current scoliosis management?

Ari Demirel, Peter Heide Pedersen, Søren Peter Eiskjær

Abstract

Introduction:

Patients undergoing scoliosis management are exposed to repeated radiological imaging. Previous studies have shown an increase in incidence of cancer among these patients. The primary aim of this study was to evaluate the radiographic examinations and cumulative radiation dose to which scoliotic patients are exposed. Secondly, to compare in-house algorithms of scoliosis management and radiographic follow-up to international spine-centers and current consensus literature.

Materials and methods: A single-center retrospective review evaluating type and frequency of radiographic imaging and total cumulative radiation exposure to patients treated for scoliosis. Inclusions: patients followed for idiopathic scoliosis in the years 2013-2016. A survey asking for information on management and radiological follow-up algorithms was sent to a number of international spine centers for comparison with in-house algorithm.

Results:

Patients who underwent surgery received an approximately 10-fold higher median cumulative radiation dose than those treated conservatively. Variety of radiological follow-up algorithms among 8 spine centers was observed.

Conclusion:

Cumulative radiation dose during scoliosis treatment varies substantially depending on radiographic follow-up protocol, intraoperative and ancillary imaging. By using low-dose x-ray systems in combination with low-dose protocol for intraoperative navigation it is possible to keep exposure to patients at a minimum, while still providing optimal care.

Funding: No funding received

TRIAL REGISTRATION: not relevant

Introduction

Scoliosis patients are exposed to repeated radiological imaging, during assessment, treatment and follow-up. Previous studies have shown a correlation between increased risk of cancer and exposure to ionizing radiation during scoliosis follow-up[1–3], especially an increase of breast cancer mortality has been of concern. In recent years much effort has gone into optimization of X-ray

equipment and imaging protocols in order to reduce exposure of ionizing radiation to our patients[4, 5]. As of today, there is no known lower limit of the amount of ionizing radiation which might lead to radiation-induced cancer and thus we have to limit the use of ionizing radiation, while maintaining adequate image quality for correct treatment of our patients. The primary aim of this study was to evaluate the frequency and type of radiographic examinations to which scoliotic patients are exposed at our institution and to estimate the total cumulative radiation dose to which a typical scoliotic patient is subjected. Secondly, a survey was sent out to nine international spine-centers asking for information on scoliosis assessment and follow-up in order to compare to our in-house algorithms and the current consensus literature.

Methods

A single center retrospective review of medical charts on patients treated for idiopathic scoliosis was performed. Ethical approval for the study was not needed according to the Regional Committee on Health Ethics, approval for establishing a data base was obtained according to Danish law.

Inclusions: all patients aged 0-18 years of age, who were either treated surgically or conservatively, at our institution in the years 2013-2016. Braced patients and patients followed only by radiological observation of curve progression were gathered in the same group and termed conservative. Patients with neuromuscular disease or any type of severe syndromic disease were excluded.

Medical records and the Picture Archiving and Communication System (PACS) were scrutinized to retrieve information on the number and types of radiographic imaging to which patients were subjected. Included were all imaging in relation to the assessment, follow-up and treatment of idiopathic scoliosis used at our institution. This included conventional digital full-spine scoliosis radiographs (CR), EOS® (EOS-imaging, Paris, France) low-dose full-spine stereo-radiography and computerized tomography (CT), including both intraoperative navigation (O-arm® Cone beam CT, Medtronic Inc.) and ancillary CT and PET-CT.

The numbers and projections of full-spine CR were registered as separate exposures, eg. coronal and lateral imaging of the spine was counted as two exposures. In the case of splicing/stitching of full-spine images, each separate exposure was counted. The same method was used to quantify the numbers and projections of EOS images.

Estimation of cumulative radiation dose

The total cumulative radiation dose to the scoliotic patients was estimated by calculating the theoretic amount of full-body absorbed radiation dose in terms of effective dose in millisieverts (mSv). In order to calculate the cumulative radiation dose from CR and EOS, the number of images divided by two (coronal and lateral

planes) were multiplied by effective dose references for CR-and EOS stereo-radiography for full-spine examinations. The reference doses for full-spine examinations were estimated based on phantom dosimetry[6]. Reference doses: CR anterior-posterior-lateral (APL) projections (0.545 mSv) and EOS standard-dose APL projections (0.220 mSv) All doses had been calculated according to the International Commission of Radiologic Protection (ICRP), ICRP-103 approach[7].

Effective doses for the O-arm 3D cone beam CT scans and ancillary CT and PET-CT were calculated based on Dose Length Product (DLP) and CT conversion factors according to the Danish National Board of Health, Institute of Radiation Protection (SIS)[8]. Effective doses for intra- operative 2D fluoroscopy using the O-arm were calculated by using dose area product (DAP) values and x-ray conversion factors according to the Danish National Board of Health, Institute of Radiation Protection (SIS). At our institution we routinely use low-dose intraoperative scan protocol (70kVp/20mA) introduced by Petersen et al in 2012[9], whereby CT dose from the O-arm was reduced by almost 90% compared with default protocol.

Algorithms for scoliosis follow-up at our institution

Follow-up for scoliosis at our institution comprises clinical examination and biplane full- spine imaging. Since the fall of 2014 EOS low-dose stereo-radiography has been first choice for full-spine radiography, and CR biplane imaging solely used in cases where EOS was not available. Figure 1, illustrates the EOS low-dose scanner, a system that has been described to markedly reduce radiation dose exposure to patients. The system has been described in detail previously**(10).** Figure 2, illustrates the follow-up and treatment algorithms at our institution.
If brace treatment is initiated, the Charleston Nighttime bending brace (Charleston® bending brace, South Carolina, USA) is the treatment of choice.
Postoperative radiographs are performed for all cases of scoliosis: before discharge from hospital and, at 6 months, 1 year and 2 years postoperatively.

Consensus survey for scoliosis follow-up at international spine centers

A survey was forwarded to nine international orthopedic spine centers, in Denmark, Norway, Sweden, Spain, UK, France and USA, dealing with the assessment and treatment of scoliosis, by using a web based survey tool (Survey Monkey, https://www.surveymonkey.com). All centers served a population larger than 1 million, four of these were high volume centers performing more than 100 surgeries for scoliosis per year.
The survey included questions about the practice of radiological follow-up of scoliotic patients to illustrate the similarities or differences among centers, and to compare the answers with current published international consensus guidelines[11–13]. The questionnaire used can be found at the following link: https://www.dropbox.com/s/mlladixj2dwy8bm/SurveyMonkey_160922409-2.pdf?dl=0

Results

Final inclusions

Demographics for the 61 patients included in this study are shown in Table 1. Six patients underwent more than one surgery; three were managed initially with growing rod systems and secondly final correction surgery with posterior spinal fusion. Another three patients underwent additional revision surgeries; two cases owing to progression of curves adjacent to fusion, and one patient owing to implant failure (screw loosening and rod breakage).

Radiological exposure

Radiologic imaging and exposure has been expressed in terms of numbers of images and radiation dose (effective dose) to patients from all modalities during assessment, treatment and follow-up, Table 1. In 66%(73/111) of the intraoperative scans used for safe instrumentation, the O-arm low-dose protocol was used. Dose from a single low-dose scan of 70kVp/20mA was found to be 0.45mSv, comparatively a default scan of 120kVp/40mA was 4.02mSv.

Patients who underwent surgery received an approximately 10-fold higher median cumulative radiation dose (excluding ancillary CT and PET-CT) than those treated conservatively.

Ancillary radiological imaging, from CT and PET-CT, on average resulted in an approximate 100% increase of total dose from all routine imaging (CR, EOS and Intra-operative O- arm based navigation and fluoroscopy), Table 2.

Approximately 25% (39.04mSv/161.82mSv) of total intraoperative radiation dose from the O-arm was a result of 2D fluoroscopy.

Mean/median weight and height at time of surgery were 54.9/54kg (range 42-80) and 166.2/165cm (range147-184), values directly comparable to the female dosimetry phantom, from which the reference doses were estimated; weight 55 kg and height 160 cm[11].

Survey

Eight out of nine international spine-centers, each serving a population size from 1 million to more than 10 million, answered our survey regarding treatment and radiological follow-up algorithms on patients with adolescent idiopathic scoliosis. The usual interval between preoperative imaging varied among the centers, half (3/6) of those who answered this question saw patients for radiographic controls every 3 months, the other half every 6 months. Surgically treated patients were seen anywhere from one to four times for radiographic follow-up over a period of time, ranging from 6 months to 2 years postoperatively. Five centers saw patients every six months after instituted brace treatment, three centers once every year. A variety of radiographic systems and techniques used at the different centers are shown in Table 3.

Discussion

To the best of our knowledge, this retrospective study represents the first assessment of the cumulative radiation dose from CR, EOS stereo-radiography and the O-arm for a typical patient undergoing current management for idiopathic scoliosis. Patient demographics and magnitude of perioperative x- ray/EOS acquisitions were comparable to other studies[1,2,15–17], as well as the mean number of levels fused.

Exposures and radiation dose

As expected and previously shown by Presciutti et al[16], the patients who underwent surgery had substantially more radiographic imaging than the conservative group, and thus received higher levels of absorbed radiation dose. The large difference in observed absorbed radiation dose among the two groups was mainly due to intraoperative imaging as well as ancillary imaging. Apart from this, the combined observation time for the conservative group was shorter, to some extent caused by the fact that a part of the conservative group was only assessed once or just a few times resulting in a low number of total follow-up images.

Intraoperative imaging from O-arm CT and fluoroscopy made up roughly 50% of the total amount of absorbed radiation dose in the surgical group. In the study by Presciutti et al[16] intraoperative imaging accounted for 78% of total accumulated dose. The reason for our percentage being lower may very well owe to the low-dose intraoperative scan protocols used at our institution. However, our intraoperative dose exposure would have been even lower if a higher degree of adherence to the low-dose protocol had been observed.

The fact that just one ancillary CT or PET-CT resulted in a two-fold increase of total cumulative radiation dose is a very disturbing finding seen in relation to the overall dose assessment of these patients, and once again emphasizes the importance of keeping the number of CT scans at a bare minimum.

Survey and consensus

Our survey showed that most of the spine centers agreed on surgical technique and not to use post-operative CT. However, the survey also illustrated some of the discrepancies among different centers as for how often to assess and for how long to follow patients with idiopathic scoliosis, as well as choice of radiographic systems, Table 4. Roughly half of the centers used a follow-up algorithm similar to our algorithm which is in line with the consensus guidelines of Kleuver et al[11] and Knott et al[12].Implementation of international consensus guidelines on follow- up algorithms for scoliosis can be various depending on the department, local tradition, and depending on which consensus guideline was used.

In fact, there is still a lack of clear international consensus as how often and how many x- rays are needed in course of scoliosis treatment. A review of recent literature does not give a clear picture of this[11–13,17]. There is agreement as to the needs of at least one coronal and lateral radiograph during or after surgery, but not as to the timing of subsequent follow-up intervals and for how long to

follow patients.

Only one in eight used routine postoperative CT as well as one in eight using intraoperative navigation. We use intraoperative navigation at our institution for all scoliosis surgery, based on studies showing significantly less screw misplacements than freehand technique and or fluoroscopy based instrumentation[18,19].

Limitations

Our study has some limitations. The size of the study population was small, and thus not well suited for statistical analysis, eg.; on various possible correlations. As a result of low numbers of patients we combined braced patients and observation patients in the same group for comparison with the surgical group. This comparison provides an overview of the variation of doses among the groups, but will not reflect very well what is the typical dose for braced patients specifically.

Reducing dose

There are several ways to achieve reduction of radiation exposure. The most simple way is to reduce the number of x-rays and avoid CT scans, while optimizing radiological equipment is an continuously ongoing process. In fact, little might be gained from routine imaging unless the patient has unexpected symptoms, Garg et al[17] found that only 2.9 /1000 spine x-rays led to revision surgery. Thus, it may very likely be possible to lower the number of spine radiographs without affecting the quality of treatment.

Conclusion

The magnitude of cumulative radiation during scoliosis treatment varies substantially depending on radiographic follow-up protocol, intraoperative and ancillary imaging. Future studies are needed for highlighting the clinical consequences of lowered or elevated frequency of x-ray monitoring, founding the basis of future consensus guidelines on radiographic follow-up. By using low-dose x-ray systems such as EOS stereo-radiography in combination with low-dose protocol for intraoperative navigation it is possible to keep exposure to patients at a minimum balancing potential risks of adverse effects such as screw misplacement and radiation induced cancer, while still providing optimal care. One ancillary CT scan may double total cumulative full-body absorbed radiation dose.

References

1. Doody MM, Ronckers CM, Land CE, et al. Cancer mortality among women frequently exposed to radiographic examinations for spinal disorders. Radiat Res 2010;174:83–90.

2. Simony A, Carreon LY, Jensen KE, et al. Incidence of cancer and infertility, in patients treated for adolescent idiopathic scoliosis 25

years prior. Eur Spine J 2015;24:S740.

3. Pace N, Ricci L, Negrini S. A comparison approach to explain risks related to X-rayimaging for scoliosis, 2012 SOSORT award winner. Scoliosis 2013 Jul 2;8(1):11.

4. Deschênes S, Charron G, Beaudoin G, et al. Diagnostic imaging of spinal deformities: reducing patients radiation dose with a new slot-scanning X-ray imager. Spine (Phila Pa 1976). 2010 Apr 20;35(9):989-94. doi: 10.1097/BRS.0b013e3181bdcaa4.

5. Dietrich TJ, Pfirrmann CW, Schwab A, et al. Comparison of radiation dose, workflow, patient comfort and financial break-even of standard digital radiography and a novel biplanar low-dose X-ray system for upright full-length lower limb and whole spine radiography. Skeletal Radiol. 2013 Jul;42(7):959-67. doi: 10.1007/s00256-013-1600-0. Epub 2013 Mar 28.

6. Pedersen PH, Petersen AG, Østgaard SE, et al. EOS Micro-dose Protocol: First Full-spine Radiation Dose Measurements in Anthropomorphic Phantoms and Comparisons with EOS Standard-dose and Conventional Digital Radiology. Spine (Phila Pa 1976) 2018;43:E1313– 21.

7. The International Commission on Radiological Protection. The 2007 Recommendations of the International Commission on Radiological Protection. ICRP Publication 103. Ann ICRP 2007;37.

8. Sundhedsstyrelsen. CT Referencedoser. Indsamling og Vurder af patientdoser ved CT - © Sundhedsstyrelsen, 2015 2015. http://sundhedsstyrelsen.dk/da/udgivelser/2015/~/media/5FFD01914F8A430A8407C9B46D94AA6E.ashx

9. Petersen AG, Eiskjær S, Kaspersen J. Dose optimisation for intraoperative cone-beam flat- detector CT in paediatric spinal surgery. Pediatr Radiol 2012;42:965–73.

10. Després P, Beaudoin G, Gravel P, et al. Physical characteristics of a low-dose gas microstrip detector for orthopedic x-ray imaging. Med Phys 2005;32:1193–204

11. De Kleuver M, Lewis SJ, Germscheid NM, et al. Optimal surgical care for adolescent idiopathic scoliosis: an international consensus. Eur Spine J 2014;23:2603–18.

12. Knott P, Pappo E, Cameron M, et al. SOSORT 2012 consensus paper: reducing x-ray exposure in pediatric patients with scoliosis The epidemiology of x-ray exposure in pediatric patients with spinal

deformity. Scoliosis2014 9:4

13. Fletcher ND, Glotzbecker MP, Marks M, et al. Development of Consensus-Based Best Practice Guidelines for Postoperative Care Following Posterior Spinal Fusion for Adolescent Idiopathic Scoliosis. Spine (Phila Pa 1976) 2017;42:E547–54.

14. Body W, Organ D, Therapeutic D. ATOM Dosimetry Phantoms Size and Age Related Dose Calculations Features

15. Law M, Ma W-K, Lau D, et al. Cumulative radiation exposure and associated cancer risk estimates for scoliosis patients: Impact of repetitive full spine radiography. Eur J Radiol Elsevier Ireland Ltd; 2016;85:625–8.

16. Presciutti SM, Karukanda T, Lee M. Management decisions for adolescent idiopathic scoliosis significantly affect patient radiation exposure. Spine J 2014;14:1984–90.

17. Garg S, Kipper E, La Greca J, et al. Are routine postoperative radiographs necessary during the first year after posterior spinal fusion for idiopathic scoliosis? A retrospective cohort analysis of implant failure and surgery revision rates. J Pediatr Orthop 2014;35:33–8.

18. Ughwanogho E, Patel NM, Baldwin KD, et al. Computed tomography-guided navigation of thoracic pedicle screws for adolescent idiopathic scoliosis results in more accurateplacement and less screw removal. Spine (Phila Pa 1976) 2012;37:473–8.

19. Baky FJ, Milbrandt T, Echternacht S, et al. Intraoperative Computed Tomography–Guided Navigation for Pediatric Spine Patients Reduced Return to Operating Room for Screw Malposition Compared With Freehand/Fluoroscopic Techniques. Spine Deform 2019 Jul;7(4):577-581

Table 1 Demographics and Radiation exposure			
Treatment	**Conservative**	**Surgery**	**Both groups**
Patients	19	42	61
Males	6	11	17
Females	13	31	44
Age at initial assessment*	**15 (5-18)**	**14 (3-17)**	14 years (3-18)
Age at final assessment*	**15 (9-19)**	**17 (14-20)**	17 years (9-20)
Time of follow-up*	9 months (0-52)	38 months (13-163)	
Cobb angle (°) initial assessment*	19 (10-50)	45 (10-80)	
Cobb angle (°) before surgery**		52 (36-82)	
Cobb angle (°) final assessment*	23 (12-65)	16 (4-30)	
Mean number of fused vertebrae		11	
Radiation exposure	**Conservative group[1] (Median and range)**	**Surgery group (Median and range)**	
Conventional spine X-rays (CR) number[2] / radiation dose	4 (0-20)/1.1mSv(0-5.5)	14.5 (2-57)/4.1mSv(0.6-15.5)	
Biplanar EOS imaging Number[2] / radiation dose	2 (0-17)/ 0.58mSv(0-2.4)	10.5 (0-26)/ 1.3mSv(0-3.1)	
O-arm 3d scans Number/ dose		2(1-4)/ 3.8mSv(0.9-10.0)	
O-arm 2D fluoroscopy time in seconds/ dose		33.7(20.3-136.0)/ 0.9mSv(0.4-3.5)	
Radiation dose combined (CR, EOS, O-arm)	1.1mSv(0.2-7.2)	10.3mSv(3.8-20.4)	
Additional CT and PET-CT[3]	0	1(1-2)	
Radiation dose	0	11.9mSv(0.6-20.1)	
Total radiation dose all modalities	1.1mSv(0.2-7.2)	10.8mSv(3.8-35.9)	

*Median values and range
**The Cobb angle just prior to surgery
[1]Braced and observational
[2]Total number of coronal and lateral images
[3]A total of 6 patients had additional imaging owing to various reasons explained in the results section.

Table 2. The magnitude of radiation dose from ancillary CT and Pet-CT				
Patient id	Modality	Radiation dose	Factor of increase in total radiation dose**	Percentage of total radiation dose***
13	CT cervical spine	5.38 mSV	2.0	50%
27	CT thoraco-lumbar spine*	17.03 mSV	1.9	48%
34	PET-CT full spine and CT lumbar spne*	20.13mSV	3.1	67%
38	CT lumbar spine	6.70 mSv	1.7	42%
45	CT cervical spine	0.57 mSv	1.1	6%
46	CT thoraco-lumbar spine*	18.03 mSv	2.1	53%

*MARS (metal artefact reducing software) technique
** Total radiation (CR, EOS, O-arm and ancillary CT and Pet-CT)/ ancillary CT and PET-CT
*** Ancillary radiation dose/total radiation dose from all modalities

Table 3. Differences of radiographic systems used for scoliosis follow-up and intraoperatively. Number of centers using out of 8 spine centers.							
Conventional radiography	1	Digital radiography	3	EOS biplanar slotscanner	2	EOS and Digital radiography	1
Freehand technique only	5	Fluoroscopy (C-arm)	1	O-arm intraoperative navigation	1	Postoperative CT scan routinely	1

Figure 1: Illustration of the EOS low-dose scanner and the outcome

Figure 2.

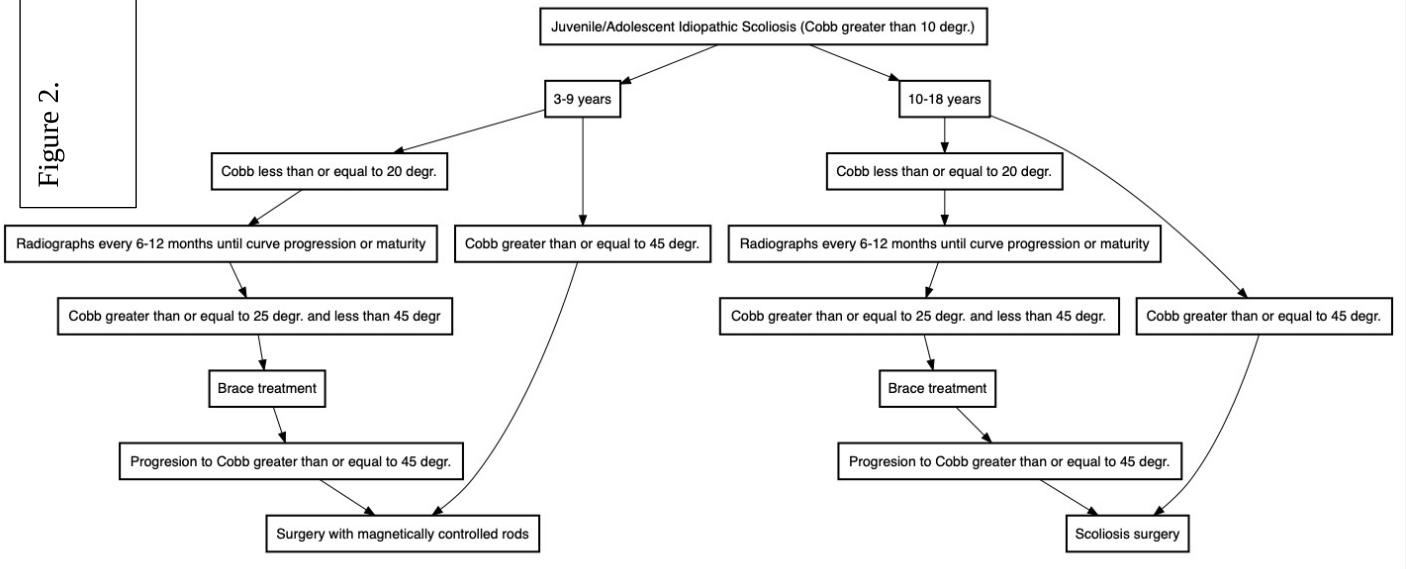
Juvenile/Adolescent Idiopathic Scoliosis (Cobb greater than 10 degr.)
3-9 years
10-18 years
Cobb less than or equal to 20 degr.
Cobb less than or equal to 20 degr.
Radiographs every 6-12 months until curve progression or maturity
Cobb greater than or equal to 45 degr.
Radiographs every 6-12 months until curve progression or maturity
Cobb greater than or equal to 25 degr. and less than 45 degr
Cobb greater than or equal to 25 degr. and less than 45 degr.
Cobb greater than or equal to 45 degr.
Brace treatment
Brace treatment
Progresion to Cobb greater than or equal to 45 degr.
Progresion to Cobb greater than or equal to 45 degr.
Surgery with magnetically controlled rods
Scoliosis surgery

Study V

Title page

Title:

HOW MANY DOSEMETERS ARE NEEDED FOR CORRECT MEAN ORGAN DOSE ASSESSMENT WHEN PERFOMING PHANTOM DOSIMETRY? A PHANTOM STUDY EVALUATING LIVER ORGAN DOSE AND INVESTIGATING TLD NUMBERS AND WAYS OF DOSEMETER PLACEMENT.

Authors' list:

Peter H. Pedersen[1,2] · Asger G. Petersen[3] · Svend E. Ostgaard[1] · Torben Tvedebrink[4] · Søren P. Eiskjær[1]

Authors' affiliations:

[1]Department of Orthopaedic Surgery, Aalborg Universitetshospital,Syd, Hobrovej 18-22, 9000 Aalborg, Denmark.

[2]Department of Clinical Medicine, Aalborg University, Fredrik Bajers Vej 5, 9100 Aalborg, Denmark.

[3]Region Nordjylland, Røntgenfysik, Merkurvej 13, 9700 Brønderslev, Denmark.

[4]Department of Mathematical Sciences, Aalborg University, Skjernvej 4A, 9220 Aalborg Øst, Denmark.

Corresponding author contact details:

Peter H. Pedersen, ORCID ID: 0000-0001-8475-9687

Phone: (+45)97660000
Fax: (+45)97662354
Email: php@rn.dk

Short running title:

ORGAN DOSIMETRY AND TLDS NEEDED

OXFORD UNIVERSITY PRESS | Radiation Protection Dosimetry

HOW MANY DOSEMETERS ARE NEEDED FOR CORRECT MEAN ORGAN DOSE ASSESSMENT WHEN PERFOMING PHANTOM DOSIMETRY? A PHANTOM STUDY EVALUATING LIVER ORGAN DOSE AND INVESTIGATING TLD NUMBERS AND WAYS OF DOSEMETER PLACEMENT.

Journal:	*Radiation Protection Dosimetry*
Manuscript ID	Draft
Manuscript Type:	Paper
Subject Index Term:	Organ doses, Phantoms, Angular dependence/response, Annealing/thermal treatment, Lithium fluoride, Models/modelling, Thermoluminescence, X rays

SCHOLARONE™
Manuscripts

ABSTRACT

This study evaluated repeated mean organ dose measurements of the liver by phantom dosimetry and statistical modelling in order to find a way to reduce the number of dosemeters needed for precise organ dose measurements. Thermoluminescent dosemeters were used in an adult female phantom exposed to a biplanar x-ray source at three different axial phantom rotations. Generalized mixed linear effect modelling was used for statistical analysis. A subgroup of five to six organ specific locations out of 28 yielded mean liver organ doses within 95% confidence intervals of measurements based on all 28 liver specific dosemeter locations. No statistical difference of mean liver dose was observed with rotation of the phantom either 10° clockwise or counter-clockwise as opposed to the coronal plane. Phantom dosimetry handling time during organ dose measurements can be markedly reduced, in this case the liver, by 79% (22/28), while still providing precise mean organ dose measurements.

For Peer Review

INTRODUCTION

Performing full-body radiation dose dosimetry in anthropomorphic phantoms is demanding and time consuming. Therefore, usually only a subset of available dosemeter positions within phantoms are used hoping that these will reflect mean absorbed radiation dose to the specific organs and the body as a whole. However, one cannot be sure that the chosen subset of positions used represent the "true" mean organ doses of the organs of interest. For instance, the liver, an organ of irregular symmetry, most often presents with numerous options for dosemeter allocations. In a typical anthropomorphic phantom, such as the ATOM female phantom[1] the liver holds 28 different liver dosemeter positions, picking only a few of these positions will result in thousands of different possible TLD placement combinations, many with statistically significant different mean doses as a consequence. If all 290 predefined organ specific thermoluminescent dosemeter (TLD) positions in this particular anthropomorphic phantom were to be used, according to own experience, it would most likely take in excess of 18 hours of continuous work effort to prepare dosemeters (annealing and calibration), instalment of dosemeters in the phantom, expose the phantom, remove dosemeters and measure dose exposure. This being for a single phantom with mean organ dose measurements and calculation of effective dose. As such, preparing phantoms and dosemeters for organ dose measurements is potentially a very time consuming and costly process. Thus, it is of great importance to investigate ways to reduce the number of TLDs needed to make consistent and precise dose monitoring. Then, the question is how the best and most precise measurements can be obtained by the least amount of effort? This is a methodological study investigating the influence of different factors on mean absorbed organ dose (liver) and on the basis of this aiming to propose a method to determine the optimal placement and number of TLDs allowing for precise repeated and efficient monitoring of mean organ doses. Secondly, this study offered an opportunity to evaluate TLD (MCP-N) sensitivity changes over the course of repeated radiation cycles.

MATERIALS AND METHODS

Phantom

An adult female anthropomorphic ATOM phantom, 702-D, (CIRS- computerized imaging reference systems, INC. Virginia, USA)[1] was used to investigate liver organ radiation dose absorption (Figure 1). The ATOM phantom has been designed for the purpose of investigating organ dose and image quality, it consists of tissue-equivalent epoxy resins. The phantom represents an adult female with a height of 165cm and a weight of 55 kg. The phantom consists of 38, 25mm thick, axial slices. Each slice holds a number of organ specific locations, each location has a 5mm diameter hole containing a tissue specific cylindrical plug for TLD placement. Each TLD is placed in the middle of each of the vertical tissue-equivalent cylindrical plugs. The adult female phantom holds a total of 290 locations for TLD positioning, the liver holds 28 locations.

Imaging system

For exposure of the phantom, the EOS low-dose slot scanning system (EOS imaging, Paris, France) (www.eos.imaging.com) was used. The EOS system provides two simultaneous full-body X-ray images, allowing for full body assessment in two planes (sagittal and coronal). In daily clinical practice at our institution the EOS system is used for routine evaluation of postural assessment in spine deformity patients. The EOS system has been described in detail previously [2]. The system comes with different imaging protocols, the protocol used for phantom exposure in this study was the standard low-dose setting shown in Table 1.

Exposure and dose measurements

All 28 organ-specific dosemeter locations of the liver were utilized. The phantom was placed in the isocenter of the EOS scanner defined by the intersection of two orthogonal laser beams, custom fitted in the EOS. An isocenter of the phantom was marked corresponding to the intersection of the two perpendicular lines produced by the laser on phantom slice number 25 out of the 38 slices total. By adding overlying slices one at the time subsequent isocenters of each slice containing liver TLD locations were defined and marked. The cross-section of the laser lined up with the phantom isocenter provided very precise repositioning of the phantom between dose readings. From this position, with the same isocenter, three series of exposures were executed. Three different fixed positions of the phantom were chosen: Anteroposterior (AP), AP-10°(10 degrees of axial rotation counter-clock wise to the left side of the phantom) and AP+10° (10 degrees of axial rotation to the right side of the phantom). Figure 2 shows the intersection of the laser beams on the defined isocenter of the phantom. For each of the above-mentioned three positions a series of seven scans were performed, each with a total of five consecutive standard-dose exposures followed by dose readings. This resulted in a total of 105 liver-organ exposures and 21 dose measurements. The organ specific dose for each set of five exposure was

For Peer Review

calculated by summing the dose measured for each internal dosimeter position, preceded by subtraction of mean ambient background dose (ad). The mean liver organ dose in μGy for one phantom exposure thus being: $\hat{D}_{liver} = \frac{1}{28}\sum_{i=1}^{28} \frac{d_i - \overline{d}_a}{5}$, where d_i is the dose at position i and $\overline{d}_a$ is the estimated mean ambient background dose estimated from four non-exposed dosemeters calibrated at the same time as the dosemeters exposed within the liver.

For each of the 28 internal dosimeter location a specific TLD was allocated. Four TLDs were used for registration of accumulated background dose from the time of calibration to the time of dose readings after phantom exposure. The specific TLD for each position was annealed, calibrated and repositioned in the exact same position for each round of exposure and subsequent dose reading. This allowed for measuring intra-object dose readings for each tablet, for each internal positioning, for each of the three phantom positions. Furthermore, the same TLDs were annealed and calibrated systematically in the same order allowing for observations on variability with regard to calibrated dosemeter reference dose readings after one exposure to a ^{90}Sr source. Mean reference dose values for the 32 TLDs were registered prior to each of the 21 exposure cycles.

MCP-N Dosemeter, Irradiator and Reader

For dose measurements MCP-N (Krakow, Poland) TLDs were used. The MCP-N is a solid Lithium-fluoride dosemeter doped with magnesium, copper and phosphorus (LiF:Mg, Cu, P). It is a highly sensitive dosemeter with 30 times higher sensitivity to gamma ray doses than the MTS-N TLD, and is well-suited for low-dose measurements[3].
The PTW Freiburg Annealing Oven (TLDO. PTW**,** Freiburg Germany) was used for annealing of the dosemeters. The TLDs were annealed using a specific time temperature profile (TTP) heating the dosemeters to 240 degrees Celsius for a time period of 15 minutes. After annealing the TLDs were calibrated using the Rados IR-2000 - ^{90}Sr Irradiator (RadPro International GmbH, Wermelskirchen, Germany). The IR-2000 of this study held a ^{90}Sr source of approximately 0.290 mGy, which was used to provide background dose to the dosemeters. Each TLD received one background dose exposure during calibration. The Rados RE-2000 reader (RadPro International GmbH, Wermelskirchen, Germany) was used for dose readings.

Statistical and data analyses

Statistical analyses on relationship between dose absorption, TLD location and phantom rotation was performed, relaying information on liver organ doses and variability. Mean organ doses for each phantom position was calculated and uncertainty doses expressed within 95% confidence intervals. In order to evaluate the effect of rotation of the phantom with regard to x-ray sources and the relayed effect on the individual location of the TLDs, generalized mixed effect linear modelling[4],[5] using R (R-Project for Statistical Computing, version 3.6.1) was performed, when nothing else is mentioned R

For Peer Review

Base was used. Subsequently, an investigation into whether a subset (reduced number) of TLDs could relay precise information of total mean organ dose was undertaken:

Photos and coordinate calculations
Digital images of each of the 7 slices holding liver positions were photographed with a high resolution digital camera, Figure 3. The camera position was the same for all images – same distance to the slice and the camera was positioned at a zero degree angle (parallel) to the phantom slice. Two key distances were measured on each of the slices corresponding to the length of the 2 perpendicular lines drawn on the phantom slices through the isocenter from front to back and from left to right. The coordinates for each of the TLD positions were calculated from the digital images, the known line lengths of the 2 lines mentioned above and the line placement as seen on the digital images using the R package Digitize[6] and the function digitize. The rotated positions were calculated with the formulas $x' = x \cos(\theta) + y \sin(\theta)$, $y' = y \cos(\theta) - x \sin(\theta)$, where θ is the angle of rotation and x' and y' the coordinates after rotation.

Generalized Mixed Linear Effects Model analysis
Due to the hierarchical nature of the data a generalized mixed linear effects model was used to analyse the data with the count variable as the dependent variable and the independent variables x-coordinate, y-coordinate, difference in x-coordinate by rotation, difference in y-coordinate by rotation, the angle of rotation (factor), slice number (factor) and the random factor 1 + replicate number | TLD position. Replicate number refers to the 7 consecutive series of exposures and subsequent measurements. The formula can simplified be written as:

$$\text{Count} \sim \beta_0 + \beta_1 * \text{X-coordinate} + \beta_2 * \text{Y-coordinate} + \beta_3 * \text{difference in X-coordinate} + \beta_4 * \text{difference in Y-coordinate} + \beta_5 * \text{Rotation-factor} + \beta_6 * \text{Slice factor} + \beta_7 * \text{Replicate-factor} + \beta_8 * (1 + \text{Replicate-factor} \mid \text{TLD position})$$

Where β zero to eight represent the regression coefficients, Table 2. We chose not to include any interaction terms in the analysis as the meaning of such terms would be difficult to interpret and complicate the model. The R package lme4 and the function glmer.nb[7] and anova function and the change in Akaike Information Criteria (AIC) was used for the generalized mixed linear effects model analysis. Model assumptions were checked by plotting the Pearson residuals against predicted values and by plotting the standardized residuals against predicted values and by plotting the standardized residuals against leverage. Collinearity was evaluated with the Variable Inflation Factor (VIF).

Subset analysis
The aim was to determine the best possible subset of TLD positions giving approximately the same estimate of the dose as the full set of TLD's (28 positions). We chose to use subsets of 1 to 8 tablets or TLD positions. The subsets were generated using the R package gRbase[8] and the function combnPrim. The average and standard deviations for the full dataset were calculated (base R) and compared to the absorbed dose for the subset of 1 to 8 tablets or TLD positions using only the observations in the specific subset. The difference to the estimate based on the full set of tablets or TLD positions was calculated. The subsets were sorted according to their signed deviation from zero (concordant estimates of the subset estimate and full set estimate) and plotted against the difference to the estimate based on the full data set. The total number of different subsets for each of the 1 to 8 subsets were calculated and the number of acceptable subsets were calculated (deviations from zero not significant,

For Peer Review

95% confidence limits). Lastly, based on the physics of radiation and the architecture of the EOS scanner we pointed out what we thought would be the most optimal choice of TLD positions (the way we think other researchers might have done to minimize the time used to do the measurements), subsets of three to six TLDs were compared to the estimates based on the full dataset.

RESULTS

The TLD positions are plotted in Figure 4, numbered and colour coded according to position and rotation. Besides the colour coding the rotation is also indicated by the suffix A, B or C. This was illustrated by using the R package ggplot [9].

Mean organ doses for the three exposure positions are shown in Figure 5. A trend towards differences of mean organ doses with clockwise or anti-clockwise rotation was found, but regardless of rotation, no statistically significant differences were observed. The generalized mixed linear effects model is summarized in table 2. The slice factor variable did not add anything to the model. Only the intercept of the random factor replicate number was part of the model. All other variables mentioned earlier was in the model (see formula). Model validation indicated no problems. All VIF's were below 4.

Subset analysis

Figure 6, shows the result of all possible combinations of 1-8 TLDs and the dispersion around the mean organ dose based on all 28 TLDs.

Table 3 illustrates the relationship between number of TLDs in a subset and number of acceptable combinations of TLDs yielding mean organ dose within the 95% CI of the "true" mean dose from all 28 dosemeter locations. Table 4 shows the four combinations of 3-6 TLD positions reaching values closest to the "true" mean based on the subset analysis. A list of combinations from 1-8 TLDs reaching up to ten best combinations of TLDs can be found in appendix 1.

Table 5 shows the subsets (empirically chosen) and subsequent mean liver dose values, for comparison with table 4, values within 95% CI of true mean dose are marked in bold. In the subset of three TLDs, six in twelve had a mean dose within the 95% CI of the "true" mean organ.. For the subset of four TLDs it was seven in twelve, in the subset of five TLDs twelve out of twelve had a value within the 95% CI of each specific rotation of the phantom. The subset of six TLDs resulted in eleven out of twelve with a mean dose within the 95% CI.

TLD sensitivity changes

A total of 672 reference dose measurements were performed for the 28 position specific TLDs and the four TLDs used for registration of background dose. Figure 7 shows the mean reference dose for all 32 TLDs measured over the course of the 21 radiation cycles, illustrating a downwards trend. The mean

For Peer Review

reference dose value at initial measurements was 231078 counts +/-2SD (211,531-250,625) vs 206187 counts +/-2SD (182,997-229,377) at final measurements. An almost 10% difference, but no statistically significant difference. We did not observe the same trend of decreased measures of radiation dose for the three rotational positions where all measurements were calibrated against the new specific reference dose measurements. This is illustrated in Figure 6 where liver doses were also compared to previously published values by the same authors[10]. No significant variation in dose reading was observed for any of the TLD tablets.

DISCUSSSION

The primary aim of this study was to analyse doses absorbed in different rotations of an anthropomorphic phantom holding 28 liver specific TLD locations, and to investigate a way to extrapolate information in order to reduce the number of TLDs needed for the use of estimating precise mean organ doses within the human body. In the subset analysis of 1-8 TLDs, all possible combinations were investigated as shown in Table 3 and Figure 5, and proved the validity of our method. In combination the latter two show the number of possible combinations and the number of ”acceptable” combinations, and illustrate that no unanticipated deviations occurred. The mathematically generated subsets of 3-6 TLDs of Table 4 are as anticipated much more precise than the empirically chosen subsets of Table 5. However, the subsets of 4-6 were very likely to yield mean liver doses within the 95 confidence interval of the “true” liver dose based on the 28 TLD locations. In fact, 35 out of 36 mean doses were within these boundaries. Thus, by either calculating best fits for subsets of 1-8 TLDs based on measured radiation dose from all available measuring points, or by symmetrically choosing subsets of 5-6 TLDs around the isocenter of the phantom and in relation to x-ray sources, mean doses within 95% CI of “true” mean dose could be achieved. This indicates that a reduced number of TLDs can provide an acceptable approximation of true organ dose. One option being the calculation of best fits from all 28 measuring points to elect specific subset, another option, however not as precise would be the more simple approach of logical selection of positions as shown above. As a result, handling time during organ dose measurements can be markedly reduced, in this case the liver, by at least 79% (22/28), while still providing precise mean organ dose measures.

Secondly, this study evaluated the effect of minor movement that could imitate unintended movement of the patient or alterations in patient positioning during radiographic exposure, on the absorbed radiation dose of the liver in an anthropomorphic phantom. No statistically significant change of mean absorbed dose to the liver regardless of clockwise or anti-clockwise phantom rotation of 10° was found. This implies that minor movement of a patient within the scene of x-ray exposure will not affect absorbed radiation dose much.

TLD reference dose readings over time showed an apparent sensitivity loss after repeated cycles of annealing and dose reading. In fact, a trend towards a reduced sensitivity of almost 11% after 21 radiation cycles was observed. This was similar to the findings of Poirier et al 2018[11] who experienced a drop of approximately 20% over 44 cycles. What is the exact cause of this reduction of sensitivity is not clear. Lüpke et al (RPD)2006[12], found that TLD sensitivity could be altered significantly if

annealing temperatures for MCP tablets exceeded 240 degrees, they observed a drop in sensitivity of 0.45% per cycle. Differences in cooling rates have also been found to influence sensitivity of dosemeters [13], however all dosemeters of this study were cooled at the same speed for each cycle. Fernandez et al 2016[14] found that low-intensity traps were cleared insufficiently causing a residual signal. However, this would result in a higher dose reading and not lower as experienced in our study, likewise during dose-readings we custom-made a 5 second delay to allow for release of low-intensity traps. We do not consider the impact of decay from the ^{90}Sr source to be of significance in this study. The half-life of the ^{90}Sr source is 28.8 years, and measurements were made over a time period of 64 days, resulting in a 0.43% reduction of the source activity (1-exp(-(ln(2)/28.8 years)0.18 years)). The findings of reduced sensitivity of the TLDs over time emphasizes the importance of careful calibration of TLDs over time. Mixing of dosemeters from different batches after diverging number of cycles/ radiation history should be avoided, in order to keep heterogeneity at a minimum.

The findings of the generalized mixed linear effects model analysis correlated well with what we would expect. The coordinates of the TLD position were a significant factor which is in accordance with the laws of physics especially the inverse square law. The differences in the x- and y-coordinates with rotation were significant factors in our model which we would also expect for the same reason as mentioned above. However, the angle of rotation (as factor) was also a significant factor. As a consequence of geometrical relations the distance of the radiation beam through tissue will increase for some TLDs and for others this distance will decrease, or be almost the same depending on the amount of rotation and the position . With axial phantom rotation the amount and type of "tissue" that the radiation beam must pass will also change, so the effect of rotation cannot be described entirely with the change in coordinates. It did not matter to which slice the TLDs belonged. The y-axis intercept for the TLDs did vary significantly but we did not find any random effect over time for the calibrated TLDs (measurements 1-21) - since the same TLD was repositioned in the same location within the phantom during all scans.

For Peer Review

Limitations

The study was as most organ dose studies limited by the fact that organ dose measurements were estimated based on in vitro phantom dosimetry and not direct in vivo measurements. However, it is the belief of the authors that in-phantom dosimetry in anthropomorphic phantoms is equivalent to or better than PCXMC[15] mathematical phantom organ dose estimations. In-phantom dosimetry is as close as one gets to real life in vivo measurements. The above-mentioned reduced sensitivity of TLDs after repeated cycles of radiation is a limiting factor if not careful calibration is performed after each cycle, of TLD sensitivity against the radiation reference source, in this case the ^{90}Sr source.

The accuracy of the digitize R package has been evaluated by Poisot et al, 2011[6]. The accuracy was deemed acceptable and the package was not difficult to apply. In this case the TLDs were somewhat bigger than the points in most scatterplots making it possible to vary how you mark the TLD positions on the phantom slices. However, we do not consider this to be of any importance as these differences were only observed in the second decimal when repeating the measurements.

The estimation of liver organ dose from the empirically selected subset of TLDs were few and only one person performed the selection of TLD positions. And it could be argued that a larger number of empirically chosen subsets should have been evaluated. However, the trend was very clear with almost 100% of mean doses within the 95% CI of measured liver doses when choosing five or six TLD positions in a logical symmetrical fashion.

CONCLUSIONS

Through phantom dosimetry and a combination of generalized mixed effect analysis and subset analysis we have constructed a model proposing a reduced number of TLD locations that can be relied upon when estimating liver mean organ dose. In the current study five or six locations versus 28 possible locations for TLD placement offered a mean organ dose not statistically significantly different from the mean dose using all 28 TLD organ specific locations. Axial rotation of the phantom either clockwise or anti-clockwise with regard to x-ray source, mimicking patient movement or inter-operator alterations in patient positioning, did not have a significant impact on mean organ dose.

For Peer Review

REFERENCES

1. Dose, W. B., Dose, O. and Radiation, T. *ATOM Dosimetry Phantoms*. (2013).at <http://www.cirsinc.com/file/Products/701_706/701 706 DS 080715(1).pdf>
2. Després, P., Beaudoin, G., Gravel, P. and Guise, J. A. De *Physical characteristics of a low-dose gas microstrip detector for orthopedic x-ray imaging*. Med. Phys. **32**, 1193–1204 (2005).
3. González, P. R., Furetta, C. and Azorín, J. *Comparison of the TL responses of two different preparations of LiF:Mg,Cu,P irradiated by photons of various energies*. Appl. Radiat. Isot. **65**, 341–344 (2007).
4. Schielzeth, H. and Nakagawa, S. *Nested by design: Model fitting and interpretation in a mixed model era*. Methods Ecol. Evol. **4**, 14–24 (2013).
5. Pinheiro, J.C., Bates, D. . *Mixed-Effects Models in S and S-PLUS (Linear Mixed-Effects Models: Basic Concepts and Examples)*. Springer, New York, NY, (2000).at <https://doi.org/10.1007/0-387-22747-4_1>
6. Poisot, T. *The digitize package: Extracting numerical data from scatterplots*. R J. **3**, 25–26 (2011).
7. Kuznetsova, A., Brockhoff, P. B. and Christensen, R. H. B. *lmerTest Package: Tests in Linear Mixed Effects Models* . J. Stat. Softw. **82**, (2017).
8. Højsgaard, S. *Package gRbase*. (2018).at <http://people.math.aau.dk/~sorenh/software/gR/>
9. Gómez-Rubio, V. *ggplot2 - Elegant Graphics for Data Analysis (2nd Edition)* . J. Stat. Softw. **77**, 3–5 (2017).
10. Pedersen, P. H., Petersen, A. G., Østgaard, S. E., Tvedebrink, T. and Eiskjær, S. P. *EOS Micro-dose Protocol: First Full-spine Radiation Dose Measurements in Anthropomorphic Phantoms and Comparisons with EOS Standard-dose and Conventional Digital Radiology*. Spine (Phila. Pa. 1976). **43**, E1313–E1321 (2018).
11. Poirier, Y., Kuznetsova, S. and Villarreal-Barajas, J. E. *Characterization of nanoDot optically stimulated*

luminescence detectors and high-sensitivity MCP-N thermoluminescent detectors in the 40-300 kVp energy range. Med. Phys. **45**, 402–413 (2018).

12. Lüpke, M., Goblet, F., Polivka, B. and Seifert, H. *Sensitivity loss of Lif: Mg,Cu,P thermoluminescence dosemeters caused by oven annealing*. Radiat. Prot. Dosimetry **121**, 195–201 (2006).

13. Piters, T. M. and Bos, A. J. J. *Influence of the Cooling Rate on Repeatability of LiF:Mg,Cu,P Thermoluminescent Chips*. Radiat. Prot. Dosimetry **33**, 91–94 (1990).

14. Sol Fernández, S. Del, García-Salcedo, R., Mendoza, J. G., Sánchez-Guzmán, D., Rodríguez, G. R., Gaona, E. and Montalvo, T. R. *Thermoluminescent characteristics of LiF: MG, Cu, P and CaSO4: Dy for low dose measurement*. Appl. Radiat. Isot. **111**, 50–55 (2016).

15. Servomaa, a. and Tapiovaara, M. *Organ Dose Calculation in Medical X Ray Examinations by the Program PCXMC*. Radiat. Prot. Dosimetry **80**, 213–219 (1998).

For Peer Review

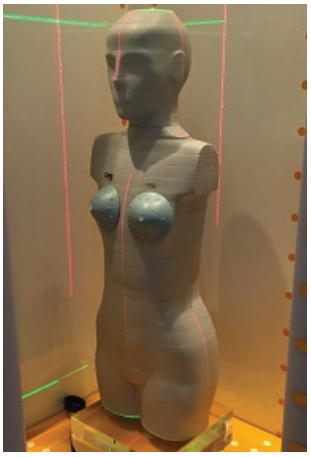

Figure 1. A female adult phantom (ATOM model 702-D, CIRS).

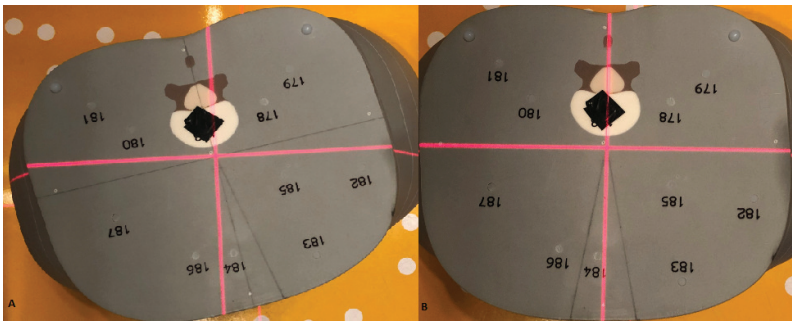

Figure 2. Phantom slice with orthogonal laser positioning marking. (A) 10° of counter-clockwise axial rotation of phantom. (B) Neutral Anteroposterior (AP) positioning of phantom.

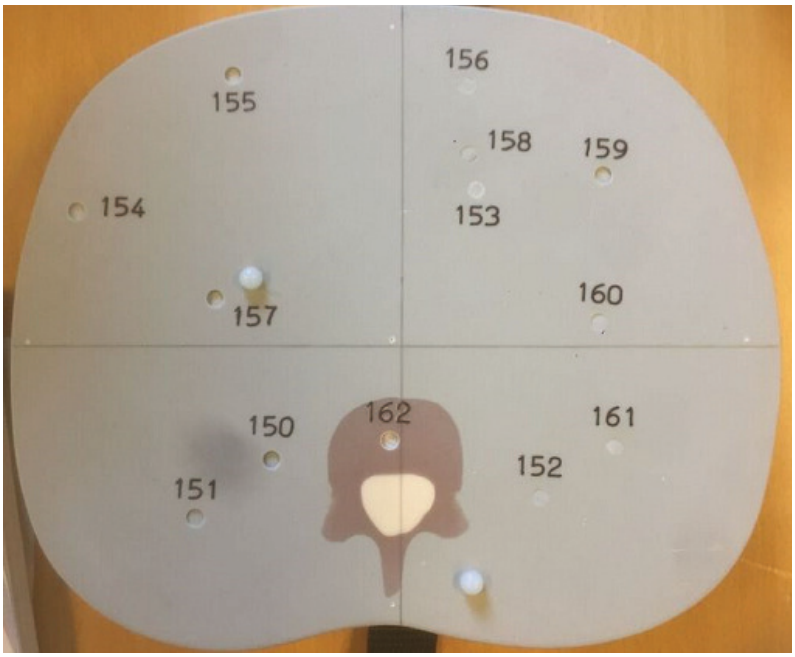

Figure 3. Example of phantom slice holding liver positions.

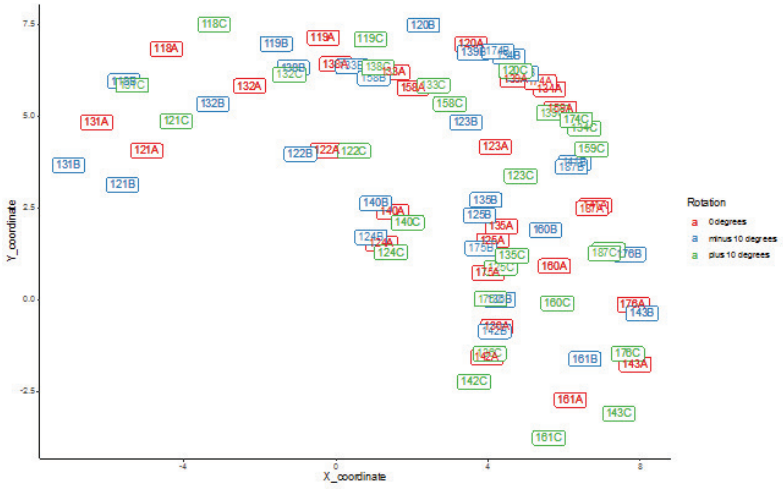

Figure 4. The TLD positions within the phantom, colour coded according to position and axial rotation of the phantom. Besides the colour coding the rotation is also indicated by the suffix A, B or C.

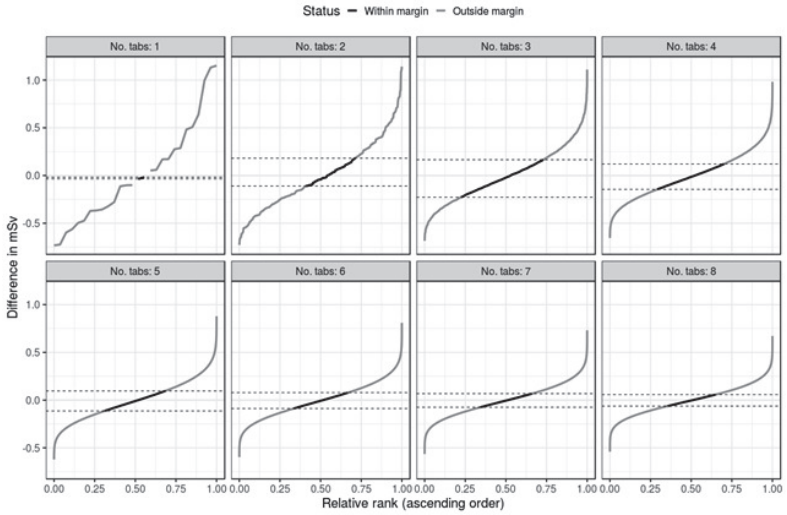

Figure 5. The variation (rank) of deviation from the mean dose from all 28 TLDs, calculated from subsets of 1-8 Tabs.(TLD positions).

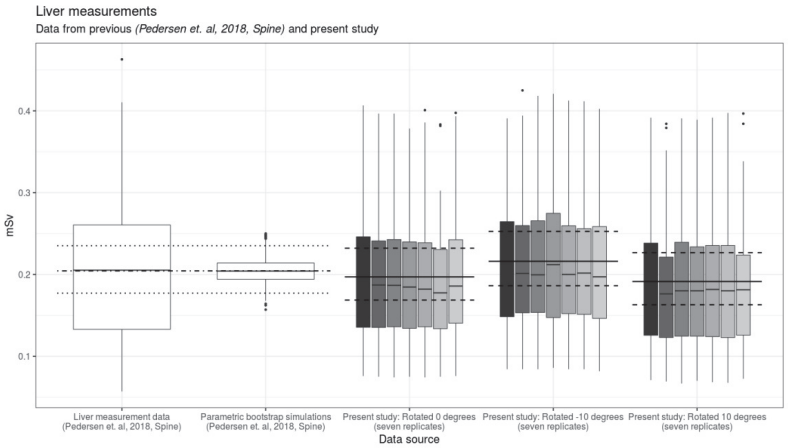

Figure 6. Radiation doses for the three axial rotational positions as well as liver doses previously measured and published by same authors(10).

493x282mm (72 x 72 DPI)

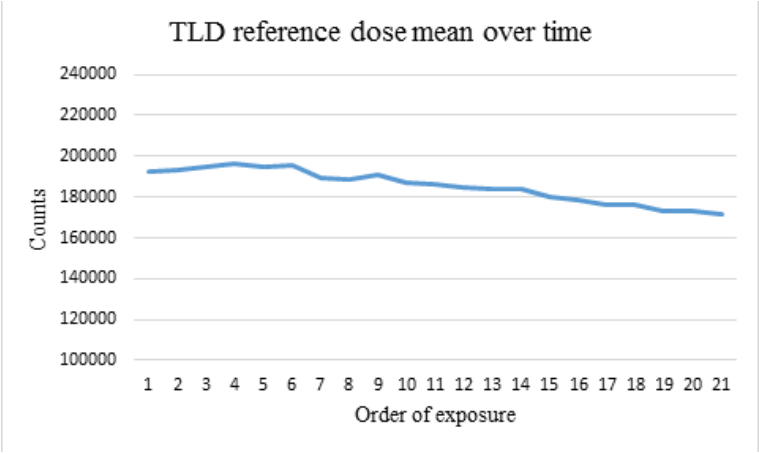

Figure 7. The mean reference dose for all 32 TLDs over the course of the 21 radiation cycles. (28 liver positions, and the four TLDs used to measure background dose)

Table 1. EOS imaging parameters.

Standard-dose protocol used for a single biplanar full-spine scan of an adult female phantom

	Anteroposterior exposure	Lateral exposure
Morphotype	Medium	Medium
Scan speed	4	4
Scan time seconds	12.5	12.5
Tube potential (kV)	90	105
Tube Current (mA)	250	250
Filtration	1.5mm AL+0.1mm Cu	1.5mm AL+0.1mm Cu
Scan Height	95 cm	95 cm
Distance source-to-isocenter	987mm	918mm
Distance source-to-detector	1300mm	1300mm
Dose-area product (mGy x cm^2)	436.6	648.0

For Peer Review

Table 2. Estimated regression parameters, standard errors, z-values and p-values for the final negative binomial generalized mixed linear effect model.

Variable	Estimate	Std.error	Z-value	p-value
Intercept	19.618	0.042	471.232	0.000
X-coordinate	-0.063	0.004	-14.013	0.000
Y-coordinate	-0.087	0.004	-19.623	0.000
X-coordinate difference	-0.019	0.008	-2.508	0.012
Y-coordinate difference	-0.037	0.005	-7.852	0.000
Rotation minus 10 degr.	0.068	0.009	7.725	0.000
Rotation plus 10 degr.	-0.013	0.009	-1.514	0.130

For Peer Review

Table 3. The number of TLDs in a subset in relation to possible combinations and acceptable combinations yielding a "true" mean dose.

No. TLDs	Combinations	Acceptable combinations	1/Ratio[a]
1	28	2	0.071
2	378	25	0.066
3	3276	314	0.096
4	20475	2240	0.109
5	98280	11486	0.117
6	376740	46218	0.123
7	1184040	151884	0.128
8	3108105	413259	0.133

[a]The probability of an acceptable combination

For Peer Review

Table 4, mean liver doses based on best subset values of TLDs with specific locations and rotation of phantom, in relation to "true" mean liver dose.

Position of phantom:	AP +10° µGy	Ap µGy	AP -10° µGy		AP +10° µGy	Ap µGy	AP -10° µGy		AP +10° µGy	AP µGy	AP -10° µGy		AP +10° µGy	AP µGy	AP -10° µGy
TLD 3 Locations				TLD 4 Locations				TLD 5 Locations				TLD 6 Locations			
134,139, 140	**185**	**197**	**217**	119,140, 141,159	**189**	**197**	**219**	123,131, 134,135, 143	**189**	**197**	**213**	119,124, 135,139, 158,175	**191**	**197**	**218**
119,140, 160	**191**	**197**	**218**	120,122, 159,175	**189**	**197**	**219**	122,124, 138,139, 143	**188**	**197**	**218**	119,124, 139,140, 158,176	**190**	**197**	**219**
119,139, 142	**189**	**197**	**220**	125,132, 139,141	**186**	**197**	**217**	119,123, 124,174, 175	**191**	**197**	**217**	133,138, 158,159, 160,175	**187**	**197**	**218**
123,138, 187	**195**	**197**	**216**	118,139, 160,161	**192**	**197**	**216**	131,134, 142,143, 158	**191**	**197**	**214**	119,123, 125,131, 160,161	**182**	**197**	**213**

All doses are marked in bold and are within the 95% confidence intervals of mean liver doses for each phantom position using all 28 measuring points.
Mean liver doses for each position with 95% confidence intervals for mean values:
AP+10°: 191 µGy (163-227)
AP: 197 µGy (169-232)
AP-10°: 216 µGy (186-253)

For Peer Review

Table 5, mean liver doses based on empirically selected subsets of TLDs with specific locations and rotation of phantom, in relation to "true" mean liver dose.

Position of phantom:	AP +10° µGy	Ap µGy	AP -10° µGy		AP +10° µGy	Ap µGy	AP -10° µGy		AP +10° µGy	AP µGy	AP -10° µGy		AP +10° µGy	AP µGy	AP -10° µGy
TLD 3 Locations				TLD 4 Locations				TLD 5 Locations				TLD 6 Locations			
118,120, 125	250	253	**247**[a]	118,120 124,125	232	251	256	118,120, 122,124, 125	**202**	**204**	**227**	118,120, 124,125, 136,140	**205**	**207**	**225**
131,134, 136	244	**231**	**246**	120,131, 134,136	231	**219**	**204**	122,124, 132,136, 140	**202**	**207**	**223**	118,132, 138,158, 160,161	**210**	**215**	**235**
118,120, 124	263	243	289	118,120, 124,125	232	**218**	**232**	132,140, 143,158, 160	**176**	**183**	**202**	118,134, 138,140, 160,161	**185**	**191**	**208**
138,140 143	**172**	**182**	**200**	138,139, 140,143	**177**	**188**	**207**	132,138, 140,159, 187	**206**	**218**	**237**	118,122, 124,136, 142,143	**169**	**170**	184

[a]All doses marked in bold are within the 95% confidence intervals of mean liver doses for each phantom position using all 28 measuring points.
Mean liver doses for each position with 95% confidence intervals:
AP+10°: 191 µGy (163-227)
AP: 197 µGy (169-232)
AP-10°: 216 µGy (186-253)

For Peer Review

Appendix I, Study V

No. TLDs	TLD positions within phantom*	Difference [mSv] (9 decimal precision)	P-value
1	134	-0.01752381	0.18447
1	140	-0.035666667	0.07835
2	133,135	-0.000880952	0.93666
2	121,142	-0.000952381	0.99471
2	138,160	0.004619048	0.63268
2	122,135	0.00497619	0.66299
2	119,136	0.006119048	0.53228
2	136,138	-0.006666667	0.56817
2	139,140	0.00847619	0.55396
2	140,174	0.012047619	0.37574
2	122,125	-0.016880952	0.17556
2	134,139	0.017547619	0.16183
3	123,139,174	-0.000142857	0.9867
3	134,139,140	-0.000190476	0.98874
3	119,140,160	-0.000285714	0.97264
3	121,140,176	0.000285714	0.99697
3	123,138,141	-0.000285714	0.97064
3	122,133,142	0.000380952	0.96348
3	119,139,142	-0.00052381	0.93598
3	121,135,175	-0.000952381	0.99057
3	123,138,187	0.001190476	0.87052
3	132,135,187	-0.001666667	0.89695
4	121,123,139,176	0.00002381	0.99964
4	119,140,141,159	-0.00002381	0.99754
4	133,138,140,143	-0.00002381	0.99826
4	120,122,159,175	0.000047619	0.99224
4	125,132,139,141	-0.000130952	0.99168
4	118,139,160,161	-0.000130952	0.98775
4	132,159,174,176	-0.000130952	0.99084
4	119,120,139,161	-0.000238095	0.96795
4	119,122,125,160	0.000261905	0.97344
4	118,124,125,161	-0.00027381	0.97344
4	124,134,138,187	-0.00027381	0.97432
5	121,123,124,159,175	-0.000002381	0.99995
5	121,133,134,141,142	0.000004762	0.99991
5	123,131,134,135,143	-0.000009524	0.99927
5	122,124,138,139,143	-0.000009524	0.99902
5	119,123,124,174,175	-0.000009524	0.99858
5	125,131,136,139,187	-0.000009524	0.99934
5	119,122,141,158,176	-0.000009524	0.99908
5	121,133,135,161,174	-0.000016667	0.99967
5	131,134,142,143,158	0.000019048	0.99883
5	123,131,133,142,161	0.000019048	0.9986
6	131,133,136,139,176,187	0	1
6	119,124,135,139,158,175	0	1
6	119,124,139,140,158,176	0	1
6	121,124,132,136,141,175	0	1
6	121,132,140,141,142,175	0	1
6	133,138,158,159,160,175	0	1

6	119,123,125,131,160,161	0	1
6	119,132,139,159,161,187	0	1
6	125,131,132,136,175,176	0	1
6	124,131,133,159,160,161	0	1
7	119,121,122,134,136,141,176	0	1
7	119,121,122,125,136,143,174	0.000003401	0.9999
7	119,121,122,124,135,141,161	-0.000003401	0.9999
7	121,138,139,142,158,159,161	-0.000003401	0.99989
7	119,121,125,138,140,143,176	-0.000003401	0.99989
7	119,120,122,134,135,139,143	0.000006803	0.99903
7	121,124,138,140,141,142,159	0.000006803	0.99978
7	119,123,131,133,160,161,176	0.000006803	0.99931
7	120,122,123,134,135,139,159	0.000006803	0.99889
7	122,123,124,132,138,143,160	0.000006803	0.99933
7	124,132,133,134,136,158,160	0.000006803	0.99951
7	123,125,131,134,136,158,175	0.000006803	0.99951
7	124,125,131,133,134,141,176	0.000006803	0.99949
8	121,122,132,134,136,139,142,176	-0.00000085	0.99996
8	121,123,132,134,136,140,161,174	-0.00000085	0.99996
8	121,123,133,138,139,142,160,175	-0.00000085	0.99997
8	119,121,124,138,142,143,174,175	-0.00000085	0.99997
8	119,121,122,135,140,159,160,176	-0.00000085	0.99997
8	119,121,138,139,140,141,161,176	-0.00000085	0.99997
8	121,132,133,136,159,160,174,176	-0.00000085	0.99996
8	121,133,138,139,142,159,160,187	-0.00000085	0.99997
8	121,134,138,142,158,160,174,175	0.000001701	0.99993

8	118,121,124,134,135,136,175,176	0.000001701	0.99993
8	119,120,121,125,132,161,175,176	0.000001701	0.99994
8	119,121,131,139,142,143,161,187	0.000001701	0.99993

*Adult female anthropomorphic ATOM phantom, 702-D, (CIRS- computerized imaging reference systems, INC. Virginia, USA)

ISSN (online): 2246-1302
ISBN (online): 978-87-7210-547-5

AALBORG UNIVERSITY PRESS